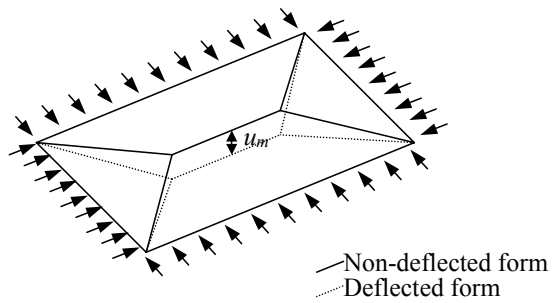Tim Gudmand-Høyer

Yield line Theory for Concrete Slabs Subjected to Axial Force

Volume 2

BYG · DTU

Yield line Theory for Concrete Slabs Subjected to Axial Force

Tim Gudmand-Høyer

Non-deflected form
Deflected form

1 Preface

This report is prepared as a partial fulfilment of the requirements for obtaining the Ph.D. degree at the Technical University of Denmark.

The work has been carried out at the Department of Structural Engineering and Materials, Technical University of Denmark (BYG•DTU), under the supervision of Professor, dr. techn. M. P. Nielsen.

I would like to thank my supervisor for the valuable advise, for the inspiration and the many and rewarding discussions and criticism to this work.

Thanks are also due to my co-supervisor M. Sc. Ph.D. Bent Steen Andreasen, RAMBØLL, M. Sc. Ph.D.-student Karsten Findsen, BYG•DTU, M. Sc. Ph.D.-student Lars Z. Hansen, BYG•DTU, M. Sc. Ph.D.-student Jakob L. Laugesen, BYG•DTU, M. Sc. Ph.D. Bent Feddersen RAMBØLL and Architect MAA Søren Bøgh MURO for their engagement and criticism to the present work and my Ph.D.-project in general.

Finally I would like to thank my wife and family for their encouragement and support.

Lyngby, December 2003

Tim Gudmand-Høyer

2 Summary

This paper treats the subject Yield line Theory for Concrete Slabs Subjected to Axial Force.

In order to calculate the load-carrying capacity from an upper bound solution the dissipation has to be known.

For a slab without axial force the usual way of calculating this dissipation is by using the normality condition of the theory of plasticity together with the yield condition. This method is equivalent to the original proposal by K. W. Johansen. This method has shown good agreement with experiments and has won general acceptance.

In this paper the dissipation in a yield line is calculated on the basis of the Coulomb yield condition for concrete in order to verify K. W. Johansen's method. It is found that the calculations lead to the same results if the axes of rotation are the same for adjacent slab parts. However, this is only true if the slab is isotropic and not subjected to axial load.

An evaluation of the error made using K. W. Johansen's proposal for orthotropic rectangular slabs is made and it is found that the method is sufficiently correct for practical purposes.

For deflected slabs it is known that the load-carrying capacity is higher. If it is assumed that the axis of rotation corresponds to the neutral axis of a slab part and the dissipation is found from the moment capacities about these axes K. W. Johansen's proposal may be used to find the load-carrying capacity in these cases too. In this paper this is verified by comparing the results with numerical calculations of the dissipation. Also for deflected slabs it is found that the simplified method is sufficiently correct for practical purposes.

The same assumptions are also used for rectangular slabs loaded with axial force in both one and two directions and sufficiently good agreement is found by comparing the methods.

Interaction diagrams between the axial load and the transverse load are developed at the end of the paper for both methods. Different approaches are discussed.

Only a few comparisons between experiments and theory are made. These indicate that the theory may be used if a proper effectiveness factor is introduced and the deflection at failure is known.

If the deflection is unknown an estimate of the deflection based on the yield strains of the concrete and the reinforcement seems to lead to acceptable results.

3 Resume

Denne rapport behandler emnet brudlinieteori for plader belastet med normalkræfter og tværbelastning.

For at kunne beregne bæreevnen ud fra en øvreværdibetragtning er det nødvendigt at kunne udregne dissipationen.

Plader uden normalkraft beregnes normalt ud fra plasticitetsteoriens normalitetsbetingelse kombineret med pladens flydebetingelse. Denne metode er ækvivalent med K. W. Johansens oprindelige forslag. Denne metode har vist god overensstemmelse med forsøg og er almindeligt benyttet.

I denne rapport udregnes dissipationen i en brudlinie ud fra dissipationsformlerne for et Coulomb materiale og dette sammenholdes med K. W. Johansens metode. Af dette fremgår det at resultatet er det samme hvis rotationsakserne for tilstødende pladedele ligger i samme højde. Dette vil dog kun være rigtigt for isotrope plader og der er derfor gennemført en vurdering af fejlen ved beregninger af ortotrope plader. Fejlen vurderes at være uden praktisk betydning.

Det vides at bæreevnen for en plade stiger under udbøjning. Det er her vist at hvis man antager at rotationsaksen svarer til nullinien for den enkelte pladedel og beregner dissipationen efter K. W. Johansens fremgangsmåde kan man beregne bæreevnen. Dette er eftervist ved at sammenligne med numeriske beregninger der baserer sig på dissipationsudtrykkene for et Coulomb materiale. Beregningerne viser, at afvigelserne er uden praktisk betydning.

Beregninger af plader med normalkraft og udbøjede plader med normalkraft i både en og to retninger viser tilsvarende god overensstemmelse.

Interaktionsdiagrammer for normal og tværlast behandles til sidst og der gives forskellige bud på hvordan dette kan gribes an.

Kun ganske få forsøg er her fundet brugbare til verifikation af teorien. Disse data er for kvadratiske plader med normalkraft i én retning.

Ved sammenligning mellem forsøg og teori er det vist at beregninger med en passende effektivitetsfaktor giver god overensstemmelse med forsøg hvis man anvender den målte brududbøjning.

Kendes brududbøjningen ikke kan man tilsyneladende anvende et skøn der baserer sig på flydetøjningen for beton og armering.

4 Table of contents

5 Notation

The most commonly used symbols are listed below. Exceptions from the list may appear, but this will then be noted in the text in connection with the actual symbol.

Geometry

h	Height of a cross-section
A	Area of a cross-section
A_c	Area of a concrete cross-section
A_s	Area of reinforcement close to the bottom face
A_s'	Area of reinforcement close to the top face
A_{sc}	Area of reinforcement in compression
h_c	Distance from the bottom face to the centre of the bottom reinforcement
h_c'	Distance from the top face to the centre of the top reinforcement
h_I, h_{II}	Distance from the bottom face to the centre of the bottom reinforcement about axis I and II, respectively
h_{cI}', h_{cII}'	Distance from the top face to the centre of the top reinforcement about axis I and II, respectively
y_0	Compression depth
L	Length of an element
L_x, L_y	Length of a slab in the x and y direction, respectively
e	Eccentricity
u	Deflection
u_m	Deflection in the mid section
x, y, z	Cartesian coordinates
w	Angle between axis I and II
v	Angle between axis II and yield line

Physics

ε	Strain
σ	Stress
σ_c	Stress in concrete

f_c	Compressive strength of concrete
f_y	Yield strength of reinforcement
ρ	Reinforcement ratio
Φ_0, Φ_0'	Degree of reinforcement for the bottom- and top reinforcement, respectively
Φ_{0x}, Φ_{0y}	Degree of bottom reinforcement in the x and y direction, respectively
Φ_{0x}', Φ_{0y}'	Degree of top reinforcement in the x and y direction, respectively
Φ_{0I}, Φ_{0II}	Degree of bottom reinforcement in the I and II direction, respectively
Φ_{0I}', Φ_{0II}'	Degree of top reinforcement in the I and II direction, respectively
p	Line load, uniform load per unit length
q	Surface load, uniform load per area unit
m_p	Yield moment in pure bending
m_{px}, m_{py}	Yield moment in pure bending in the x and y direction, respectively
m_f	Yield moment for a given axial load
m_{fx}, m_{fy}	Yield moment for a given axial load in the x and y direction, respectively
n	Axial load per unit length
n_x, n_y	Axial load per unit length in the x and y direction, respectively
W_i, W_e	Internal and external work, respectively
W_c, W_s	Concrete and reinforcement contribution to the dissipation, respectively
M_f	Total moment capacity of a yield line
$M_{f,c}$	Contribution to the total moment capacity of a yield line from the concrete
$M_{f,s}, M_{f,s}'$	Contribution to the total moment capacity of a yield line from the bottom- and top reinforcement, respectively

6 Introduction

This paper has two main purposes.

The first one is to investigate the possibility of calculating the load-carrying capacity of a slab in a simplified way based on an interpretation of K. W. Johansen´s proposal regarding the dissipation and C. R. Calladine´s proposal regarding the axes of rotation.

The second purpose is to investigate the possibility of finding a calculation method for the relation between axial load-carrying capacity and lateral load-carrying capacity.

In order to determine the load-carrying capacity for slabs by using an upper bound approach the dissipation in a yield line has to be found.

In section 7.1 the contribution from the concrete and the reinforcement are found separately. In both cases formulas for the dissipation are developed for all possible yield lines starting in a corner, followed by the formulas for the special case of a right-angled corner.

Section 7.2 treats beams. This illustrates the basic problems in these calculations.

The following sections (7.3 to 7.5) treat different cases of rectangular slabs starting with the square slab without axial force and initial deflection and ending up with rectangular slabs with axial force and initial deflections.

In section 7.6 a conservative proposal for an interaction curve between the axial load and the transverse load is given.

In chapter 8 test results are compared with theory.

Finally conclusions are made in chapter 9.

7 Theory

7.1 Dissipation in a yield line

If the axes of rotation for two slab parts are not at the same depth measured from the slab surface, the relative displacement discontinuity is no longer perpendicular to the yield line. The angle between the displacement discontinuity and the yield line changes with the depth from the slab surface and this must be taken into account when calculating the dissipation.
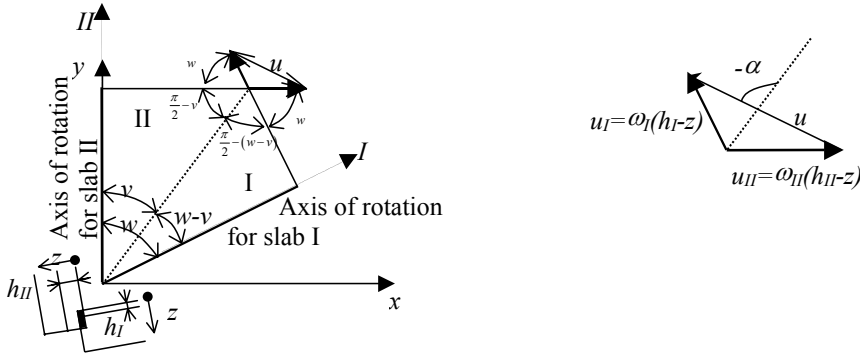

Figure 7.1. Displacement for two slab parts.

7.1.1 The contribution from the concrete

The concrete dissipation in the yield line may be calculated from the dissipation formulas for plane stress assuming a modified Coulomb material. Setting the tensile strength of concrete to zero, the contribution to the dissipation (per unit length) from the concrete may be calculated as:

$$W_c = \int_0^h \frac{1}{2} f_c u \left(1 - \sin\left(\alpha\right)\right) dz \tag{7.1}$$

u being the relative displacement and α the angle between the displacement and the yield line. Formula for plane stress has been used, see [5].

Both u and α depends on z, which is the depth from the top surface to the point considered. u_I and u_{II} are the displacements of slab part I and II, respectively. Depending on whether the displacements u_I and u_{II} are positive or not, α and u has to be calculated from one of the following cases:
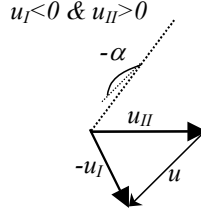
Case 1:

$u_I > 0$ & $u_{II} > 0$

$$u = \sqrt{u_I^2 + u_{II}^2 - 2u_I u_{II} \cos(\pi - w)} \qquad (7.2)$$

$$\alpha = -\left(\frac{\pi}{2} + v - Arc\cos\left(\frac{u^2 + u_{II}^2 - u_I^2}{2u_{II}u} \right) \right) \qquad (7.3)$$
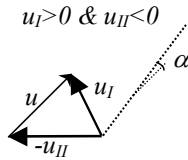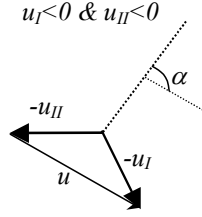
Case 2:

$u_I < 0$ & $u_{II} > 0$

$$u = \sqrt{u_I^2 + u_{II}^2 - 2(-u_I)u_{II} \cos(w)} \qquad (7.4)$$

$$\alpha = -\left(\frac{\pi}{2} + v + Arc\cos\left(\frac{u^2 + u_{II}^2 - (-u_I)^2}{2u_{II}u} \right) \right) \qquad (7.5)$$

Case 3:

$u_I > 0$ & $u_{II} < 0$

$$u = \sqrt{u_I^2 + u_{II}^2 - 2u_I u_{II} \cos(\pi - w)} \qquad (7.6)$$

$$\alpha = \frac{\pi}{2} - v - Arc\cos\left(\frac{u^2 + u_{II}^2 - u_I^2}{-2u_{II}u} \right) \qquad (7.7)$$

Case 4:

$$u_I < 0 \ \& \ u_{II} < 0$$

$$u = \sqrt{u_I^2 + u_{II}^2 - 2u_I u_{II} \cos(\pi - w)} \tag{7.8}$$

$$\alpha = \frac{\pi}{2} - v + Arc\cos\left(\frac{u^2 + u_{II}^2 - (-u_I)^2}{-2u_{II}u}\right) \tag{7.9}$$

It is seen that the calculation of u is the same in all the cases and u may in general be calculated as:

$$u = \sqrt{u_I^2 + u_{II}^2 + 2u_I u_{II} \cos(w)} \tag{7.10}$$

The angle between the displacement and the yield line α varies with respect to u_I and u_{II} depending on whether they are positive or negative.

The relation between the two rotations about I and II may be found from the geometrical conditions demanding the same displacement at a point of the yield line.

Figure 7.2. Geometrical relation between the rotations.

It appears from Figure 7.2 that the rotations may be calculated as

$$\omega_I = \frac{\omega}{\sin(w-v)}$$

$$\omega_{II} = \frac{\omega}{\sin(v)} \tag{7.11}$$

Here ω is the rotation of slab part line about an axis along to the yield line.

In the calculation of the displacement it is assumed that the rotation is small and the displacement may therefore be calculated as the rotation multiplied with the height. The displacements u_I, u_{II} and u may be calculated as

$$u_I = h\frac{\omega}{\sin(w-v)}\left(\frac{h_I}{h}-\frac{z}{h}\right) \Leftrightarrow$$

$$\frac{u_I}{h\omega} = \frac{1}{\sin(w-v)}\left(\frac{h_I}{h}-\frac{z}{h}\right)$$

(7.12)

$$u_{II} = h\frac{\omega}{\sin(v)}\left(\frac{h_{II}}{h}-\frac{z}{h}\right) \Leftrightarrow$$

$$\frac{u_{II}}{h\omega} = \frac{1}{\sin(v)}\left(\frac{h_{II}}{h}-\frac{z}{h}\right)$$

(7.13)

Inserting (7.12) and (7.13) into (7.10) leads to:

$$u = \sqrt{\left(h\frac{\omega}{\sin(w-v)}\left(\frac{h_I}{h}-\frac{z}{h}\right)\right)^2 + \left(h\frac{\omega}{\sin(v)}\left(\frac{h_{II}}{h}-\frac{z}{h}\right)\right)^2 + 2\left(h\frac{\omega}{\sin(w-v)}\left(\frac{h_I}{h}-\frac{z}{h}\right)\right)\left(h\frac{\omega}{\sin(v)}\left(\frac{h_{II}}{h}-\frac{z}{h}\right)\right)\cos(w)} \Leftrightarrow$$

$$\frac{u}{h\omega} = \sqrt{\left(\frac{\left(\frac{h_I}{h}-\frac{z}{h}\right)}{\sin(w-v)}\right)^2 + \left(\frac{\left(\frac{h_{II}}{h}-\frac{z}{h}\right)}{\sin(v)}\right)^2 + \frac{2\left(\frac{h_I}{h}-\frac{z}{h}\right)\left(\frac{h_{II}}{h}-\frac{z}{h}\right)\cos(w)}{\sin(w-v)\sin(v)}}$$

(7.14)

The angle α may be calculated as:

Case 1 ($u_I>0$ & $u_{II}>0$):

$$\alpha = -\left(\frac{\pi}{2}+v-Arc\cos\left(\frac{u^2+u_{II}^2-u_I^2}{2u_{II}u}\right)\right)$$

(7.15)

Case 2 ($u_I<0$ & $u_{II}>0$):

$$\alpha = -\left(\frac{\pi}{2}+v+Arc\cos\left(\frac{u^2+u_{II}^2-(-u_I)^2}{2u_{II}u}\right)\right)$$

(7.16)

Case 3 ($u_I>0$ & $u_{II}<0$):

$$\alpha = \frac{\pi}{2}-v-Arc\cos\left(\frac{u^2+u_{II}^2-u_I^2}{-2u_{II}u}\right)$$

(7.17)

Case 4 ($u_I<0$ & $u_{II}<0$):

$$\alpha = \frac{\pi}{2}-v+Arc\cos\left(\frac{u^2+u_{II}^2-(-u_I)^2}{-2u_{II}u}\right)$$

(7.18)

It is seen that the contribution to the dissipation from the concrete is a function of both the position of the axes of rotation h_I, h_{II}, the depth h, the rotation ω and the compressive strength f_c. The dissipation may be calculated in a dimensionless form as:

$$\frac{W_c}{h^2 \omega f_c} = \int_0^1 \frac{1}{2} \frac{u}{h} \left(1 - \sin(\alpha)\right) d\frac{z}{h} \tag{7.19}$$

A general analytical expression has not been found. However, for the special case of right-angled corners ($w = \pi/2$) the dissipation becomes:

$$\frac{W_c}{h^2 \omega f_c} = \frac{1}{4 \sin(v) \cos(v)} \cdot$$

$$\left(\begin{array}{l} -1 + \left(2 + \sqrt{\left(\frac{h_I}{h}\right)^2 \sin(v)^2 + \left(\frac{h_{II}}{h}\right)^2 \cos(v)^2}\right)\left(\frac{h_I}{h} \sin(v)^2 + \frac{h_{II}}{h} \cos(v)^2\right) \\[2em] + \sqrt{1 + \left(\left(\frac{h_{II}}{h}\right)^2 - 2\frac{h_{II}}{h}\right)\cos(v)^2 + \left(\left(\frac{h_I}{h}\right)^2 - 2\frac{h_I}{h}\right)\sin(v)^2}\left(1 - \frac{h_I}{h} \sin(v)^2 - \frac{h_{II}}{h} \cos(v)^2\right) \\[2em] + \log\left(\dfrac{-\frac{h_I}{h} \sin(v)^2 - \frac{h_{II}}{h} \cos(v)^2 + \sqrt{\left(\frac{h_I}{h}\right)^2 \sin(v)^2 + \left(\frac{h_{II}}{h}\right)^2 \cos(v)^2}}{1 - \frac{h_I}{h} \sin(v)^2 - \frac{h_{II}}{h} \cos(v)^2 + \sqrt{1 + \left(\left(\frac{h_{II}}{h}\right)^2 - 2\frac{h_{II}}{h}\right)\cos(v)^2 + \left(\left(\frac{h_I}{h}\right)^2 - 2\frac{h_I}{h}\right)\sin(v)^2}}\right) \\[2em] \cdot \left(\left(2\frac{h_I}{h}\frac{h_{II}}{h} - \left(\frac{h_I}{h}\right)^2 - \left(\frac{h_{II}}{h}\right)^2\right)\left(\cos(v)^2 - \cos(v)^4\right)\right) \end{array}\right) \tag{7.20}$$
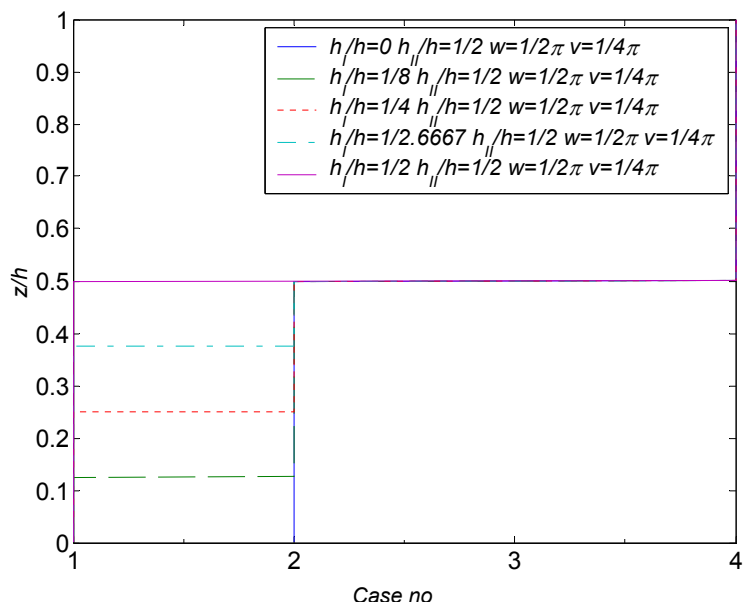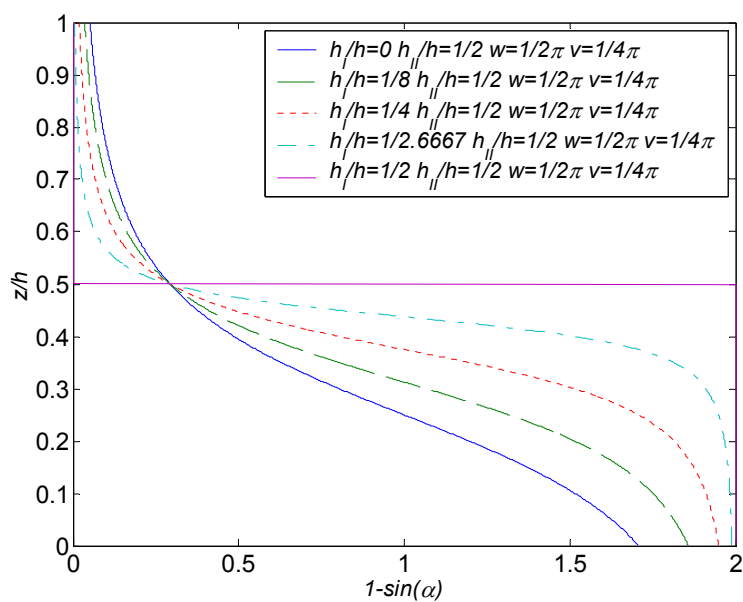
This expression is found from integrating by parts over the interval in which the expressions for α are valid. Distinctions must be made whether h_1 is larger than h_2 and whether these are larger than h. As an example it is seen that if $h_1 < h_2$ and $h_2 > h$ the formula becomes:

$$\frac{W_c}{h^2 \omega f_c} = \int_0^{h_1} \frac{1}{2} \frac{u}{h} \left(1 - \sin(\alpha_{case1})\right) d\frac{z}{h} + \int_{h_1}^1 \frac{1}{2} \frac{u}{h} \left(1 - \sin(\alpha_{case2})\right) d\frac{z}{h} \tag{7.21}$$

Fortunately all the combinations of h_1, h_2 and h lead to the result given in (7.20).

Plots of results of calculations for $h_{II}/h = 0.5$ $w = 0.5\pi$ and $v = 0.25\pi$ may be seen in Figure 7.1 to Figure 7.6.

These plots show which case has to be used in the calculation, how the different parts in the function (7.19) depends on the height and finally the function it self.

Figure 7.3. z/h as a function of the case no.
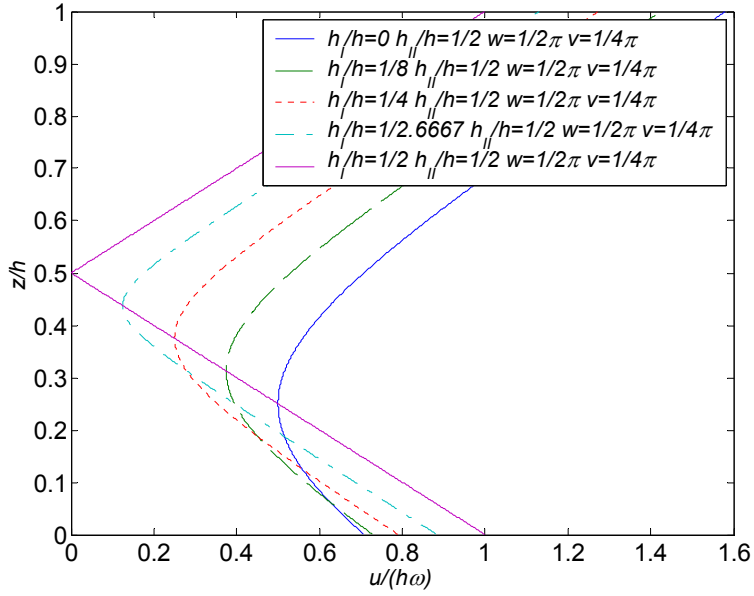

Figure 7.4. z/h as a function of 1-sin(α).
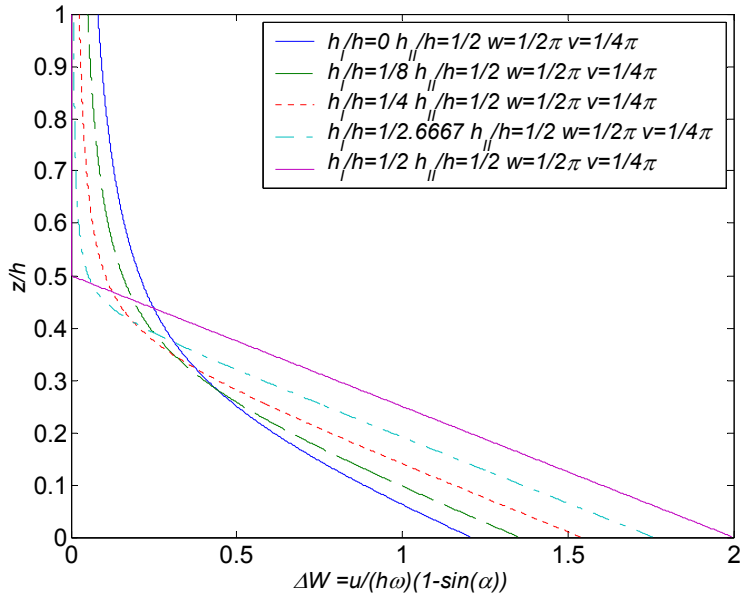
Figure 7.5. z/h as a function of u/(hω).

Figure 7.6. z/h as a function of ΔW.

As expected, most of the contribution to the dissipation is from the top (*z/h* is small).

Plots of results of calculations for $h_{II}/h = 0$ $w=0.5\pi$ and $v=0.25\pi$ may be seen in Figure 7.7 to Figure 7.10.
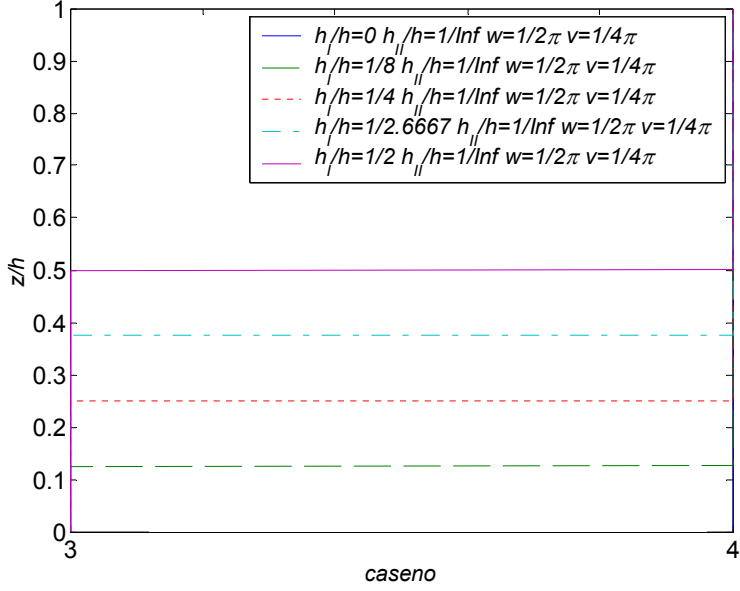

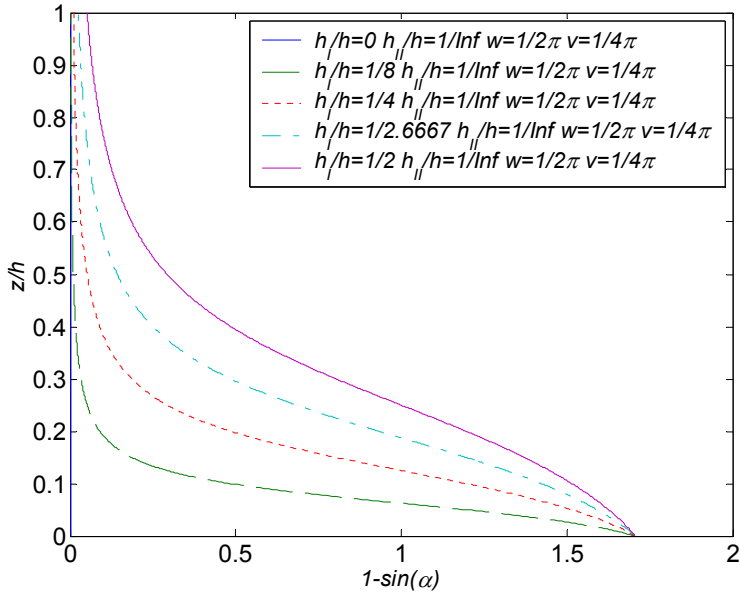*Figure 7.7. z/h as a function of the case no.*
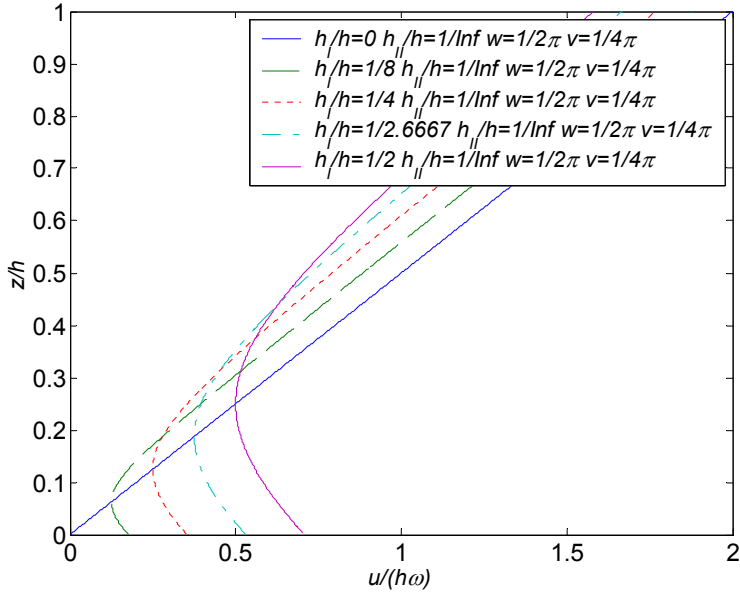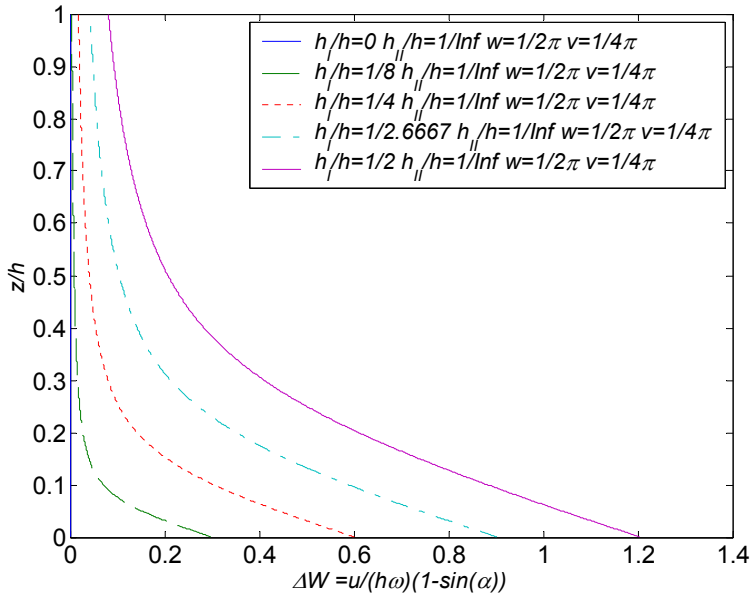

Figure 7.8. z/h as a function of 1-sin(α).

Figure 7.9. z/h as a function of u/(hω).

Figure 7.10. z/h as a function of ΔW.

In the case where one of the axes of rotation is in the top face it is seen that the main contribution is from the top of the slab.

A plot of the dimensionless dissipation contribution from the concrete is shown as a function of h_I/h and h_{II}/h for $w=0.5\pi$ and $w=0.25\pi$ in Figure 7.11 and Figure 7.12.

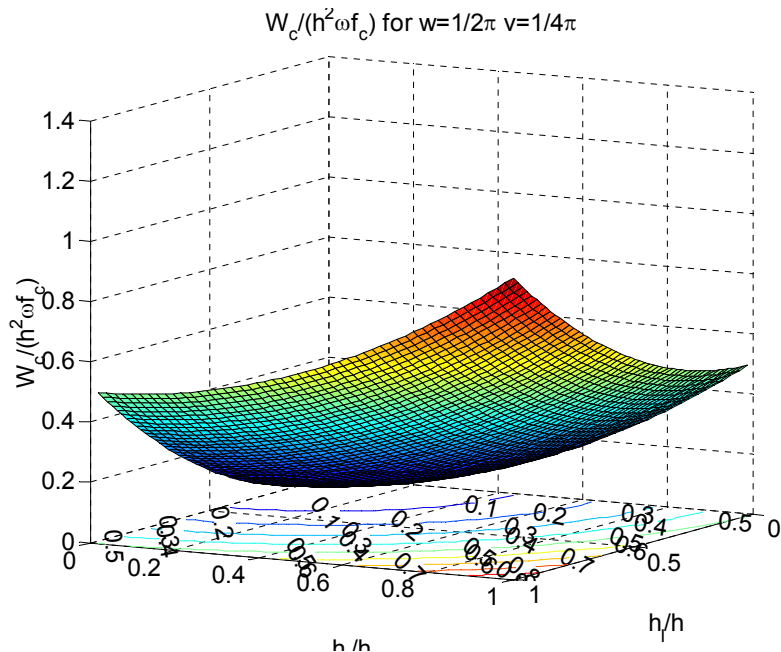These values are found from numerical integration over the depth of the section.

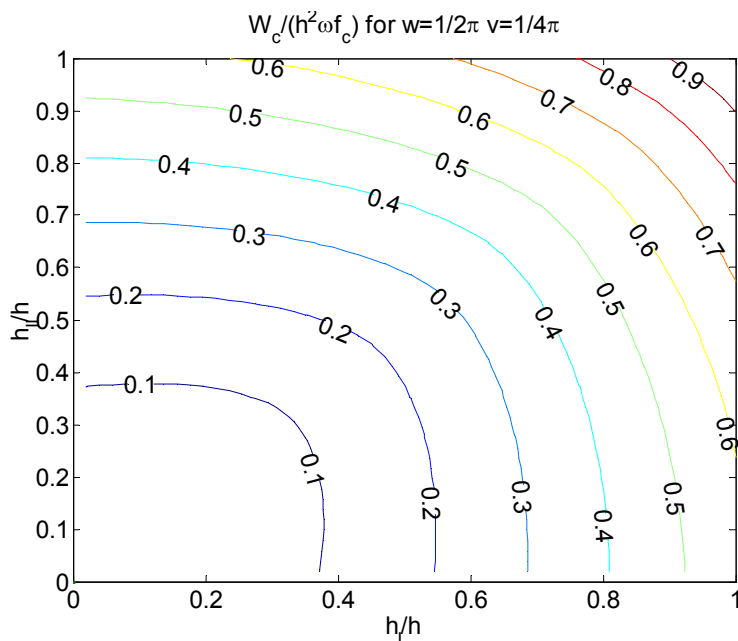Figure 7.11. Surface and contour plot of the dimensionless dissipation contribution from the concrete.

Figure 7.12Contour plot of the dimensionless dissipation contribution from the concrete.

It appears that the actual calculations are somewhat comprehensive and a simplification is therefore desirable.

K. W. Johansen, see [1], proposed that the bending moment in a section perpendicular to the yield line may be calculated as if the principal directions were coinciding with the directions of the reinforcement. The agreement between the yield condition and K. W. Johansen's proposal has been demonstrated by M. P. Nielsen in [5].

If a similar relation is valid for the dissipation, the dissipation contribution from the concrete might be calculated from the rotation about the axis, assuming a displacement perpendicular to the axis of rotation. This may be calculated quite easily since only the compression zone contributes to the dissipation and the displacement is perpendicular to the axis of rotation. In this case

$$W_{c\_K.W.J} = \int_0^h \frac{1}{2} f_c u \left(1 - \sin(\alpha)\right) dz$$

$$W_{c\_K.W.J} = \int_0^{h_I} \frac{1}{2} f_c u_I 2\cos(w-v) dz + \int_0^{h_{II}} \frac{1}{2} f_c u_{II} 2\cos(v) dz$$

$$W_{c\_K.W.J} = f_c \left(\int_0^{h_I} u_I \cos(w-v) dz + \int_0^{h_{II}} u_{II} \cos(v) dz \right)$$

$$W_{c\_K.W.J} = f_c \left(\int_0^{h_I} h \frac{\omega}{\sin(w-v)} \left(\frac{h_I}{h} - \frac{z}{h} \right) \cos(w-v) dz + \int_0^{h_{II}} h \frac{\omega}{\sin(v)} \left(\frac{h_{II}}{h} - \frac{z}{h} \right) \cos(v) dz \right)$$

$$W_{c\_K.W.J} = h\omega f_c \left(\frac{\cos(w-v)}{\sin(w-v)} \int_0^{h_I} \left(\frac{h_I}{h} - \frac{z}{h} \right) dz + \frac{\cos(v)}{\sin(v)} \int_0^{h_{II}} \left(\frac{h_{II}}{h} - \frac{z}{h} \right) dz \right)$$

$$W_{c\_K.W.J} = h\omega f_c \left(\frac{\cos(w-v)}{\sin(w-v)} \int_0^{h_L} \left(\frac{h_I}{h} - \frac{z}{h} \right) dz + \frac{\cos(v)}{\sin(v)} \int_0^{h_{II}} \left(\frac{h_{II}}{h} - \frac{z}{h} \right) dz \right)$$

$$W_{c\_K.W.J} = h^2 \omega f_c \left(\frac{1}{2} \left(\frac{h_I}{h} \right)^2 \frac{1}{\tan(w-v)} + \frac{1}{2} \left(\frac{h_{II}}{h} \right)^2 \frac{1}{\tan(v)} \right) \tag{7.22}$$

A numerical comparison between the simplified calculation and the theoretical one may be seen in Figure 7.13 to Figure 7.18 along with the deviation. These plots illustrate how large the difference is and how it depends on the position of the axis of rotation. They are made for different values for v in order to illustrate the influence of such a variation.
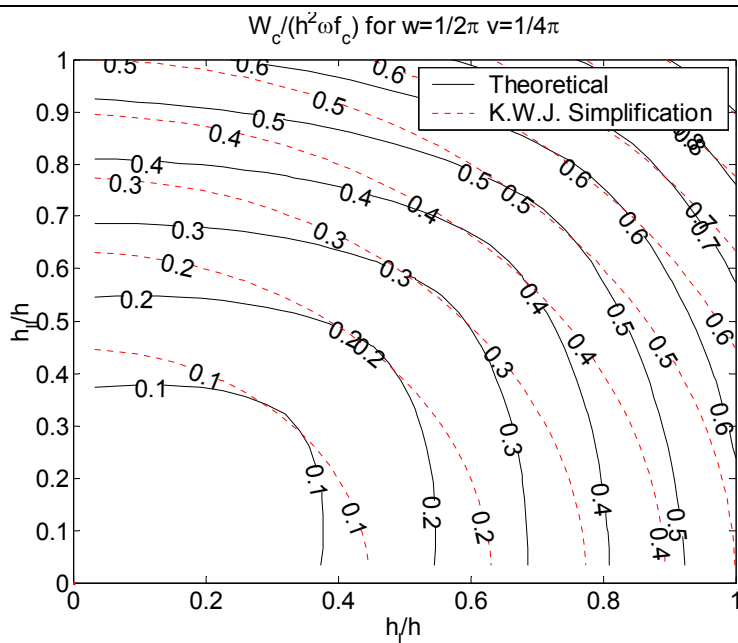
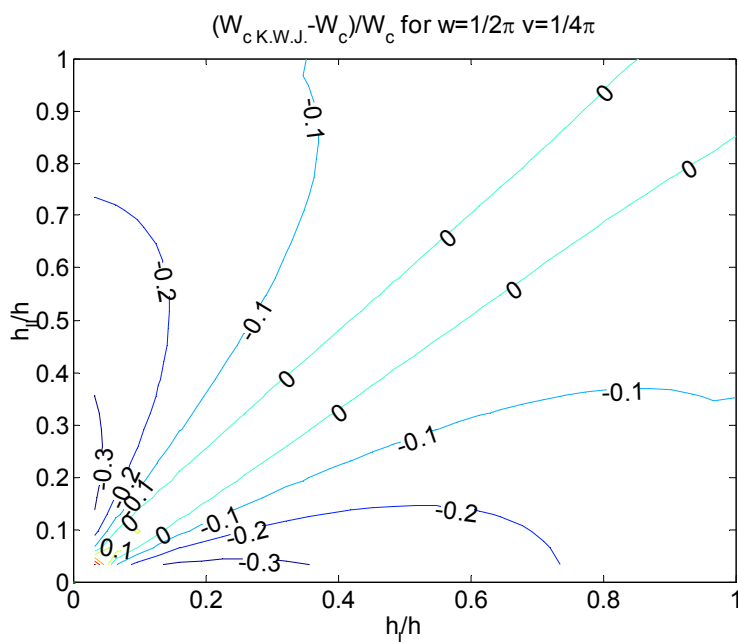*Figure 7.13 Contour plot of the dimensionless dissipation contribution from the concrete*

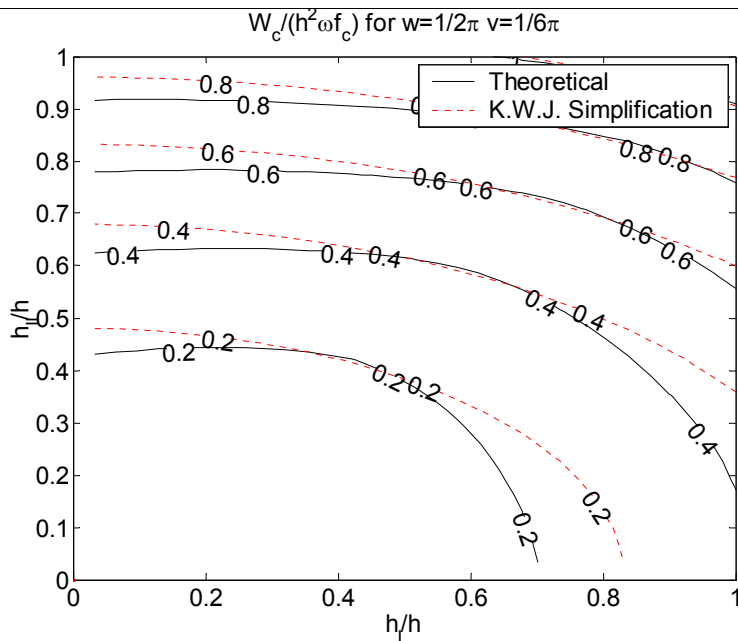*Figure 7.14. Deviation plot for the two calculation methods.*

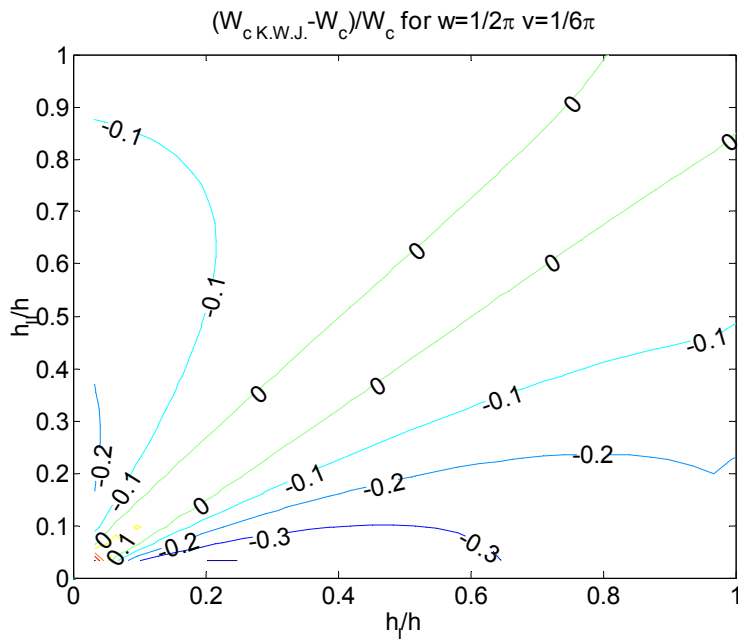Figure 7.15 Contour plot of the dimensionless dissipation contribution from the concrete

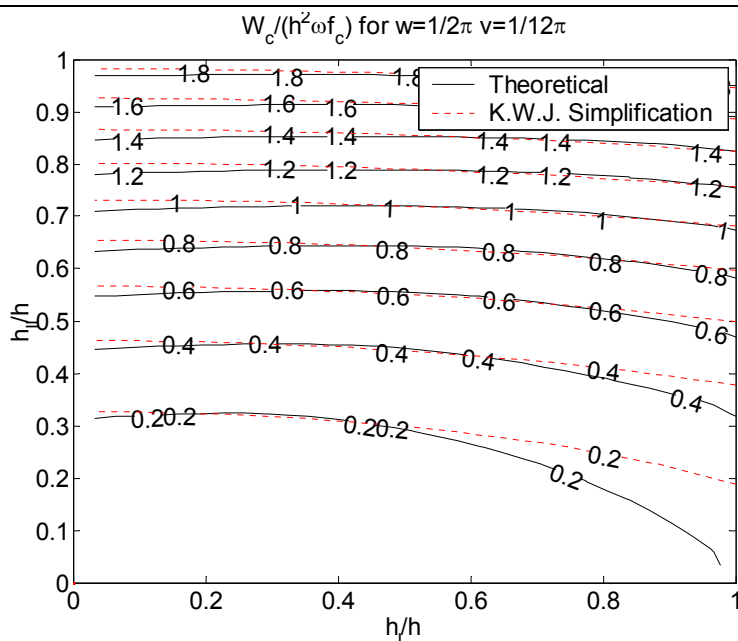Figure 7.16. Deviation plot for the two calculation methods.

Figure 7.17 Contour plot of the dimensionless dissipation contribution from the concrete
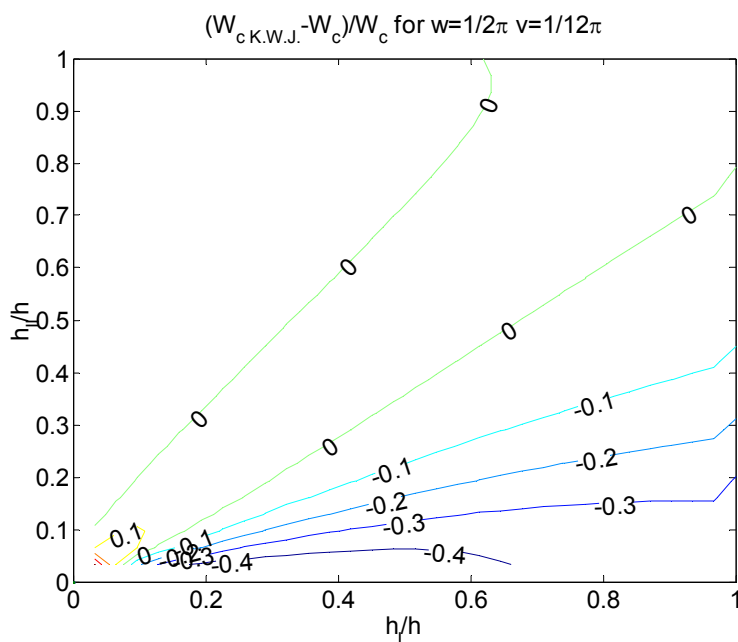

Figure 7.18. Deviation plot for the two calculation methods.

It appears that the simplification underestimates the dissipation if $w=1/2\pi$. The underestimation is large where the difference between h_I/h and h_{II}/h is large. Furthermore, it also appears that an increasing difference between v and $\pi/4$ leads to a larger underestimation.

The influence of w has also been studied and the following conclusions may be made:

If w is larger than $1/2\pi$ the simplification underestimates the dissipation as seen in Figure 7.19 to Figure 7.20

If w is less than $1/2\pi$ the simplification overestimates the dissipation as seen in Figure 7.21 to Figure 7.24.

If w is very small the overestimation becomes quite significant as seen in Figure 7.25 and Figure 7.26.

These figures (Figure 7.19 to Figure 7.26) are illustrative representations of the different situations where w is larger or smaller than $1/2\pi$.
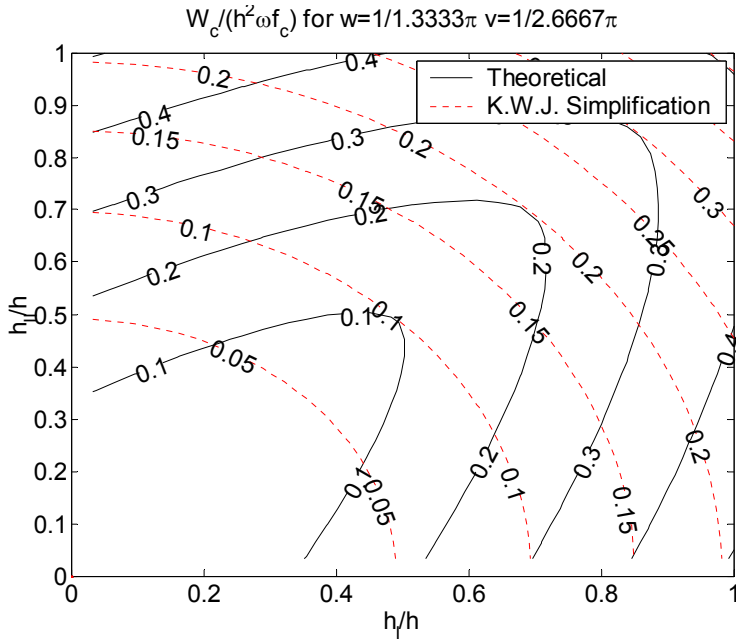

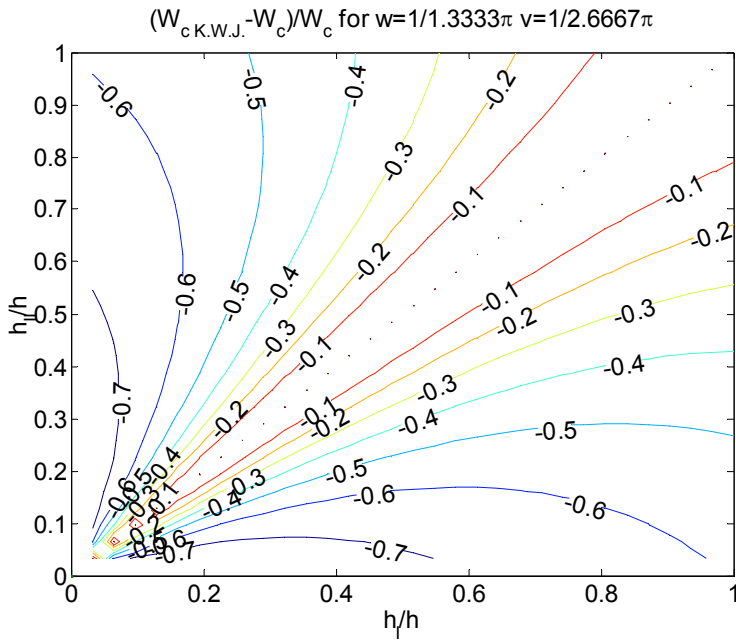*Figure 7.19 Contour plot of the dimensionless dissipation contribution from the concrete*

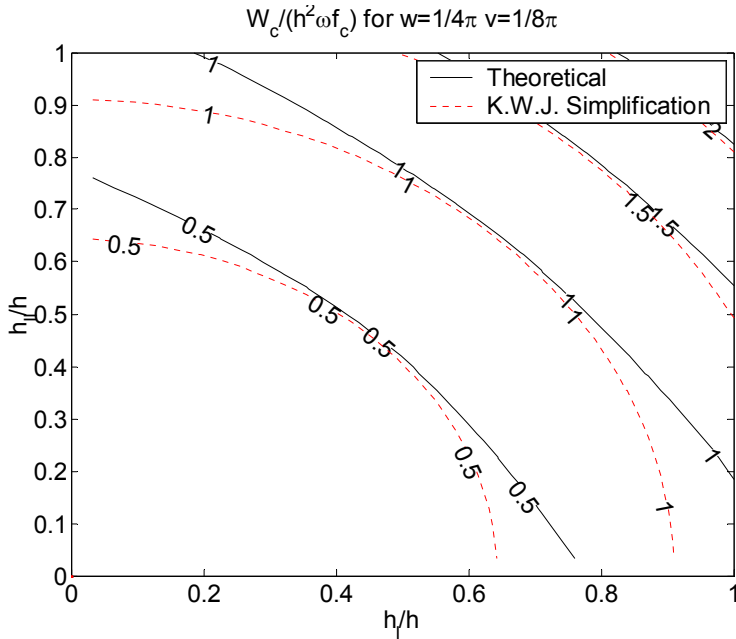*Figure 7.20. Deviation plot for the two calculation methods.*

Figure 7.21 Contour plot of the dimensionless dissipation contribution from the concrete
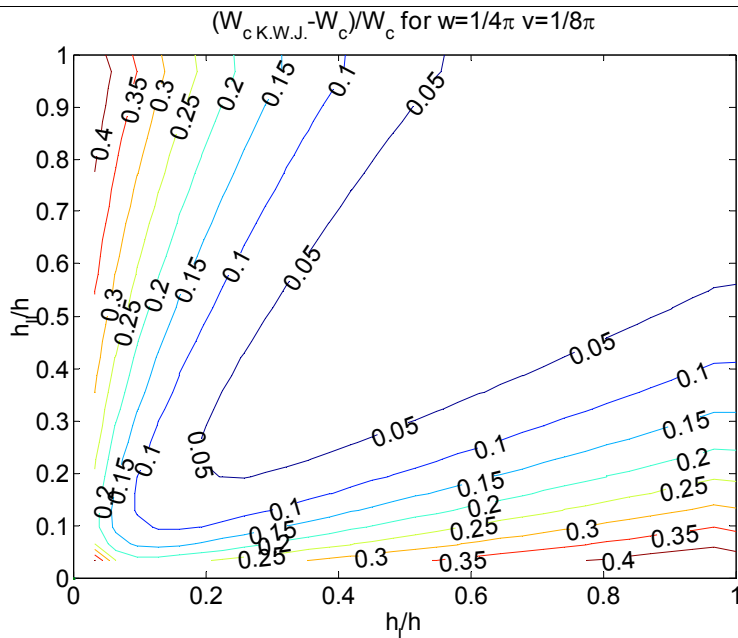
Figure 7.22. Deviation plot for the two calculation methods.
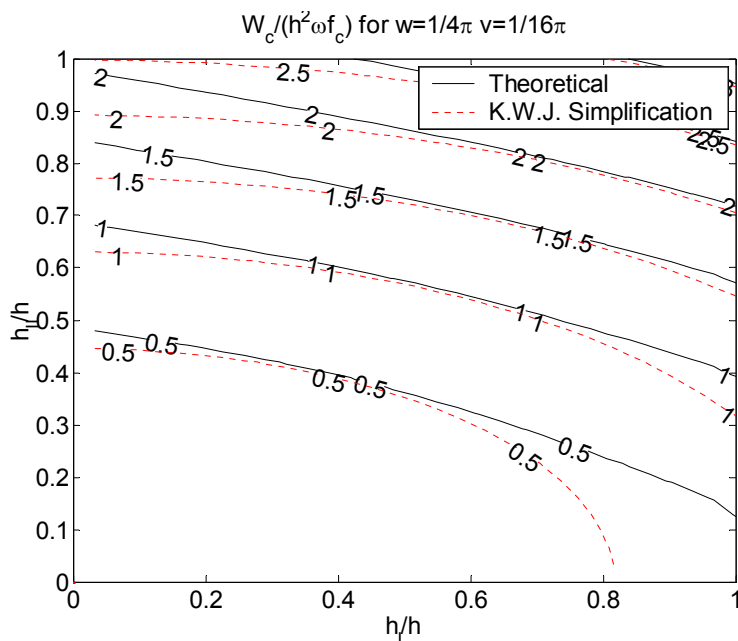

Figure 7.23 Contour plot of the dimensionless dissipation contribution from the concrete
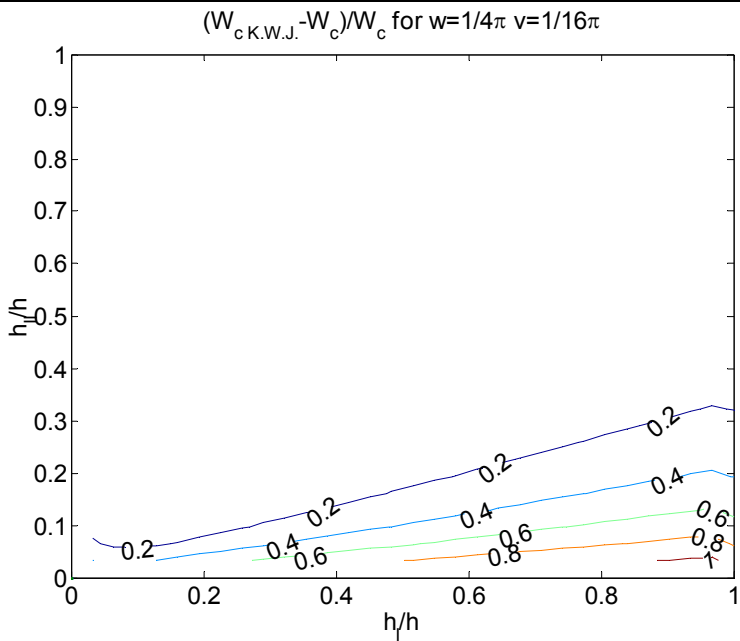
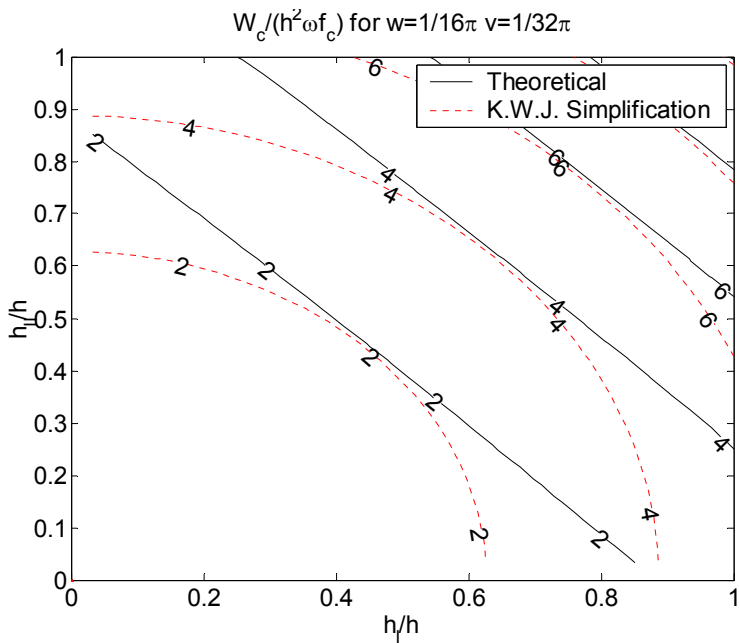*Figure 7.24. Deviation plot for the two calculation methods.*

Figure 7.25 Contour plot of the dimensionless dissipation contribution from the concrete

Figure 7.26. Deviation plot for the two calculation methods.

It appears that the formula proposed by K. W. Johansen is not accurate if *w* derivates significantly from π/2. However, this does not necessarily mean that this way of calculating leads to a similar over- and underestimations when calculating the load-carrying capacity of a slab since concrete dissipation is only a part of the dissipation.

One of the most common situations is a yield line starting from a right-angled corner and the formulas for this particular situation is therefore found. In these cases the following formula is valid:

$$\frac{W_c}{h^2 \omega f_c} = \frac{1}{4\sin(v)\cos(v)} \cdot$$

$$\begin{pmatrix} -1 + \left(2 + \sqrt{\left(\frac{h_1}{h}\right)^2 \sin(v)^2 + \left(\frac{h_2}{h}\right)^2 \cos(v)^2}\right)\left(\frac{h_1}{h}\sin(v)^2 + \frac{h_2}{h}\cos(v)^2\right) \\ + \sqrt{1 + \left(\left(\frac{h_2}{h}\right)^2 - 2\frac{h_2}{h}\right)\cos(v)^2 + \left(+\left(\frac{h_1}{h}\right)^2 - 2\frac{h_1}{h}\right)\sin(v)^2}\left(1 - \frac{h_1}{h}\sin(v)^2 - \frac{h_2}{h}\cos(v)^2\right) \\ + \log\left(\frac{-\frac{h_1}{h}\sin(v)^2 - \frac{h_2}{h}\cos(v)^2 + \sqrt{\left(\frac{h_1}{h}\right)^2 \sin(v)^2 + \left(\frac{h_2}{h}\right)^2 \cos(v)^2}}{1 - \frac{h_1}{h}\sin(v)^2 - \frac{h_2}{h}\cos(v)^2 + \sqrt{1 + \left(\left(\frac{h_2}{h}\right)^2 - 2\frac{h_2}{h}\right)\cos(v)^2 + \left(+\left(\frac{h_1}{h}\right)^2 - 2\frac{h_1}{h}\right)\sin(v)^2}}\right) \\ \cdot \left(\left(2\frac{h_1}{h}\frac{h_2}{h} - \left(\frac{h_1}{h}\right)^2 - \left(\frac{h_2}{h}\right)^2\right)\left(\cos(v)^2 - \cos(v)^4\right)\right) \end{pmatrix}$$

$$(7.23)$$

The formula for the simplified calculation becomes:

$$\frac{W_{c\_K.W.J}}{h^2 \omega f_c} = \left(\frac{1}{2}\left(\frac{h_I}{h}\right)^2 \tan(v) + \frac{1}{2}\left(\frac{h_{II}}{h}\right)^2 \frac{1}{\tan(v)}\right) \tag{7.24}$$

7.1.2 The contribution from the reinforcement

If the reinforcement is placed in a direction perpendicular to the axis of rotation at a distance from the slab surface as shown in Figure 7.27 the contribution from the reinforcement to the dissipation per unit length becomes:

$$W_s = \omega_1 \cos(w-v)\left(A_{s,I}|h - h_{cI} - h_I| + A_{s,I}'|h_I - h_{cI}'|\right) + \\ \omega_2 \cos(v)\left(A_{s,II}|h - h_{cII} - h_{II}| + A_{s,II}'|h_{II} - h_{cII}'|\right) \tag{7.25}$$

where ω_I and ω_{II} are the rotations about axis I and II, respectively. These are determined in (7.11) and the expression may be written as:

$$\frac{W_s}{\omega h^2 f_c} = \frac{1}{\tan(w-v)}\left(\Phi_{0,I}\left|1 - \frac{h_{cI}}{h} - \frac{h_I}{h}\right| + \Phi_{0,I}'\left|\frac{h_I}{h} - \frac{h_{cI}'}{h}\right|\right) + \\ \frac{1}{\tan(v)}\left(\Phi_{0,II}\left|1 - \frac{h_{cII}}{h} - \frac{h_{II}}{h}\right| + \Phi_{0,II}'\left|\frac{h_{II}}{h} - \frac{h_{cII}'}{h}\right|\right) \tag{7.26}$$
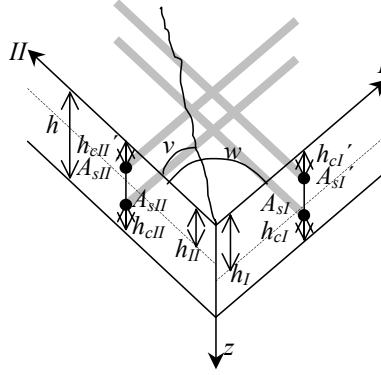
Figure 7.27. Reinforcement arrangement

If the corner is right-angled the dissipation becomes:

$$
\begin{aligned}
\frac{W_s}{\omega h^2 f_c} = \tan(v) & \left(\Phi_{0,I} \left| 1 - \frac{h_{cI}}{h} - \frac{h_I}{h} \right| + \Phi_{0,I}{}' \left| \frac{h_I}{h} - \frac{h_{cI}{}'}{h} \right| \right) + \\
\frac{1}{\tan(v)} & \left(\Phi_{0,II} \left| 1 - \frac{h_{cII}}{h} - \frac{h_{II}}{h} \right| + \Phi_{0,II}{}' \left| \frac{h_{II}}{h} - \frac{h_{cII}{}'}{h} \right| \right)
\end{aligned}
\tag{7.27}
$$

7.2 Beam example

For slabs the position of the axes of rotation are not always easily found. An exact analysis for a slab is impossible since no correct analytical expression may be found for the dissipation. Therefore, a numerical investigation has to be made in each situation.

However, it may be assumed that the axes of rotation must be placed at the same position as the neutral axis. For a beam this assumption may be shown to be correct and is therefore worth studying first.

For all combinations of transverse loads, the load-carrying capacity always depends on the dissipation for a unit rotation $\omega = 1$ in the yield line. Therefore, it is sufficient to find the minimum dissipation in order to find the minimum load-carrying capacity.
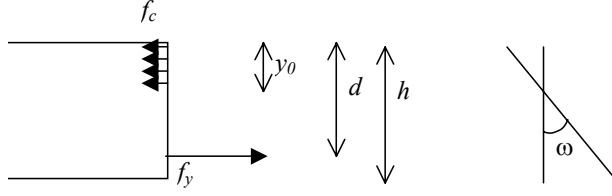
Figure 7.28 Stresses in a beam.

Considering the beam in Figure 7.28 it is seen that the position of the neutral axis may be found from a projection equation as:

$$A_s f_y = b y_0 f_c$$
$$\Phi_0 h f_c b = b y_0 f_c$$
$$y_0 = \Phi_0 h$$

(7.28)

where

$$\Phi_0 = \frac{A_s f_y}{b h f_c}$$

(7.29)

The yield moment becomes

$$M_p = \frac{1}{2} y_0 f_c b \left(d - \frac{1}{2} y_0 \right) \Rightarrow$$
$$M_p = \frac{1}{2} \Phi_0 h^2 f_c b \left(\frac{d}{h} - \frac{1}{2} \Phi_0 \right)$$

(7.30)

An upper bound approach leads to the following result:

$$W = \int_0^h \frac{1}{2} f_c b u \left(1 - \sin(\alpha) \right) dz + A_s f_y \omega (d - y_0) \Leftrightarrow$$
$$W = \frac{1}{2} f_c b \frac{1}{2} y_0 \omega y_0 (2) + \Phi_0 h f_c b \omega (d - y_0) \Leftrightarrow$$
$$W = \frac{1}{2} f_c b \omega y_0^2 - \Phi_0 h f_c b \omega y_0 + \Phi_0 h f_c b \omega d \Leftrightarrow$$
$$\frac{dW}{dy_0} = f_c b \omega y_0 - \Phi_0 h f_c b \omega$$

(7.31)

$$\frac{dW}{dy_0} = 0 \Leftrightarrow y_0 = \Phi_0 h$$

(7.32)

As seen, the minimum load-carrying capacity is found where the position of the axis of rotation equals the position of the neutral axis. Furthermore, it is seen that the dissipation found by the upper bound approach is the same as the yield moment times the rotation.

Similarly it may be shown that this assumption is valid if both top reinforcement and bottom reinforcement are included. Furthermore, it may also be shown that the assumption is valid if an axial force is applied. In these situations the dissipation plus the work caused by the dissipation of the axial force equals the yield moment (including the contribution from the axial force) times the rotation.
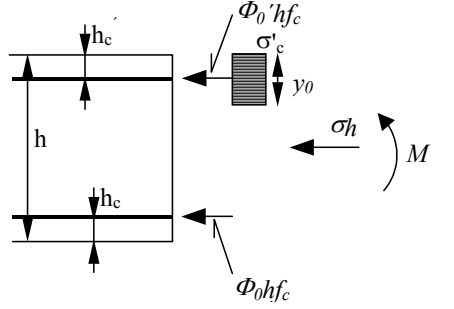

Figure 7.29. Beam with axial force.

For the reinforced beam illustrated in Figure 7.29 the position of the neutral axis may be calculated as:

For $0 \leq \dfrac{\sigma}{fc} \leq \dfrac{h_c{}'}{h} - \Phi_0 - \Phi_0{}'$

$$\frac{y_0}{h} = \frac{\sigma}{fc} + \Phi_0 + \Phi_0{}' \qquad (7.33)$$

For $\dfrac{h_c{}'}{h} - \Phi_0 - \Phi_0{}' \leq \dfrac{\sigma}{fc} \leq \dfrac{h_c{}'}{h} - \Phi_0 + \Phi_0{}'$

$$\frac{y_0}{h} = \frac{h_c}{h} \qquad (7.34)$$

For $\dfrac{h_c{}'}{h} - \Phi_0 + \Phi_0{}' \leq \dfrac{\sigma}{fc} \leq \dfrac{h - h_c}{h} - \Phi_0 + \Phi_0{}'$

$$\frac{y_0}{h} = \frac{\sigma}{fc} + \Phi_0 - \Phi_0{}' \qquad (7.35)$$

For $\dfrac{h - h_c}{h} - \Phi_0 + \Phi_0{}' \leq \dfrac{\sigma}{fc} \leq \dfrac{h - h_c}{h} + \Phi_0 + \Phi_0{}'$

$$\frac{y_0}{h} = \frac{h - h_c}{h} \qquad (7.36)$$

For $\dfrac{h - h_c}{h} + \Phi_0 + \Phi_0{}' \leq \dfrac{\sigma}{fc} \leq 1 + \Phi_0 + \Phi_0{}'$

$$\frac{y_0}{h} = \frac{\sigma}{fc} - \Phi_0 - \Phi_0{}' \qquad (7.37)$$

Knowing the position of the axis of rotation the dissipation per unit length may be calculated as:

$$\frac{W}{h^2 \omega f_c} = \frac{1}{2}\left(\frac{y_0}{h}\right)^2 + \Phi_0 \left|\left(1 - \frac{h_c}{h}\right) - \frac{y_0}{h}\right| + \Phi_0' \left|\frac{h_c'}{h} - \frac{y_0}{h}\right| \tag{7.38}$$

It appears that since the assumption about the neutral axis being the axis of rotation is valid the dissipation may be calculated quite easily for a beam.

7.3 Square slab without axial force

For slabs in general the assumption about the neutral axes being the axes of rotation can not be shown analytically.

In the following examples the results of numerical calculations will be evaluated both regarding the assumption about the axes of rotation and the error made using K. W. Johansen's simplification.

Considering a uniformly laterally loaded isotropic square slab with the same amount of reinforcement in the top and bottom and simply supported along all four edges, it is known (see [5]) that the exact solution is:

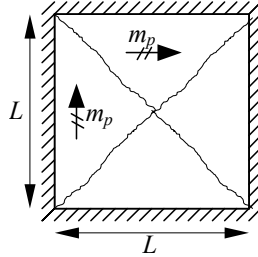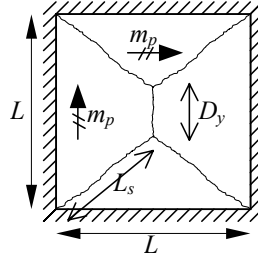$$q_{\text{Prager}} = \frac{24 m_p}{L^2} \tag{7.39}$$

Figure 7.30. Prager's exact solution for a square slab

If it is assumed that the failure mode in Figure 7.31 is the one that will occur the load-carrying capacity found from the above dissipation formulas is as follows:

Failure mode 1

Figure 7.31. Failure mode 1 for square slab.

Failure mode 1:

The external work becomes:

$$W_e = \delta q \left(\frac{1}{2} D_y L + \frac{1}{3}\left(L - D_y\right)L \right) \tag{7.40}$$

The dissipation becomes:

$$W_i = 4L_s \frac{\delta}{L_s}\left(\frac{W_{c,v}}{h^2 \omega f_c} + \frac{W_{s,v}}{h^2 \omega f_c} \right)h^2 f_c + D_y \frac{\delta}{\dfrac{L}{2}} 2\left(\frac{W_{c,0}}{h^2 \omega f_c} + \frac{W_{s,0}}{h^2 \omega f_c} \right)h^2 f_c \tag{7.41}$$

The work equation leads to:

$$q_1 = \frac{24 f_c h^2 \left(L\left(\dfrac{W_{c,v}}{h^2 \omega f_c} + \dfrac{W_{s,v}}{h^2 \omega f_c} \right) + D_y \left(\dfrac{W_{c,0}}{h^2 \omega f_c} + \dfrac{W_{s,0}}{h^2 \omega f_c} \right) \right)}{\left(D_y + 2L\right)L^2} \tag{7.42}$$

Here $W_{c,v}$ and $W_{s,v}$ are the contributions to the dissipation per unit length for the yield line (L_s) from the concrete and reinforcement, respectively. Similarly, $W_{c,0}$ and $W_{s,0}$ are the contributions to the dissipation per unit length for the yield line (D_y) from the concrete and reinforcement, respectively.

Calculating all possible combinations of the positions of the two axes of rotation and plotting the lowest load-carrying capacity for a given D_y leads to the results shown in Figure 7.32 and Figure 7.33.
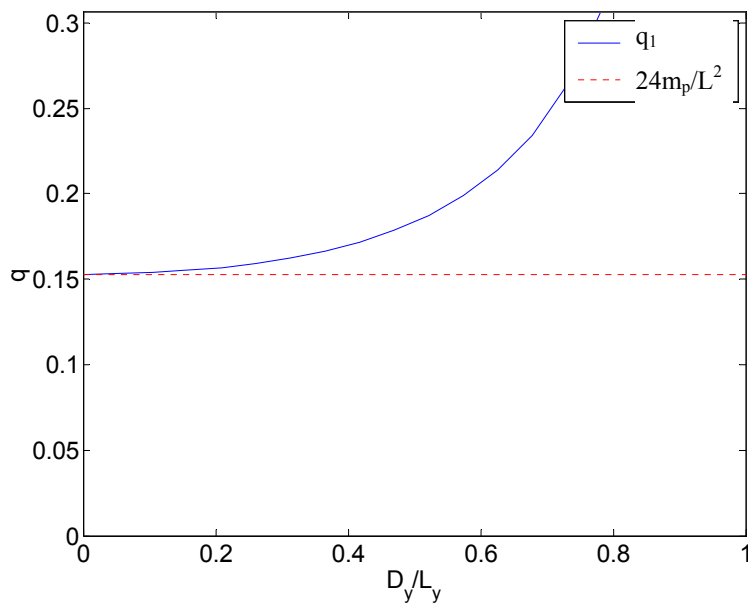
Figure 7.32. Load-carrying capacity q_1 for a square slab with L=2000mm, $\Phi_0=\Phi_0{'}=0.1$, $h_c/h= h_c{'}/h=0.1$, $f_c=30MPa$ (solid) and load-carrying capacity according to (7.39) (dashed).

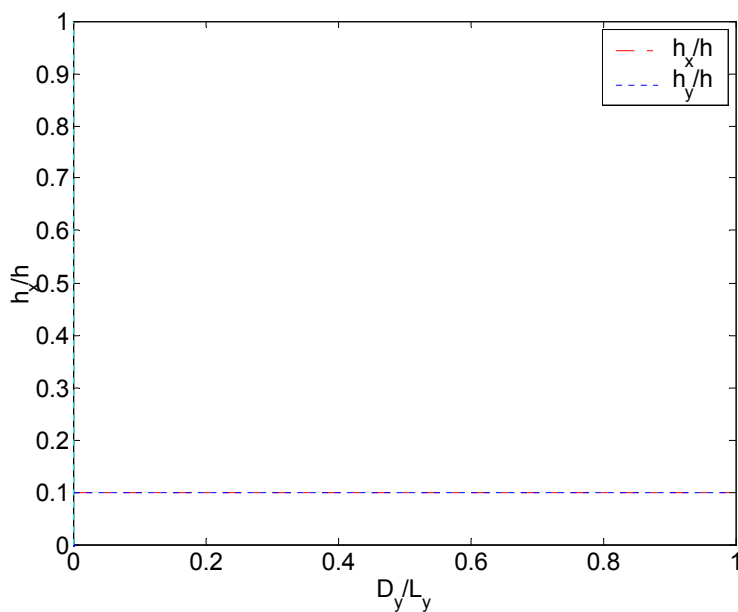*Figure 7.33 Position of the axes of rotation for a square slab with L=2000mm, $\Phi_0=\Phi_0{'}=0.1$, $h_c/h= h_c{'}/h=0.1$, $f_c=30MPa$.*

The yield moment m_p used in these calculations is calculated as described in [5] (having $h_c/h = h_c'/h$):

$$\mu = \frac{\Phi_0'}{\Phi_0} \tag{7.43}$$

For $\mu \geq 1 - \frac{1}{\Phi_0}\frac{h_c}{h}$ and $\Phi_0 \leq \frac{1}{1+\mu}\frac{h_c}{h}$

$$m_p = \left(1 - 2\frac{h_c}{h} + (1+\mu)\left(\frac{h_c}{h} - \frac{1}{2}\Phi_0(1+\mu)\right)\right)\Phi_0 h^2 f_c \tag{7.44}$$

For $\mu \geq 1 - \frac{1}{\Phi_0}\frac{h_c}{h}$ and $\Phi_0 \geq \frac{1}{1+\mu}\frac{h_c}{h}$

$$m_p = \left(1 - 2\frac{h_c}{h} + \frac{1}{2}\frac{1}{\Phi_0}\left(\frac{h_c}{h}\right)^2\right)\Phi_0 h^2 f_c \tag{7.45}$$

For $\mu < 1 - \frac{1}{\Phi_0}\frac{h_c}{h}$

$$m_p = \left(1 - 2\frac{h_c}{h} + (1-\mu)\left(\frac{h_c}{h} - \frac{1}{2}\Phi_0(1-\mu)\right)\right)\Phi_0 h^2 f_c \tag{7.46}$$

From Figure 7.32 it appears that the numerical calculations using the dissipation formulas above leads to the same solution as the one found using the yield condition for the slab when $D_y=0$. Furthermore, Figure 7.33 shows that the axes of rotation are at the same depth and this depth corresponds to the neutral axes. More plots for different degrees of reinforcement and different values of h_c/h are shown in section 11.1.1.1.

For isotropic square slabs it may be concluded that the position of the axes of rotation corresponds to the neutral axes and that the load-carrying capacity found from the above dissipation formulas corresponds to the exact solutions found from the yield conditions.

7.3.1.1   Rectangular slabs

For rectangular slabs the failure modes assumed in this paper are illustrated in Figure 7.34 (Ingerslev´s solutions). These failure modes are not always exact solutions to the problem. However, it is believed that the results are close to the exact solution and therefore acceptable.
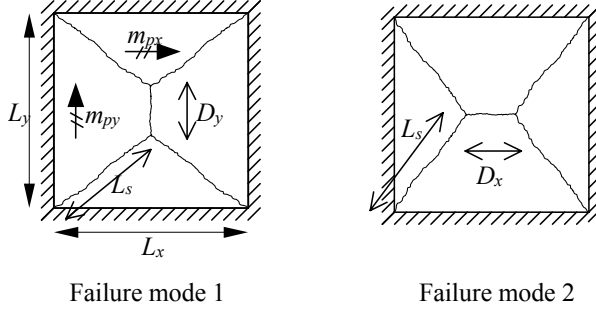
Failure mode 1   Failure mode 2

Figure 7.34. Failure modes.

An upper bound solution leads to the following load-carrying capacity for a uniformly loaded slab:

$$\mu_m = \frac{m_{py}}{m_{px}} \tag{7.47}$$

For $L_y \geq \dfrac{L_x}{\sqrt{\mu_m}}$

$$q_{\text{Ingerslev}} = \frac{24\mu_m m_{px}}{L_x^{\,2}\left(\sqrt{3+\dfrac{1}{\mu_m}\left(\dfrac{L_x}{L_y}\right)^2}-\dfrac{1}{\sqrt{\mu_m}}\dfrac{L_x}{L_y}\right)^2} \tag{7.48}$$

and

$$\frac{D_y}{L_y} = 1 - \frac{L_y}{\sqrt{\mu_m}L_x}\left(-\frac{L_y}{\sqrt{\mu_m}L_x}+\sqrt{3+\left(\frac{L_y}{\sqrt{\mu_m}L_x}\right)^2}\right) \tag{7.49}$$

For $L_y \leq \dfrac{L_x}{\sqrt{\mu_m}}$

$$q_{\text{Ingerslev}} = \frac{24 m_{px}}{L_y^{\,2}\left(\sqrt{3+\mu_m\left(\dfrac{L_y}{L_x}\right)^2}-\sqrt{\mu_m}\dfrac{L_y}{L_x}\right)^2} \tag{7.50}$$

and

$$\frac{D_x}{L_x} = 1 - \frac{\sqrt{\mu_m}L_y}{L_x}\left(-\frac{\sqrt{\mu_m}L_y}{L_x}+\sqrt{3+\left(\frac{\sqrt{\mu_m}L_y}{L_x}\right)^2}\right) \tag{7.51}$$

Formula (7.48) corresponds to failure mode 1 and (7.50) to failure mode 2. The yield moments m_{px} and m_{py} are calculated from cross-section analyses perpendicular to the x-axis and the y-axis, respectively.

For the two failure modes the equations according to the dissipation formulas becomes:

Failure mode 1:

The internal work becomes:

$$W_e = \delta q \left(\frac{1}{2} D_y L_x + \frac{1}{3} \left(L_y - D_y \right) L_x \right) \tag{7.52}$$

The external work becomes:

$$W_e = 4 L_s \frac{\delta}{L_s} \left(\frac{W_{c,v}}{h^2 \omega f_c} + \frac{W_{s,v}}{h^2 \omega f_c} \right) h^2 f_c + D_y \frac{\delta}{\frac{L_x}{2}} 2 \left(\frac{W_{c,0}}{h^2 \omega f_c} + \frac{W_{s,0}}{h^2 \omega f_c} \right) h^2 f_c \tag{7.53}$$

The work equation leads to:

$$q_1 = \frac{\frac{6 f_c h^2}{L_y^2} \left(4 \left(\frac{D_y}{L_y} - 1 \right) \left(\frac{L_x}{L_y} \left(\frac{W_{c,v}}{h^2 \omega f_c} + \frac{W_{s,v}}{h^2 \omega f_c} \right) + \frac{D_y}{L_y} \left(\frac{W_{c,0}}{h^2 \omega f_c} + \frac{W_{s,0}}{h^2 \omega f_c} \right) \right) \right)}{\left(\frac{L_x}{L_y} \right)^2 \left(\frac{D_y}{L_y} - 1 \right) \left(\frac{D_y}{L_y} + 2 \right)} \tag{7.54}$$

where $W_{c,v}$ and $W_{s,v}$ are the contributions to the dissipation per unit length for the yield line (L_s) from concrete and reinforcement, respectively. Similarly, $W_{c,0}$ and $W_{s,0}$ are the contributions to the dissipation per unit length for the yield line (D_y) from concrete and reinforcement, respectively.

The work equation for failure mode 2 leads to load-carrying capacity:

$$q_2 = \frac{\frac{6 f_c h^2}{L_x^2} \left(4 \left(\frac{D_x}{L_x} - 1 \right) \left(\frac{L_y}{L_x} \left(\frac{W_{c,v}}{h^2 \omega f_c} + \frac{W_{s,v}}{h^2 \omega f_c} \right) + \frac{D_x}{L_x} \left(\frac{W_{c,0}}{h^2 \omega f_c} + \frac{W_{s,0}}{h^2 \omega f_c} \right) \right) \right)}{\left(\frac{L_y}{L_x} \right)^2 \left(\frac{D_x}{L_x} - 1 \right) \left(\frac{D_x}{L_x} + 2 \right)} \tag{7.55}$$

Calculating all the possible combinations of the position of the two axes of rotation and plotting the lowest load-carrying capacity for a given D_y lead to the results shown in Figure 7.35.
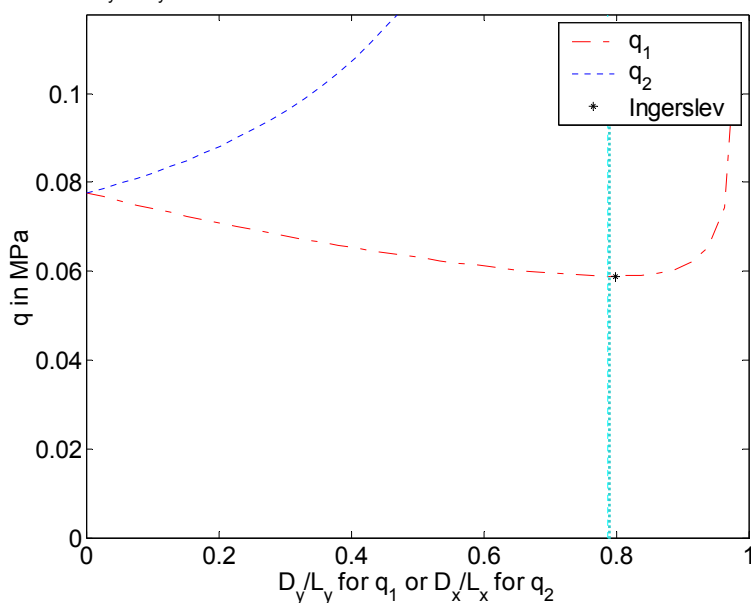
Figure 7.35. Load-carrying capacity q_1 and q_2 ,according to (7.54) (dashed dotted) and (7.55) (dotted), for a rectangular slab with $L_x=2000mm$, $L_y=16000mm$, $\Phi_0=\Phi_0{'}=0.1$, $h_c/h= h_c{'}/h=0.1$, $f_c=30MPa$ and load-carrying capacity according to (7.48) or (7.50) (*).The vertical line indicates the minium for the numerical calculculations.
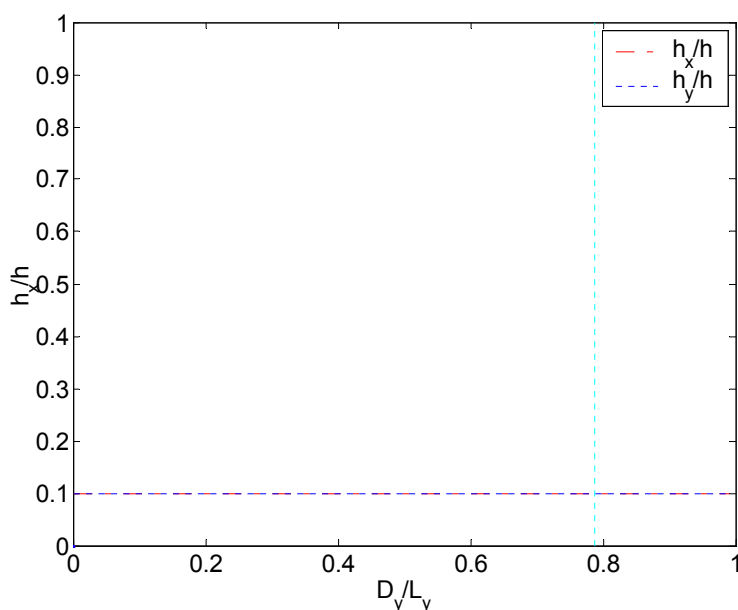

Figure 7.36 Position of the axes of rotation for a rectangular slab with $L_x=2000mm$, $L_y=16000mm$, $\Phi_0=\Phi_0{'}=0.1$, $h_c/h= h_c{'}/h=0.1$, $f_c=30MPa$.

Apparently, the assumption about the neutral axes being the axes of rotation is correct and this may also be shown for isotropic slabs. Nevertheless, as shown in Figure 7.38, the assumption is not always correct. Numerical calculations show that the assumption is incorrect if the slab is orthotropic. In Figure 7.38 it is seen that the minimum load-carrying capacity is found where the axes of rotation are at positions $0.14\ h_x/h$ and $0.1\ h_y/h$ in a slab with the reinforcement degrees $\Phi_{0x}=\Phi_{0x}{}'=0.1$ and $\Phi_{0y}=\Phi_{0y}{}'=0.05$ and not at $0.2\ h_x/h$ and $0.1\ h_y/h$ as expected. However, the minima of these curves are very flat as seen in Figure 7.39 where the load-carrying capacity is plotted as a function of the position of the axis of rotation in the x direction.
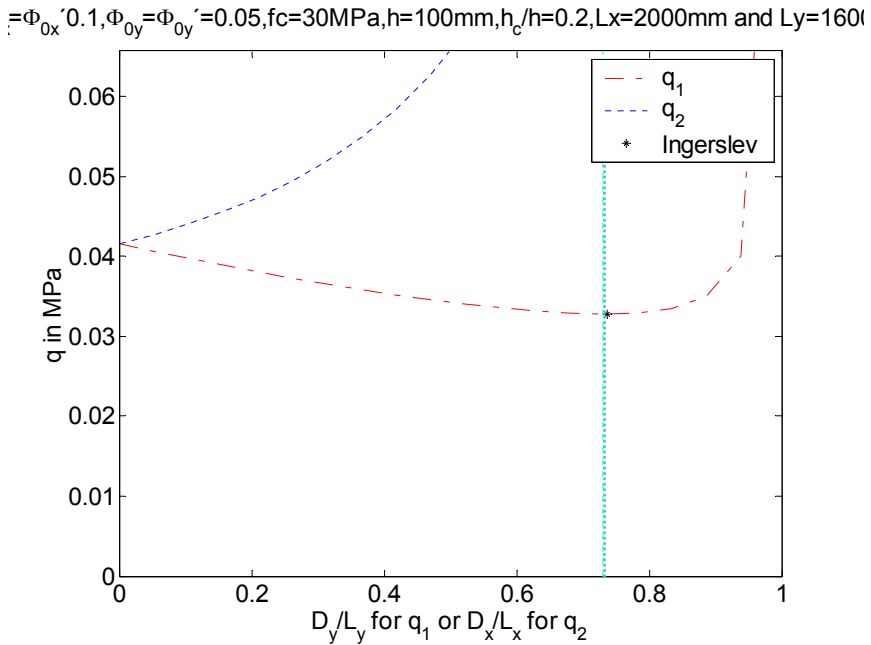

Figure 7.37. Load-carrying capacity q_1 and q_2, according to (7.54) (dashed dotted) and (7.55) (dotted), for a square slab $L_x=2000mm$, $L_y=16000mm$, $\Phi_{0x}=\Phi_{0x}{}'=0.1$, $\Phi_{0y}=\Phi_{0y}{}'=0.05$, $h_{cx}/h=h_{cx}{}'/h=h_{cy}/h=h_{cy}{}'/h=0.2$, $f_c=30MPa$ and load-carrying capacity according to (7.48) or (7.50) (*).
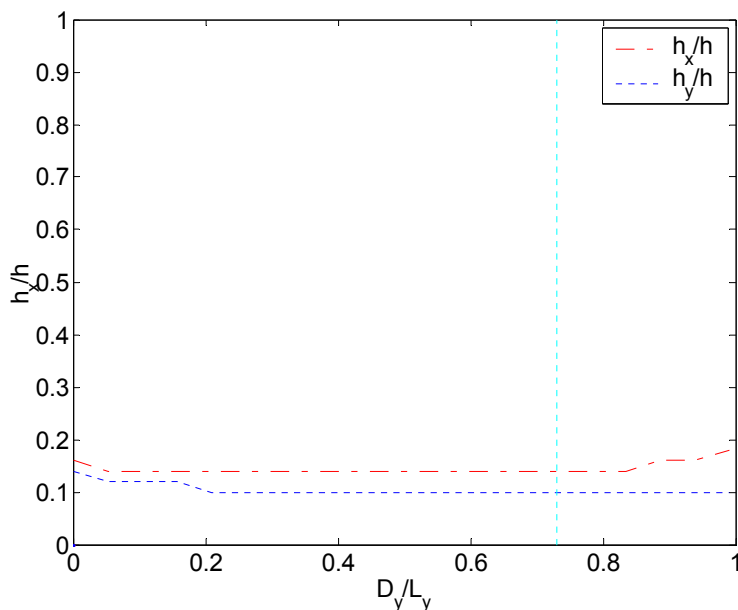
Figure 7.38 Position of the axes of rotation for a rectangular slab $L_x=2000mm$, $L_y=16000mm$, $\Phi_{0x}=\Phi_{0x}'=0.1$, $\Phi_{0y}=\Phi_{0y}'=0.05$, $h_{cx}/h= h_{cx}'/h= h_{cy}/h= h_{cy}'/h=0.2$, $f_c=30MPa$.
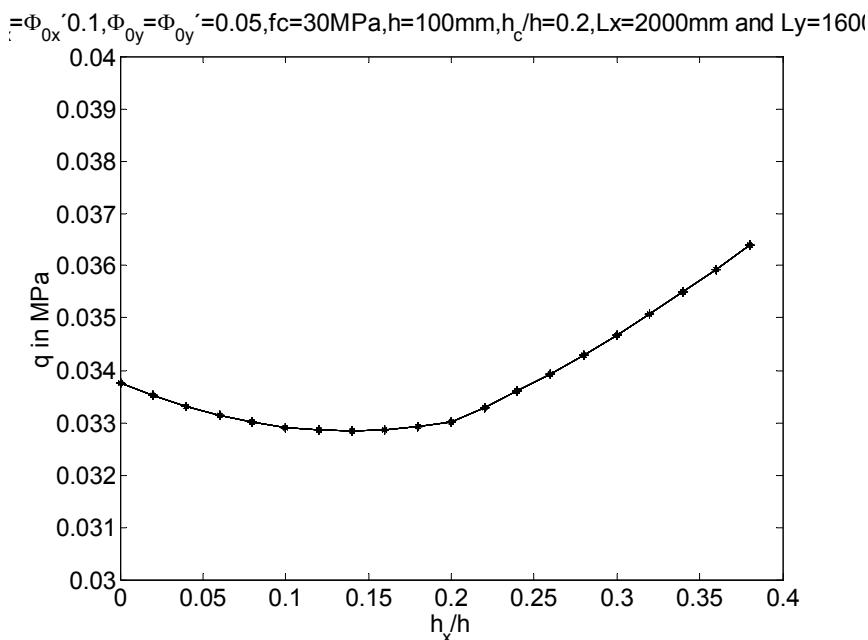

Figure 7.39 Load-carrying capacity as a function of the position of the axis of rotation in the x direction for a rectangular slab $L_x=2000mm$, $L_y=16000mm$, $\Phi_{0x}=\Phi_{0x}'=0.1$, $\Phi_{0y}=\Phi_{0y}'=0.05$, $h_{cx}/h= h_{cx}'/h= h_{cy}/h= h_{cy}'/h=0.2$, $f_c=30MPa$, $D_y/L_y=0.73$, $h_y/h=0.1$.

If the slab is reinforced in the top and bottom and $\Phi_0 + \Phi_0' > h_c'/h$ the axis of rotation will be at the neutral axis (assuming $\Phi_0 = \Phi_0'$). If $\Phi_0 + \Phi_0' < h_c'/h$ the assumption is incorrect but the error made by such assumption is negligible.

If the slab is not reinforced in the top the assumption is incorrect and the error may become noticeable. This is illustrated in Figure 7.40 and Figure 7.41 where the positions of the axes of rotation for a slab with $\Phi_{0y}' = \Phi_{0x}' = 0$, $\Phi_{0x} = 0.7$ and $\Phi_{0y} = 0.1$ are at $0.4 h_x/h$ and $0.1 h_y/h$, respectively. Even though the position of the axes of rotation is different in the two directions it is seen that the load-carrying capacity is only underestimated about 5% in this case.

$\Phi_{0x}' = \Phi_{0y}' = 0, \Phi_{0x} = 0.7, \Phi_{0y}' = 0.1, fc = 30MPa, h = 100mm, h_c/h = 0.1, Lx = 2000mm \text{ and } Ly = 16000mm$
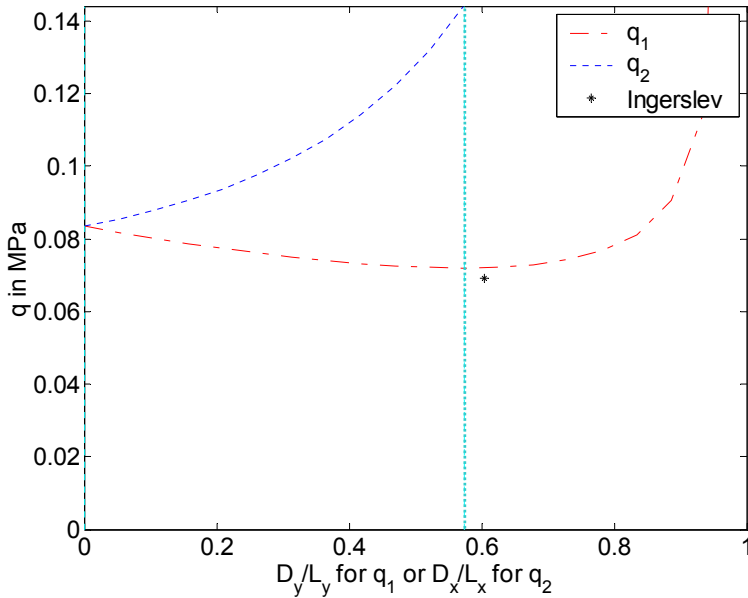
Figure 7.40. Load-carrying capacity q_1 and q_2, according to (7.54) (dashed dotted) and (7.55) (dotted), for a square slab $L_x = 2000mm$, $L_y = 16000mm$, $\Phi_{0x}' = \Phi_{0y}' = 0$, $\Phi_{0x} = 0.7$, $\Phi_{0y} = 0.1$, $h_{cx}/h = h_{cx}'/h = h_{cy}/h = h_{cy}'/h = 0.1$, $f_c = 30MPa$ and load-carrying capacity according to (7.48) or (7.50) (*).
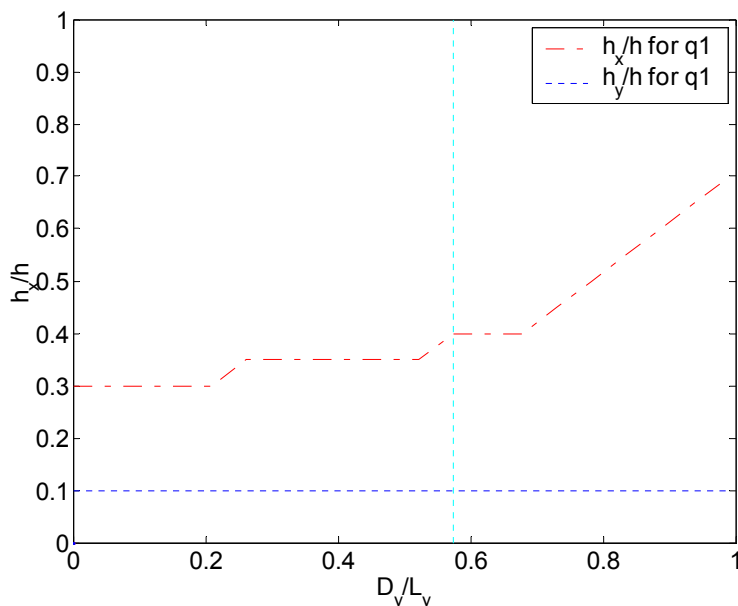
Figure 7.41 Position of the axes of rotation for a rectangular slab L_x=2000mm, L_y=16000mm, Φ_{0x}=Φ_{0x}'=0.7, Φ_{0y}=Φ_{0y}'=0.1, h_{cx}/h= h_{cx}'/h= h_{cy}/h= h_{cy}'/h=0.1, f_c=30MPa.

It is obvious that the error decreases for increasing difference between the two side lengths, since a larger difference leads to larger contribution from the yield line parallel to the supports (D_x or D_y) where the assumption is correct. In other words the slab starts to carry the load as a beam.
The fact that an increasing difference between the two degrees of reinforcement increases the error is also quite obvious. Therefore, in order to estimate the largest error a slab with the largest difference in the degrees of reinforcement and a side length ratio leading to almost no parallel parts of the yield line is considered. Setting Φ_{0y}'=Φ_{0x}'=0, Φ_{0x}=0.9 and Φ_{0y}=0.1 L_y/L_x=2.2 (see Figure 11.7) leads to an error of about 17%. However, such a degree of reinforcement is quite unrealistic. A realistic guess on the limits found in practice may be found for Φ_{0y}'=Φ_{0x}'=0, Φ_{0x}=0.3 and Φ_{0y}=0.05 L_y/L_x=2.2 (see Figure 11.8) which lead to an error less than 4%.
Keeping in mind that the assumption about the neutral axes being the axes of rotation leads to an underestimation of less than 4% for rectangular slabs, it is believed that the assumption may be acceptable for such slabs.

7.4 Rectangular slabs with axial force

For rectangular slabs with axial force the failure modes assumed are the same as for slabs without axial force. They are shown in Figure 7.42.
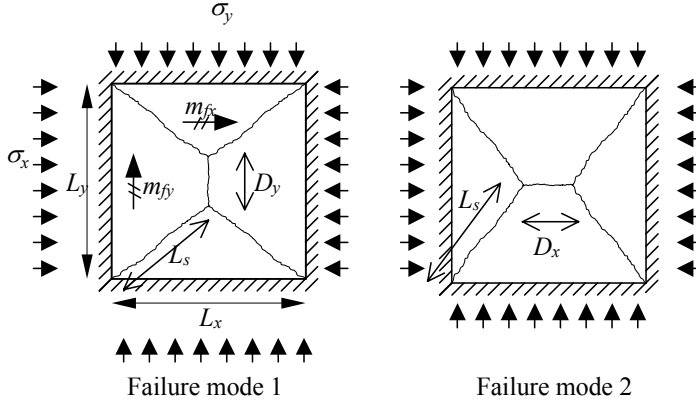

Failure mode 1   Failure mode 2

Figure 7.42. Failure modes for rectangular slabs with axial force.

An approximate solution to this problem is to calculate the yield moments in each direction including the axial force and then use these yield moments in Ingerslev´s solution. This calculation corresponds to the assumption about the neutral axes being the axes of rotation. The result is the same as if the dissipation is determined according to K. W. Johansen´s method for calculating the dissipation.
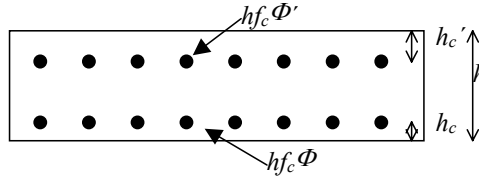

Figure 7.43. Cross section in a slab.

For the cross-section shown in Figure 7.43 the yield moments becomes:

For $0 \leq \dfrac{\sigma}{fc} \leq \dfrac{h_c{}'}{h} - \Phi_0 - \Phi_0{}'$

$$\frac{y_0}{h} = \frac{\sigma}{f_c} + \Phi_0 + \Phi_0{}' \tag{7.56}$$

$$m_p = h^2 f_c \left(\frac{1}{2} \frac{y_0}{h} \left(1 - \frac{y_0}{h}\right) + \Phi_0 \left(\frac{1}{2} - \frac{h_c}{h}\right) - \Phi_0{}' \left(\frac{1}{2} - \frac{h_c{}'}{h}\right) \right) \tag{7.57}$$

For $\dfrac{h_c{}'}{h} - \Phi_0 - \Phi_0{}' \le \dfrac{\sigma}{fc} \le \dfrac{h_c{}'}{h} - \Phi_0 + \Phi_0{}'$

$$\frac{y_0}{h} = \frac{h_c{}'}{h} \tag{7.58}$$

$$m_p = h^2 f_c \left(\frac{1}{2} \frac{y_0}{h} \left(1 - \frac{y_0}{h} \right) + \Phi_0 \left(\frac{1}{2} - \frac{h_c}{h} \right) - \left(\frac{y_0}{h} - \frac{\sigma}{f_c} - \Phi_0 \right) \left(\frac{1}{2} - \frac{h_c{}'}{h} \right) \right) \tag{7.59}$$

For $\dfrac{h_c{}'}{h} - \Phi_0 + \Phi_0{}' \le \dfrac{\sigma}{fc} \le \dfrac{h - h_c}{h} - \Phi_0 + \Phi_0{}'$

$$\frac{y_0}{h} = \frac{\sigma}{fc} + \Phi_0 - \Phi_0{}' \tag{7.60}$$

$$m_p = h^2 f_c \left(\frac{1}{2} \frac{y_0}{h} \left(1 - \frac{y_0}{h} \right) + \Phi_0 \left(\frac{1}{2} - \frac{h_c}{h} \right) + \Phi_0{}' \left(\frac{1}{2} - \frac{h_c{}'}{h} \right) \right) \tag{7.61}$$

For $\dfrac{h - h_c}{h} - \Phi_0 + \Phi_0{}' \le \dfrac{\sigma}{fc} \le \dfrac{h - h_c}{h} + \Phi_0 + \Phi_0{}'$

$$\frac{y_0}{h} = \frac{h - h_c}{h} \tag{7.62}$$

$$m_p = h^2 f_c \left(\frac{1}{2} \frac{y_0}{h} \left(1 - \frac{y_0}{h} \right) + \left(\frac{y_0}{h} - \frac{\sigma}{f_c} + \Phi_0{}' \right) \left(\frac{1}{2} - \frac{h_c}{h} \right) + \Phi_0 \left(\frac{1}{2} - \frac{h_c{}'}{h} \right) \right) \tag{7.63}$$

For $\dfrac{h - h_c}{h} + \Phi_0 + \Phi_0{}' \le \dfrac{\sigma}{fc} \le 1 + \Phi_0 + \Phi_0{}'$

$$\frac{y_0}{h} = \frac{\sigma}{fc} - \Phi_0 - \Phi_0{}' \tag{7.64}$$

$$m_p = h^2 f_c \left(\frac{1}{2} \frac{y_0}{h} \left(1 - \frac{y_0}{h} \right) - \Phi_0 \left(\frac{1}{2} - \frac{h_c}{h} \right) + \Phi_0{}' \left(\frac{1}{2} - \frac{h_c{}'}{h} \right) \right) \tag{7.65}$$

The formulas above are valid in both the *x* and *y* direction.

For the two failure modes the equations using the dissipation formulas above becomes:

Failure mode 1:

The internal work becomes:

$$W_i = 4 L_s \frac{\delta}{L_s} \left(\frac{W_{c,y}}{h^2 \omega f_c} + \frac{W_{s,y}}{h^2 \omega f_c} \right) h^2 f_c + D_y \frac{\delta}{\frac{L_x}{2}} 2 \left(\frac{W_{c,0}}{h^2 \omega f_c} + \frac{W_{s,0}}{h^2 \omega f_c} \right) h^2 f_c \tag{7.66}$$

The external work becomes:

$$W_e = \delta q \left(\frac{1}{2} D_y L_x + \frac{1}{3} \left(L_y - D_y \right) L_x \right) + \sigma_x h 2 L_y \left(h_y - \frac{h}{2} \right) \frac{\delta}{\frac{L_x}{2}} + \sigma_y h 2 L_x \left(h_x - \frac{h}{2} \right) \frac{\delta}{\frac{\left(L_y - D_y \right)}{2}} \tag{7.67}$$

where h_x and h_y are the distances from the top surface to the axes of rotation in the x and y direction, respectively.

The work equation leads to:

$$q_1 = \frac{\dfrac{12 f_c h^2}{L_y^{\,2}} \left(\begin{array}{c} 2\left(\dfrac{D_y}{L_y}-1\right)\left(\dfrac{L_x}{L_y}\left(\dfrac{W_{c,v}}{h^2 \omega f_c}+\dfrac{W_{s,v}}{h^2 \omega f_c}\right)+\dfrac{D_y}{L_y}\left(\dfrac{W_{c,0}}{h^2 \omega f_c}+\dfrac{W_{s,0}}{h^2 \omega f_c}\right)\right) \\[2mm] +\dfrac{\sigma_x}{f_c}\left(\left(\dfrac{D_y}{L_y}-1\right)+2\dfrac{h_y}{h}\left(1-\dfrac{D_y}{L_y}\right)\right)+\dfrac{\sigma_y}{f_c}\left(\dfrac{L_x}{L_y}\right)^2\left(2\dfrac{h_x}{h}-1\right) \end{array} \right)}{\left(\dfrac{L_x}{L_y}\right)^2\left(\dfrac{D_y}{L_y}-1\right)\left(\dfrac{D_y}{L_y}+2\right)} \qquad (7.68)$$

where $W_{c,v}$ and $W_{s,v}$ are the contributions to the dissipation per unit length for the yield line (L_s) from concrete and reinforcement, respectively. Similarly, $W_{c,0}$ and $W_{s,0}$ are the contributions to the dissipation per unit length for the given line (D_y) from concrete and reinforcement, respectively.

The work equation for failure mode 2 leads to:

$$q_2 = \frac{\dfrac{12 f_c h^2}{L_x^{\,2}} \left(\begin{array}{c} 2\left(\dfrac{D_x}{L_x}-1\right)\left(\dfrac{L_y}{L_x}\left(\dfrac{W_{c,v}}{h^2 \omega f_c}+\dfrac{W_{s,v}}{h^2 \omega f_c}\right)+\dfrac{D_x}{L_x}\left(\dfrac{W_{c,0}}{h^2 \omega f_c}+\dfrac{W_{s,0}}{h^2 \omega f_c}\right)\right) \\[2mm] +\dfrac{\sigma_y}{f_c}\left(\left(\dfrac{D_x}{L_x}-1\right)+2\dfrac{h_x}{h}\left(1-\dfrac{D_x}{L_x}\right)\right)+\dfrac{\sigma_x}{f_c}\left(\dfrac{L_y}{L_x}\right)^2\left(2\dfrac{h_y}{h}-1\right) \end{array} \right)}{\left(\dfrac{L_y}{L_x}\right)^2\left(\dfrac{D_x}{L_x}-1\right)\left(\dfrac{D_x}{L_x}+2\right)} \qquad (7.69)$$

Calculating all possible combinations of the position of the two axes of rotation and plotting the lowest load-carrying capacity for a given axial force in one direction lead to the results shown in Figure 7.44 to Figure 7.48.
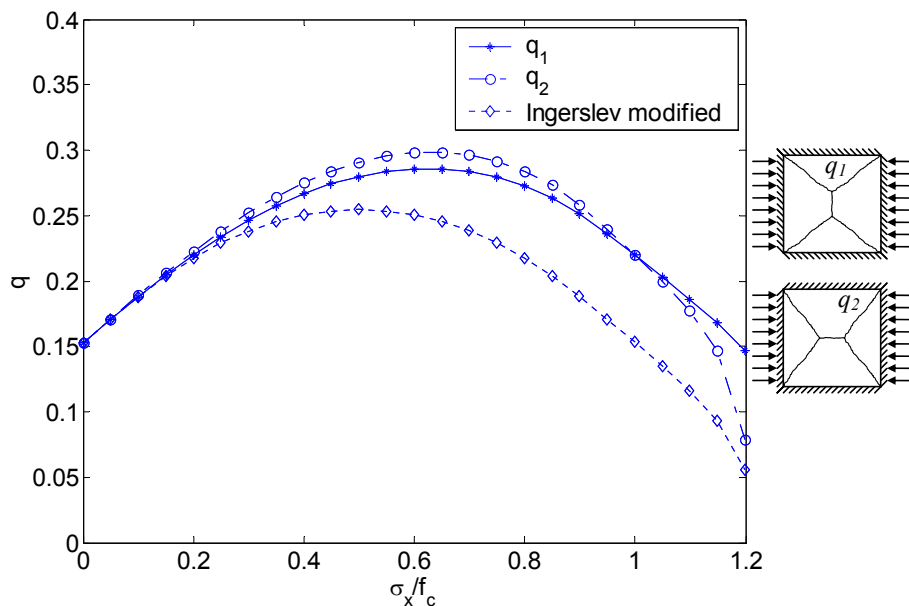
Figure 7.44. Load-carrying capacity for a rectangular slab $L_x=2000mm$, $L_y=2000mm$, $\Phi_{0x}=\Phi_{0x}{}'=0.1$, $\Phi_{0y}=\Phi_{0y}{}'=0.1$, $h_{cx}/h= h_{cx}{}'/h= h_{cy}/h= h_{cy}{}'/h=0.1$, $f_c=30MPa$, $h=100mm$, increasing σ_x and $\sigma_y=0$.
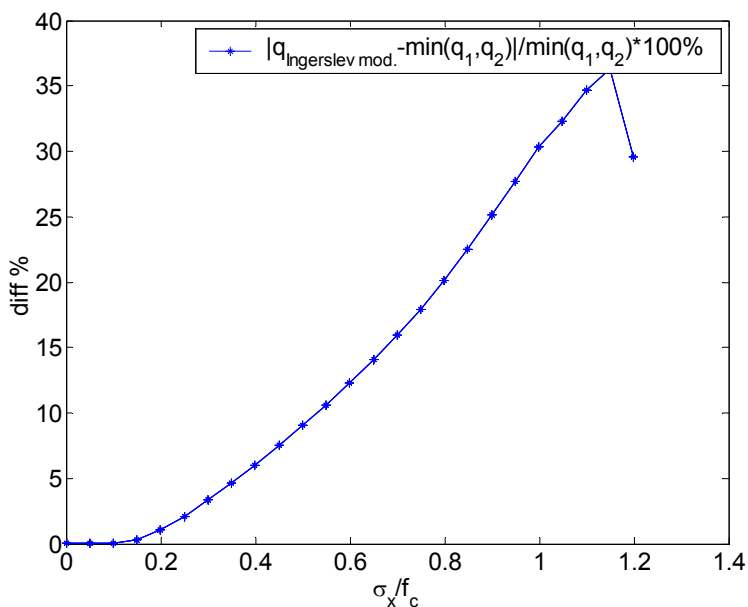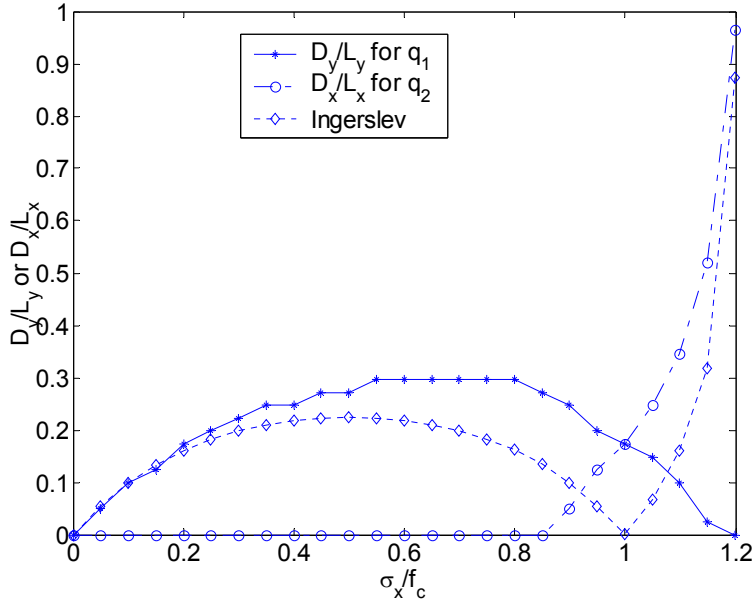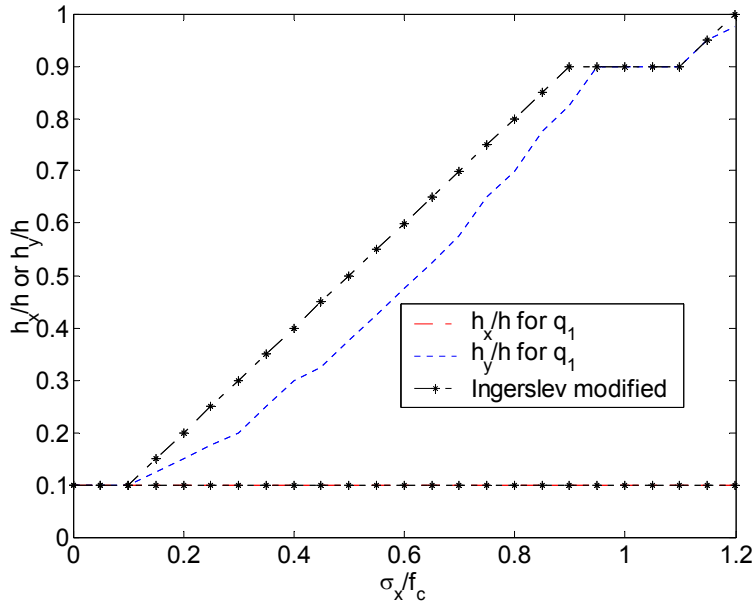

Figure 7.45 Difference between the calculation methods for a rectangular slab $L_x=2000mm$, $L_y=2000mm$, $\Phi_{0x}=\Phi_{0x}{}'=0.1$, $\Phi_{0y}=\Phi_{0y}{}'=0.1$, $h_{cx}/h= h_{cx}{}'/h= h_{cy}/h= h_{cy}{}'/h=0.1$, $f_c=30MPa$, $h=100mm$, increasing σ_x and $\sigma_y=0$.

Figure 7.46.Length of the part of the yield line parallel to the axes of rotation for a rectangular slab $L_x=2000mm$, $L_y=2000mm$, $\Phi_{0x}=\Phi_{0x}{}'=0.1$, $\Phi_{0y}=\Phi_{0y}{}'=0.1$, $h_{cx}/h=h_{cx}{}'/h=h_{cy}/h=h_{cy}{}'/h=0.1$, $f_c=30MPa$, $h=100mm$, increasing σ_x and $\sigma_y=0$.
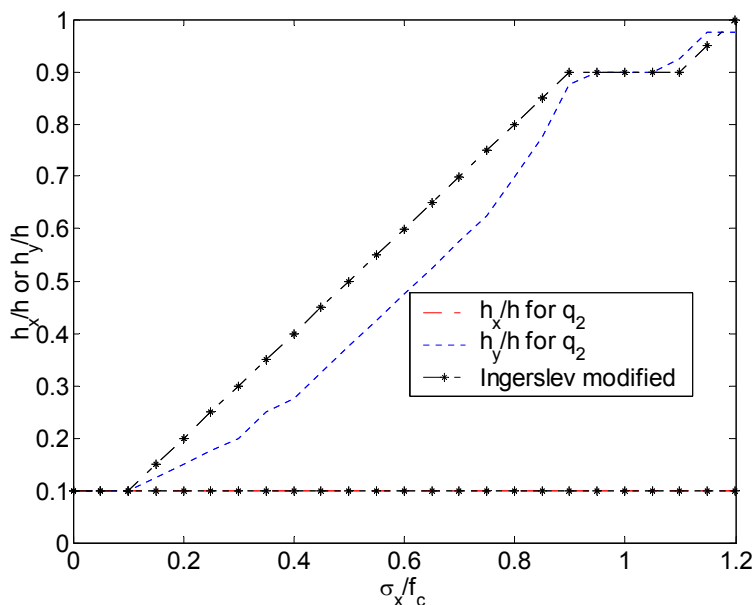

Figure 7.47.Position of the axes of rotation for failure mode 1 for a rectangular slab $L_x=2000mm$, $L_y=2000mm$, $\Phi_{0x}=\Phi_{0x}{}'=0.1$, $\Phi_{0y}=\Phi_{0y}{}'=0.1$, $h_{cx}/h=h_{cx}{}'/h=h_{cy}/h=h_{cy}{}'/h=0.1$, $f_c=30MPa$, $h=100mm$, increasing σ_x and $\sigma_y=0$.

Figure 7.48 Position of the axes of rotation for failure mode 2 for a rectangular slab $L_x=2000mm$, $L_y=2000mm$, $\Phi_{0x}=\Phi_{0x}{}'=0.1$, $\Phi_{0y}=\Phi_{0y}{}'=0.1$, $h_{cx}/h=h_{cx}{}'/h=h_{cy}/h=h_{cy}{}'/h=0.1$, $f_c=30MPa$, $h=100mm$, increasing σ_x and $\sigma_y=0$.

As expected the calculations using the method based on Ingerslev´s solution lead to an underestimation of the load-carrying capacity. In general the underestimation increases as the axial force increases. This underestimation is caused by the underestimation of the dissipation contribution from the concrete.

As seen in Figure 7.46 the length of the part of the yield line parallel to one of the axes for the Ingerslev solution is not the same as the one found from the dissipation formulas. It is seen that for $\sigma_x=f_c$ the load-carrying capacity found for failure mode 1 is the same as the load-carrying capacity found for failure mode 2 and both have a part of the yield line parallel to the axes. Ingerslev´s solution also leads to changes in failure mode at this stress but has no part of the yield line parallel to the axes.

The positions of the axes of rotation found from the two methods are also different. It is seen that the normal force does not effect the position as assumed. The position found by using the dissipation formulas determined by h_y/h, is in general lower. This means that the axis of rotation is placed closer to the top of the slab and therefore the positive effect for the load-carrying capacity is higher.

In order to evaluate the overestimation, an extreme slab is considered.

Knowing that the contribution to the dissipation from the concrete is calculated differently in the two methods it is obvious that a lower degree of reinforcement leads to a larger difference between the methods.
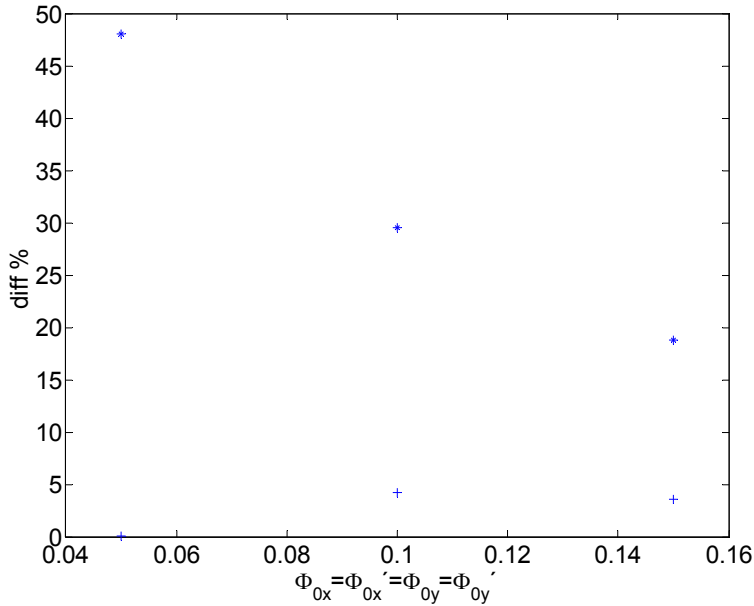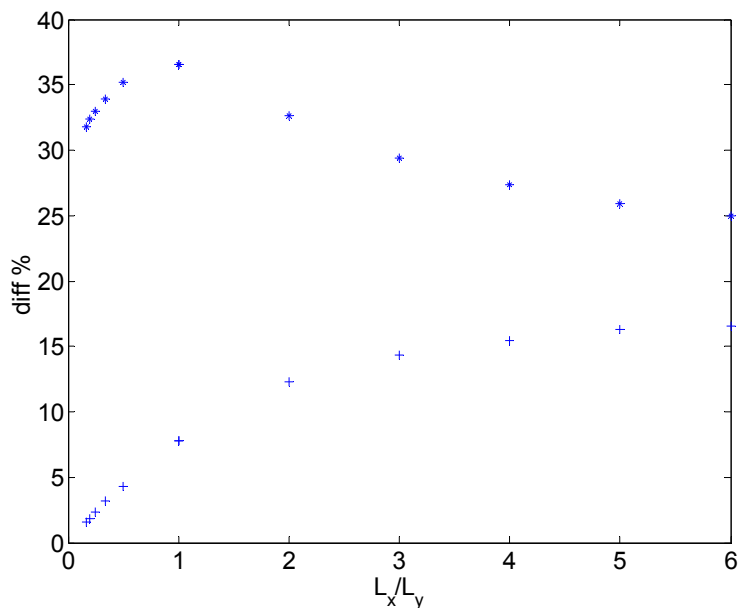

Figure 7.49. Maximum (*) and minimum (+) difference between the two calculation methods for a rectangular slab $L_x=2000mm$, $L_y=2000mm$, $h_{cx}/h= h_{cx}'/h= h_{cy}/h= h_{cy}'/h=0.1$, $f_c=30MPa$, $h=100mm$, σ_x variation from 0 to $f_c(1+\Phi_{0x}+\Phi_{0x}')$, $\sigma_y=0$ and different $\Phi_{0x}=\Phi_{0x}'= \Phi_{0y}=\Phi_{0y}'$.

When it comes to the L_x/L_y ratio an extreme case cannot be found from similar simple considerations. As illustrated in Figure 7.50 and Figure 7.51 extreme combinations of L_x and L_y changes along with the degree of reinforcement. In these plots * and + represents the maximum and minimum difference between the two calculation methods.

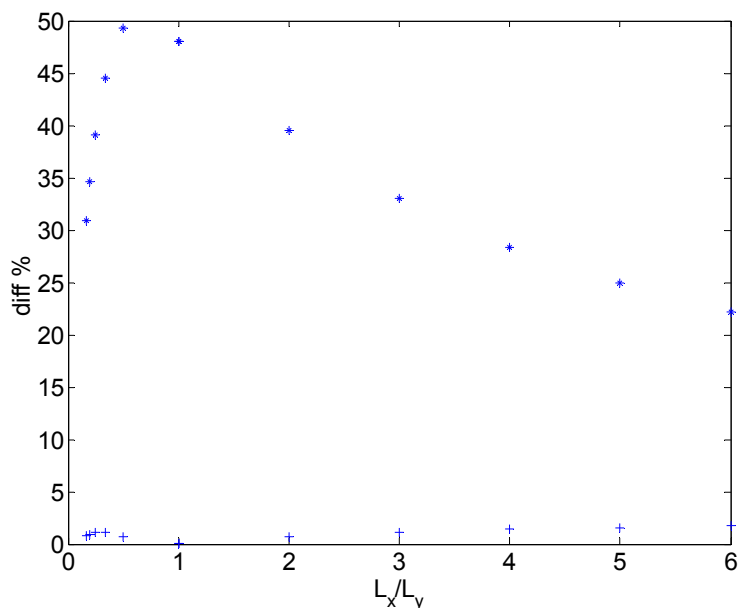*Figure 7.50. Maximum (*) and minimum (+) difference between the two calculation methods for a rectangular slab $L_x=2000mm$, $\Phi_{0x}=\Phi_{0x}{}'=0.1$, $\Phi_{0y}=\Phi_{0y}{}'=0.1$, $h_{cx}/h= h_{cx}{}'/h= h_{cy}/h= h_{cy}{}'/h=0.1$, $f_c=30MPa$, $h=100mm$, σ_x variation from 0 to $f_c(1+\Phi_{0x}+\Phi_{0x}{}')$, $\sigma_y=0$ and different L_x/L_y ratios.*

Figure 7.51. Maximum (*) and minimum (+) difference between the two calculation methods for a rectangular slab $L_x=2000mm$, $\Phi_{0x}=\Phi_{0x}{}'=0.05$, $\Phi_{0y}=\Phi_{0y}{}'=0.05$, $h_{cx}/h= h_{cx}{}'/h= h_{cy}/h= h_{cy}{}'/h=0.1$, $f_c=30MPa$, $h=100mm$, σ_x variation from 0 to $f_c(1+\Phi_{0x}+\Phi_{0x}{}')$, $\sigma_y=0$ and different L_x/L_y ratios.

Figure 7.51 shows that the maximum positive deviation is found for a L_x/L_y ratio of approximately 0.5 if the degree of reinforcement is 0.05. It is also seen that the minimum deviation is always positive and this means that the simplified calculation always underestimates the load-carrying capacity.

In Figure 7.52 to Figure 7.56 the results of the calculations for a slab with the L_x/L_y ratio of 0.5 and a degree of reinforcement of 0.05 are shown. Ingerslev modified refers to calculations using Ingerslevs solution ((7.54) or (7.55)) with the yield moment found when including the axial force ((7.57) to (7.65)) and Ingerslev 1 and Ingerslev 2 refers to the solutions for the two yield patterns..

Figure 7.52. Load-carrying capacity for a rectangular slab L_x=2000mm, L_y=4000mm, $\Phi_{0x}=\Phi_{0x}{'}$=0.05, $\Phi_{0y}=\Phi_{0y}{'}$=0.05, $h_{cx}/h= h_{cx}{'}/h= h_{cy}/h= h_{cy}{'}/h$=0.1, f_c=30MPa, increasing σ_x and σ_y=0.
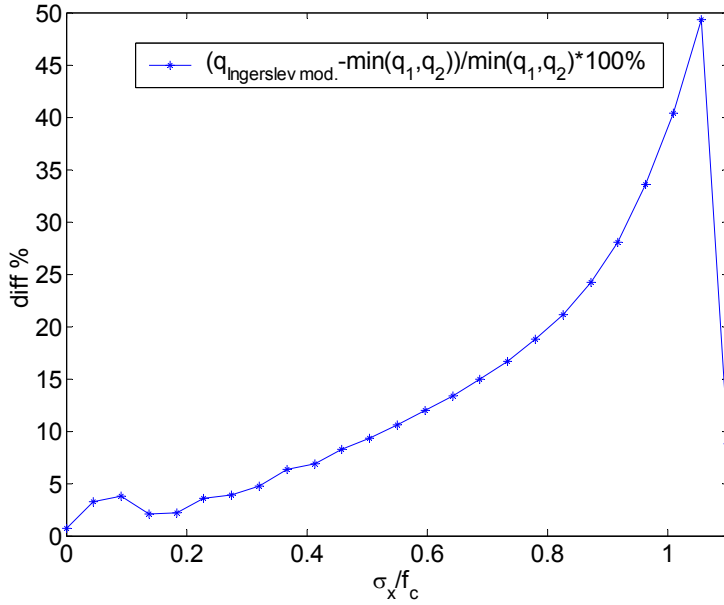
Figure 7.53 Difference between the calculation methods for a rectangularslab L_x=2000mm, L_y=4000mm, $\Phi_{0x}=\Phi_{0x}'$=0.05, $\Phi_{0y}=\Phi_{0y}'$=0.05, $h_{cx}/h= h_{cx}'/h= h_{cy}/h= h_{cy}'/h$=0.1, f_c=30MPa, increasing σ_x and σ_y=0.
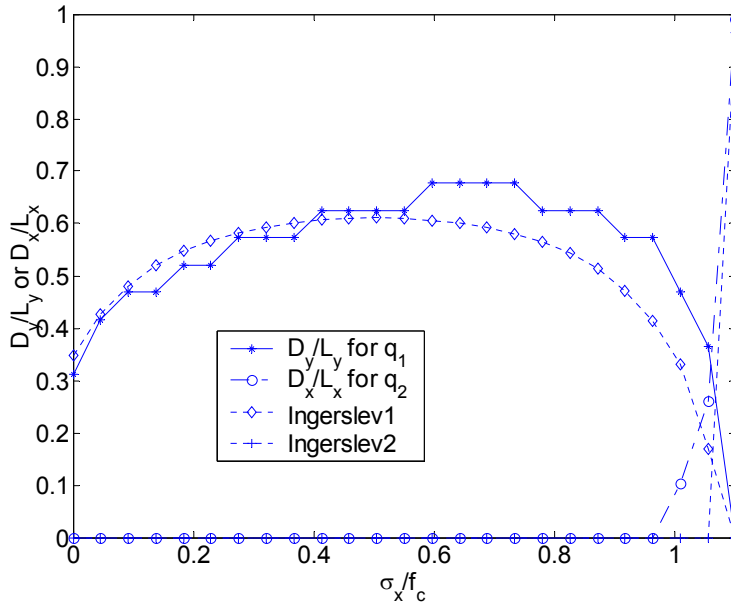

Figure 7.54.Length of the part of the yield line parallel to the axes of rotation for a rectangular slab L_x=2000mm, L_y=4000mm, $\Phi_{0x}=\Phi_{0x}'$=0.05, $\Phi_{0y}=\Phi_{0y}'$=0.05, $h_{cx}/h= h_{cx}'/h= h_{cy}/h= h_{cy}'/h$=0.1, f_c=30MPa, increasing σ_x and σ_y=0.

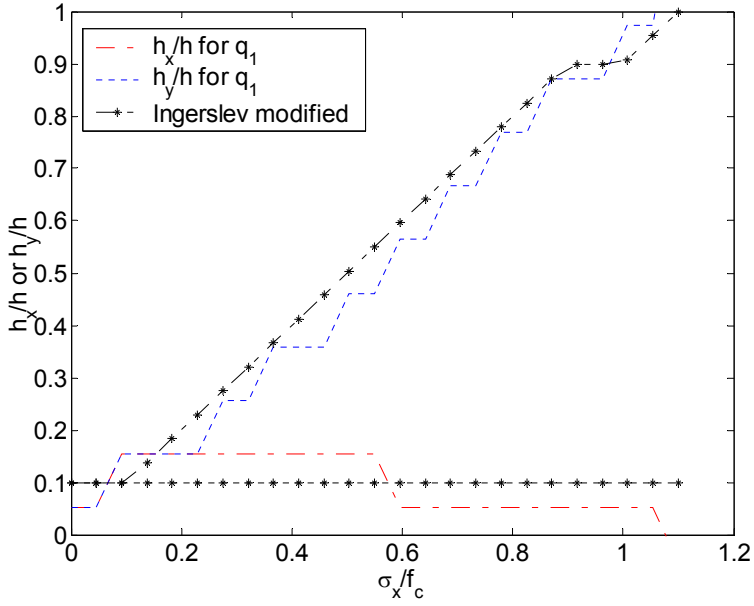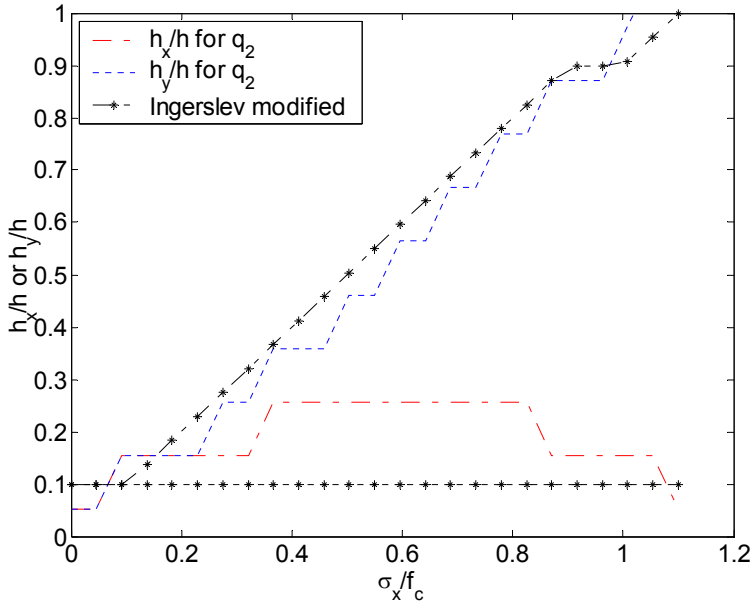*Figure 7.55.Position of the axes of rotation for failure mode 1 for a rectangular slab $L_x=2000mm$, $L_y=4000mm$, $\Phi_{0x}=\Phi_{0x}{'}=0.05$, $\Phi_{0y}=\Phi_{0y}{'}=0.05$, $h_{cx}/h=h_{cx}{'}/h=h_{cy}/h=h_{cy}{'}/h=0.1$, $f_c=30MPa$, increasing σ_x and $\sigma_y=0$.*

Figure 7.56 Position of the axes of rotation for failure mode 2 for a rectangular slab $L_x=2000mm$, $L_y=4000mm$, $\Phi_{0x}=\Phi_{0x}{'}=0.05$, $\Phi_{0y}=\Phi_{0y}{'}=0.05$, $h_{cx}/h=h_{cx}{'}/h=h_{cy}/h=h_{cy}{'}/h=0.1$, $f_c=30MPa$, increasing σ_x and $\sigma_y=0$.

It appears that the deviation between the two methods in general increases with the axial force. The largest deviation is approximately 50% and it is larger for axial stresses closer to $f_c + \Phi_0 + \Phi_0'$. However, this deviation is valid for an axial stress larger than f_c and such a stress would not be allowed in practice because of problems of stability. Assuming that the maximum axial stress is f_c, the deviation is 40%.

From this it may be concluded that the simple way (Ingerslev modified) of calculating the load-carrying capacity for a rectangular slab loaded with axial force is always safe and the method underestimates the load-carrying capacity with max 40%. A 40% deviation is an extreme case and it is believed that the simplification is acceptable for most practical purposes.

7.5 Rectangular slabs with axial force and with deflection

If the slab is deflected, the calculation of the dissipation must be changed since the distance to the axes of rotation changes along the yield line. In these calculations it is assumed that the deflection follows the yield line pattern as shown in Figure 7.57.
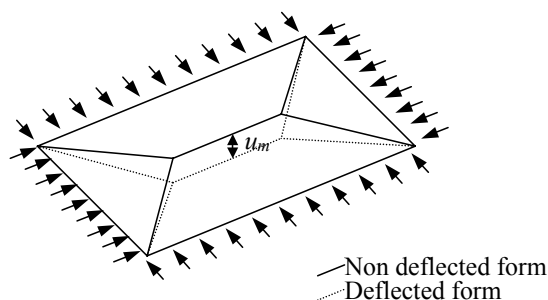

Figure 7.57. Deflection assumption for rectangular slabs.

Compared with the calculations for a slab without deflection the only difference is the calculation of the dissipation. In these calculations the vertical distance to the axes of rotation changes and this leads to different values of $W_{s,0}$ $W_{s,90}$, $W_{s,v}$, $W_{c,0}$, $W_{c,90}$, $W_{c,v}$.

Regarding $W_{s,0}$ $W_{s,90}$, $W_{c,0}$ and $W_{c,90}$ the distance from the top of the slab to the axes of rotation changes from h_x to h_x-u and from h_y to h_y-u. Regarding $W_{s,v}$ and $W_{c,v}$ the distance from the top of the slab to the axes of rotation varies along the yield line. This means that $W_{s,v}$ and $W_{c,v}$ must be calculated as average values. The calculations are made numerically.

When calculating the dissipation as described above, the formulas ((7.68) and (7.69)) for non-deflected slabs may be used to determine the load-carrying capacity.

For a square slab the calculations lead to the results shown in Figure 7.58 to Figure 7.60. Since the slab is square and the reinforcement is the same in both direction the two yield patterns leads to the same results.
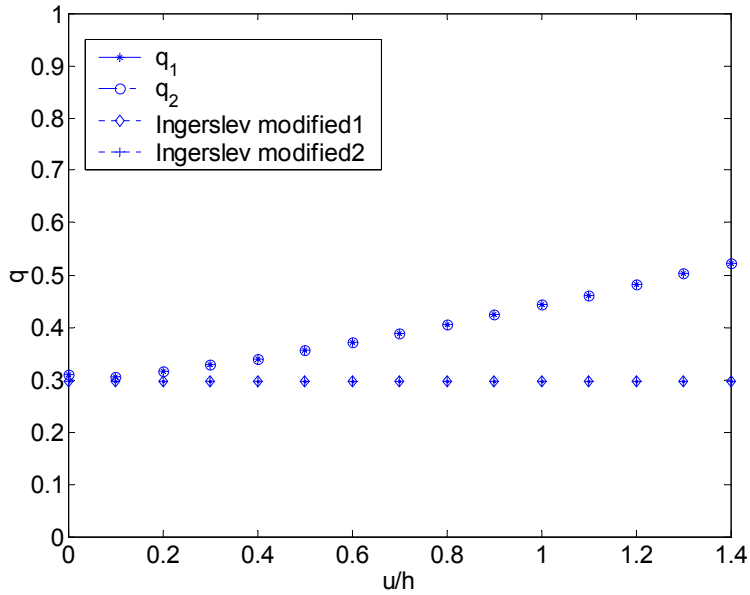

Figure 7.58 Load-carrying capacity for a rectangular slab $L_x=2000mm$, $L_y=2000mm$, $\Phi_{0x}=\Phi_{0x}{}'=0.2$, $\Phi_{0y}=\Phi_{0y}{}'=0.2$, $h_{cx}/h= h_{cx}{}'/h= h_{cy}/h= h_{cy}{}'/h=0.1$, $f_c=30MPa$, σ_x and $\sigma_y=0$
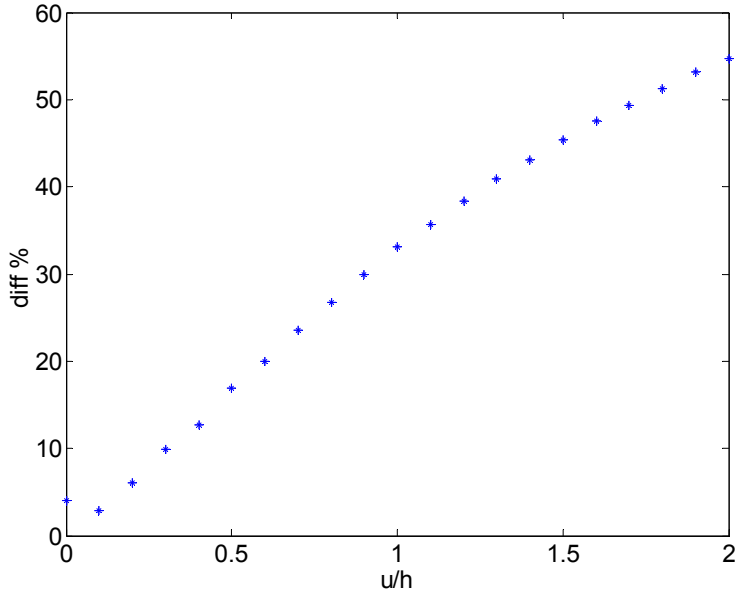
Figure 7.59 Difference between the load-carrying capacity for a non-deflected and a deflected rectangular slab with $L_x=2000mm$, $L_y=2000mm$, $\Phi_{0x}=\Phi_{0x}{'}=0.2$, $\Phi_{0y}=\Phi_{0y}{'}=0.2$, $h_{cx}/h=h_{cx}{'}/h=h_{cy}/h=h_{cy}{'}/h=0.1$, $f_c=30MPa$, σ_x and $\sigma_y=0$
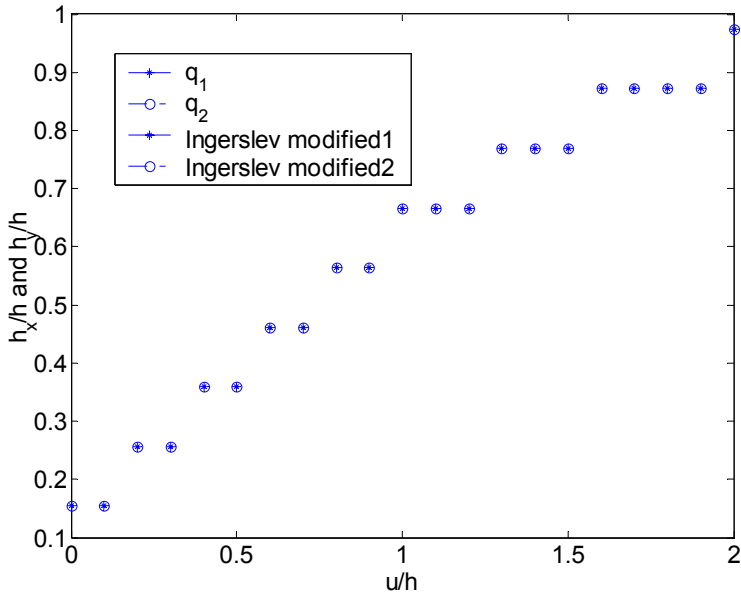

Figure 7.60 Position of the axes of rotation for failure mode 2 for a rectangular slab $L_x=2000mm$, $L_y=2000mm$, $\Phi_{0x}=\Phi_{0x}{'}=0.2$, $\Phi_{0y}=\Phi_{0y}{'}=0.2$, $h_{cx}/h=h_{cx}{'}/h=h_{cy}/h=h_{cy}{'}/h=0.1$, $f_c=30MPa$, σ_x and $\sigma_y=0$.

In these figures it is seen that the load-carrying capacity increases as the slab deflects. This phenomenon is well-known and may be explained by the change in geometry from a slab to a shallow shell. In these calculations only the displacements at failure are included in the work equation, which means that the deflected slab is calculated as a shell with the shape corresponding to the deflection.

As for non-deflected slabs it is interesting to investigate if the axes of rotation correspond to the neutral axes. Of course, the stresses are not known in the upper bound solution, but if we assume that the concrete stresses equal f_c in the direction of the displacement and the reinforcement stresses equal f_y it is found that the axes of rotation correspond to the neutral axes.

Calculations verifying this result are usually very complicated since the direction of the displacement changes along the yield line area. However, some simple cases may be used to demonstrate the result.

A square slab with $\Phi_{0x}=\Phi_{0x}{'}=0.25$, $\Phi_{0y}=\Phi_{0y}{'}=0.25$, $h_{cx}/h= h_{cx}{'}/h= h_{cy}/h= h_{cy}{'}/h=0$ is used here to demonstrate the result mentioned. The calculations of this slab lead to the results shown in Figure 7.60 to Figure 7.62.
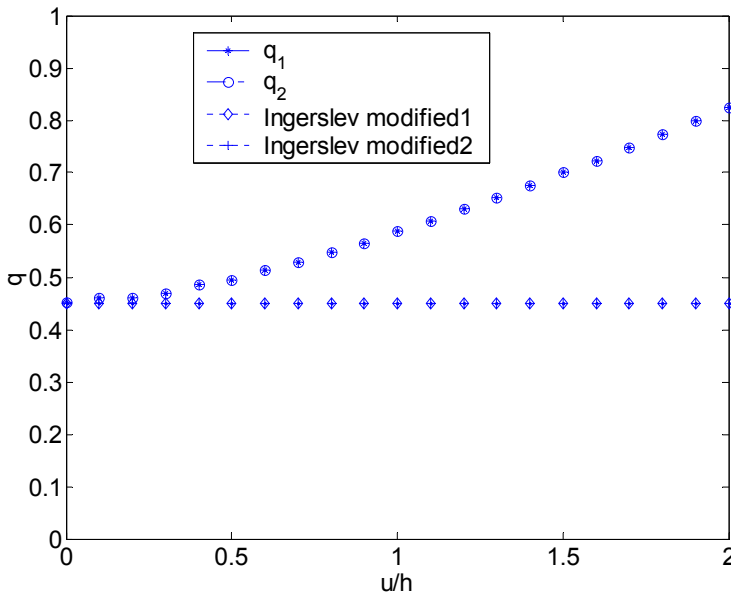

Figure 7.61 Load-carrying capacity for a rectangular slab $L_x=2000mm$, $L_y=2000mm$, $\Phi_{0x}=\Phi_{0x}{'}=0.25$, $\Phi_{0y}=\Phi_{0y}{'}=0.25$, $h_{cx}/h= h_{cx}{'}/h= h_{cy}/h= h_{cy}{'}/h=0$, $f_c=30MPa$, σ_x and $\sigma_y=0$
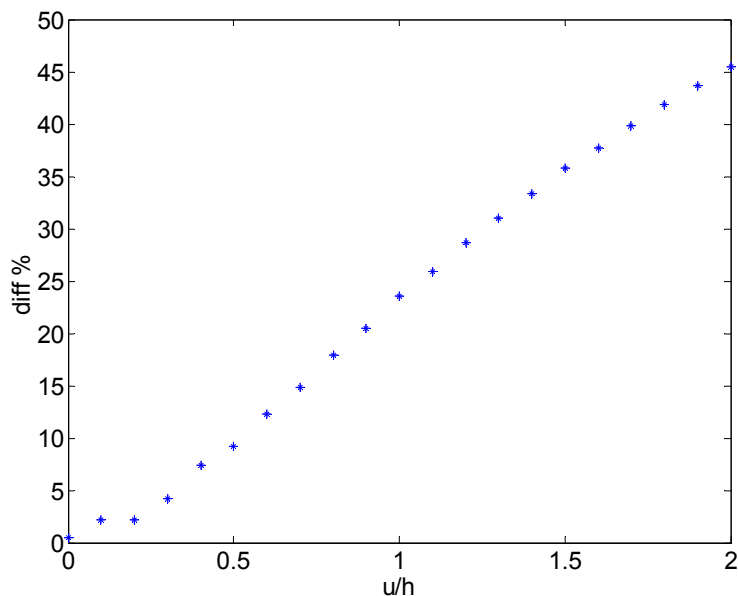
Figure 7.62 Difference between the load-carrying capacity for a non-deflected and a deflected rectangular slab with $L_x=2000mm$, $L_y=2000mm$, $\Phi_{0x}=\Phi_{0x}{'}=0.25$, $\Phi_{0y}=\Phi_{0y}{'}=0.25$, $h_{cx}/h= h_{cx}{'}/h= h_{cy}/h= h_{cy}{'}/h=0$, $f_c=30MPa$, σ_x and $\sigma_y=0$
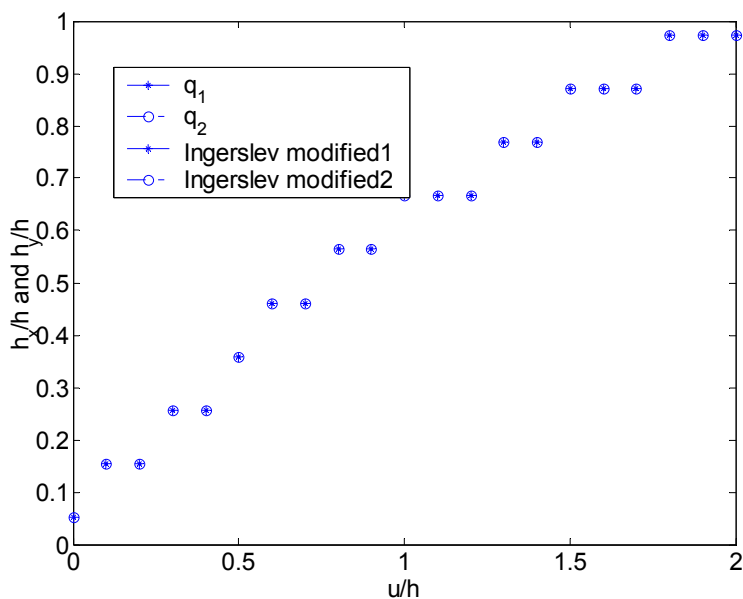

Figure 7.63 Position of the axes of rotation for failure mode 2 for a rectangular slab $L_x=2000mm$, $L_y=2000mm$, $\Phi_{0x}=\Phi_{0x}{'}=0.25$, $\Phi_{0y}=\Phi_{0y}{'}=0.25$, $h_{cx}/h= h_{cx}{'}/h= h_{cy}/h= h_{cy}{'}/h=0$, $f_c=30MPa$, σ_x and $\sigma_y=0$.

It appears that the axes of rotation move downward as the deflection increases. For the situation where u/h equals 2 it is seen that the relative position of axes of rotation is 1. This situation is illustrated in Figure 7.64.

From a projection equation in the x-direction it appears that if $u/h =2$ and $h_x=h_y=h$ the degree of reinforcement becomes:

$$\frac{f_c \cdot \tfrac{1}{2}h \cdot \tfrac{1}{2} \cdot \tfrac{1}{2}L\sqrt{2}}{\sqrt{2}} = \Phi_0 f_c h \tfrac{1}{2}L \Leftrightarrow$$
$$\Phi_0 = 0.25 \tag{7.70}$$

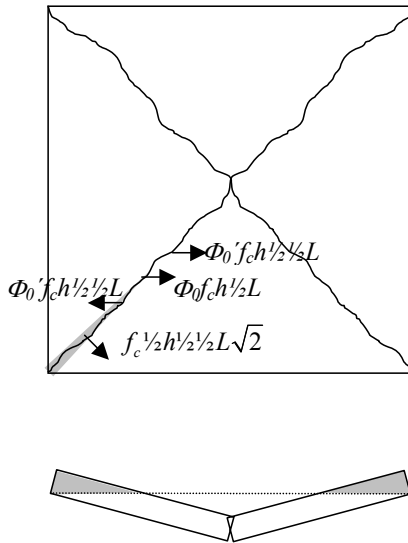This corresponds to the degree of reinforcement used in the calculations.

Figure 7.64 Failure mode for a square deflected slab.

Similar observations may be made for slabs with axial force. In Figure 7.65 to Figure 7.67 the results of calculations for a square slab with $\Phi_{0x}=\Phi_{0x}'=0.15$, $\Phi_{0y}=\Phi_{0y}'=0.15$, $h_{cx}/h= h_{cx}'/h= h_{cy}/h= h_{cy}'/h=0$ and $\sigma_y=\sigma_x=0.1f_c$ are shown. It appears that the axes of rotation correspond to the neutral axes.
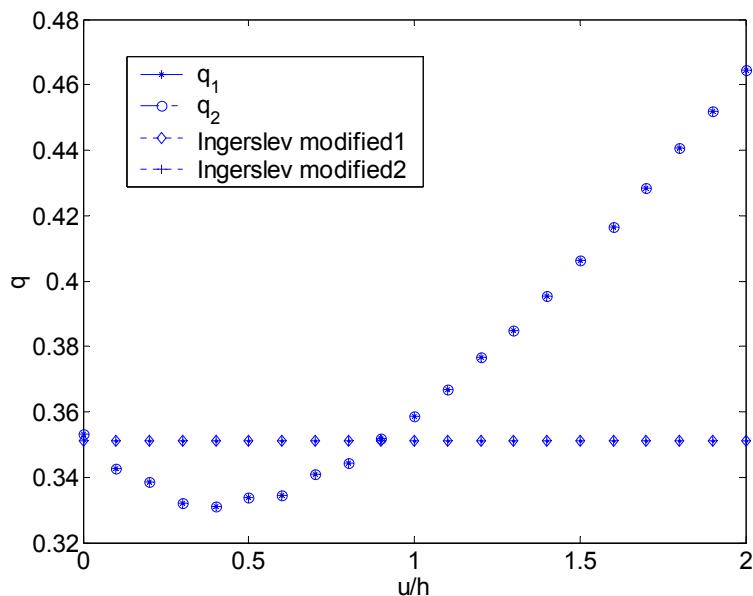
Figure 7.65 Load-carrying capacity for a rectangular slab $L_x=2000mm$, $L_y=2000mm$, $\Phi_{0x}=\Phi_{0x}'=0.15$, $\Phi_{0y}=\Phi_{0y}'=0.15$, $h_{cx}/h= h_{cx}'/h= h_{cy}/h= h_{cy}'/h=0$, $f_c=30MPa$, $\sigma_x=\sigma_y=0.1f_c$

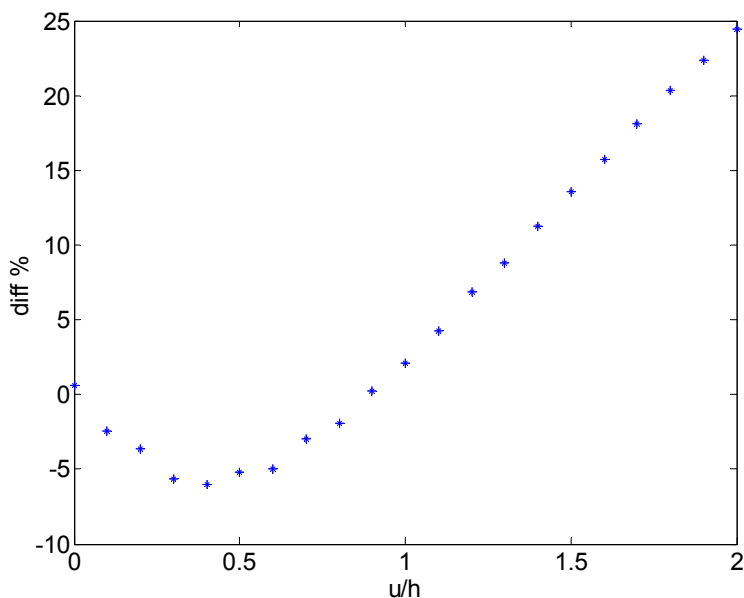*Figure 7.66 Difference between the load-carrying capacity for a non-deflected and a deflected rectangular slab with $L_x=2000mm$, $L_y=2000mm$, $\Phi_{0x}=\Phi_{0x}'=0.15$, $\Phi_{0y}=\Phi_{0y}'=0.15$, $h_{cx}/h= h_{cx}'/h= h_{cy}/h= h_{cy}'/h=0$, $f_c=30MPa$, $\sigma_x=\sigma_y=0.1f_c$*

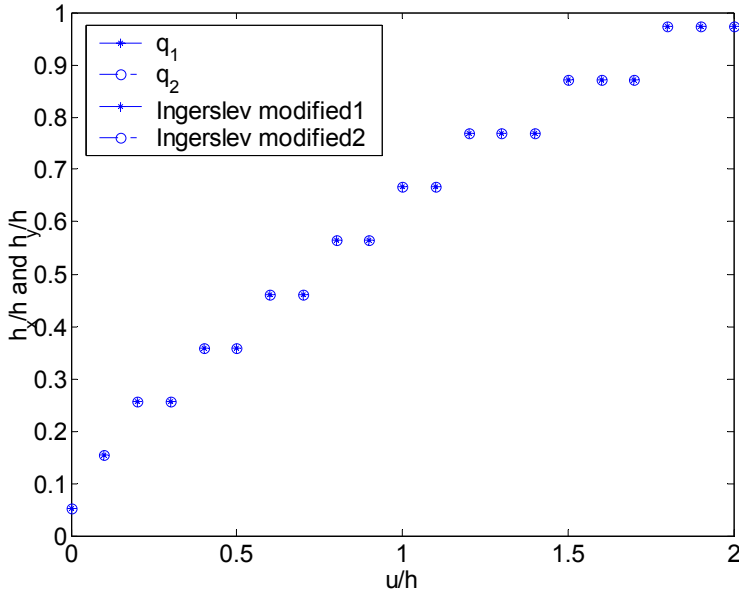*Figure 7.67 Position of the axes of rotation for failure mode 2 for a rectangular slab $L_x=2000mm$, $L_y=2000mm$, $\Phi_{0x}=\Phi_{0x}{}'=0.15$, $\Phi_{0y}=\Phi_{0y}{}'=0.15$, $h_{cx}/h= h_{cx}{}'/h= h_{cy}/h= h_{cy}{}'/h=0$, $f_c=30MPa$, $\sigma_x=\sigma_y=0.1f_c$.*

One might suspect that the assumption about the axes of rotation being the same as the neutral axes is only valid for isotropic slabs. However, numerical calculations as the one shown in Figure 7.68 to Figure 7.70, show that this is not the case. In the calculations the reinforcement is orthotropic and the slab is only subjected to axial load in one direction ($\Phi_{0x}=\Phi_{0x}{}'=0.15$, $\Phi_{0y}=\Phi_{0y}{}'=0.25$, $h_{cx}/h= h_{cx}{}'/h= h_{cy}/h= h_{cy}{}'/h=0$ and $\sigma_y=0$, $\sigma_x=0.1f_c$). Since the axial load equals the difference in the reinforcement the slab behaves as if the reinforcement was isotropic.
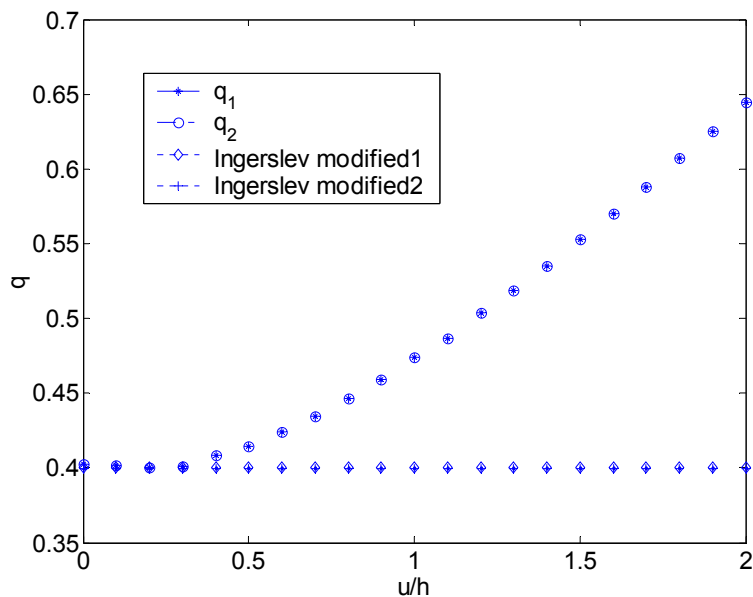
Figure 7.68 Load-carrying capacity for a rectangular slab L_x=2000mm, L_y=2000mm, Φ_{0x}=Φ_{0x}'=0.15, Φ_{0y}=Φ_{0y}'=0.25, h_{cx}/h= h_{cx}'/h= h_{cy}/h= h_{cy}'/h=0, f_c=30MPa, σ_x=0.1f_c, σ_y=0
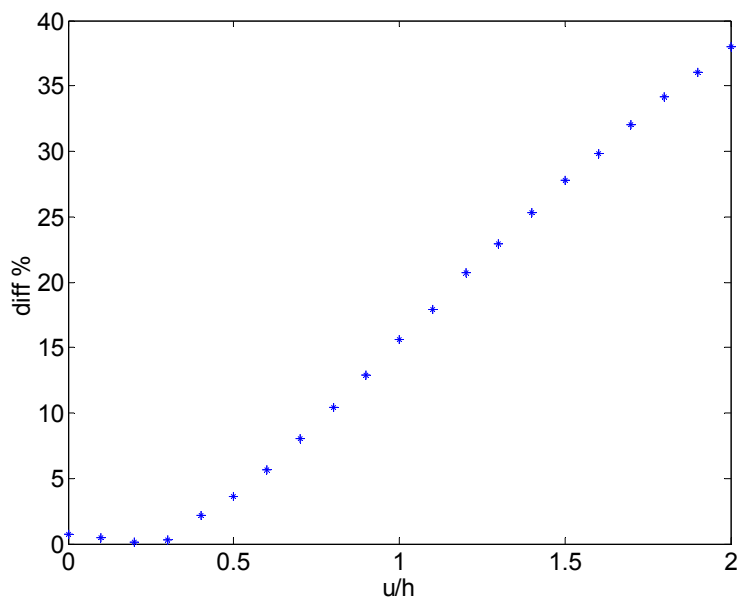

Figure 7.69 Difference between the load-carrying capacity for a non-deflected and a deflected rectangular slab with L_x=2000mm, L_y=2000mm, Φ_{0x}=Φ_{0x}'=0.15, Φ_{0y}=Φ_{0y}'=0.25, h_{cx}/h= h_{cx}'/h= h_{cy}/h= h_{cy}'/h=0, f_c=30MPa, σ_x=0.1f_c, σ_y=0
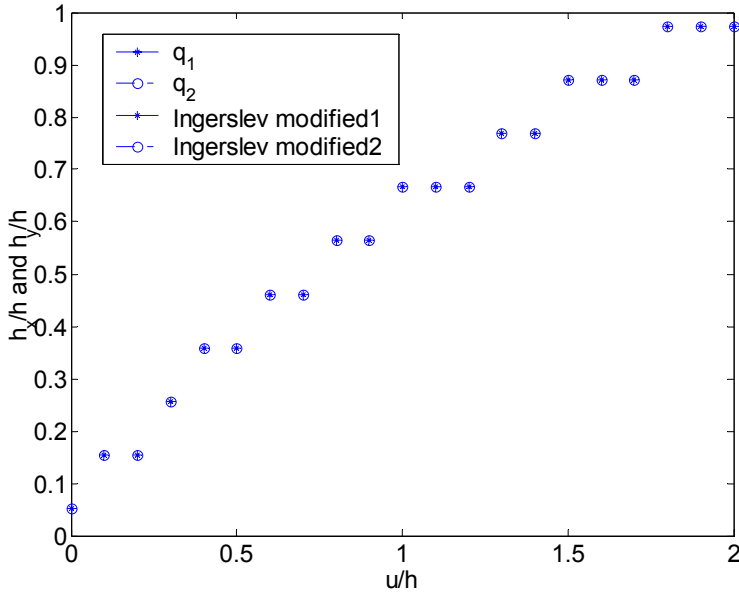
Figure 7.70 Position of the axes of rotation for failure mode 2 for a rectangular slab L_x=2000mm, L_y=2000mm, $\Phi_{0x}=\Phi_{0x}{'}$=0.15, $\Phi_{0y}=\Phi_{0y}{'}$=0.25, $h_{cx}/h= h_{cx}{'}/h= h_{cy}/h= h_{cy}{'}/h$=0, f_c=30MPa, σ_x=0.1f_c, σ_y=0.

Since the calculations are made numerically it is not possible to prove strictly that the axes of rotation and the neutral axes are identical. However, assuming that the contribution to the dissipation from the concrete may be calculated according to the simplified formulas given in section 7.1.1, it may be shown that the axes of rotation corresponds to the neutral axes.
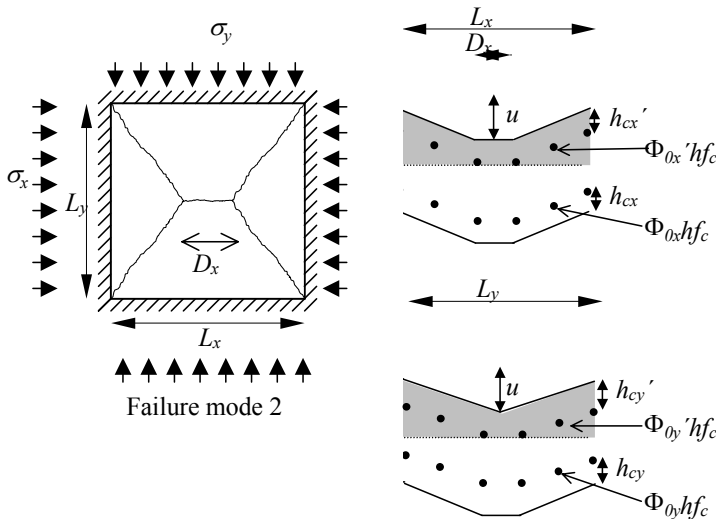

Figure 7.71. Yield pattern and cross sections.

For a failure mode as the one shown in Figure 7.71 the calculations becomes as follows.

The external work:

$$W_e = \delta q \left(\frac{1}{2} D_x L_y + \frac{1}{3} (L_x - D_x) L_y \right) + \sigma_x h 2 L_y \left(h_y - \frac{h}{2} \right) \frac{\delta}{\left(\frac{L_x - D_x}{2} \right)} + \sigma_y h 2 L_x \left(h_x - \frac{h}{2} \right) \frac{\delta}{\frac{L_y}{2}} \quad (7.71)$$

The internal work becomes:

$$W_i = f_c \left(\begin{array}{c} \dfrac{2\delta}{\frac{L_y}{2}} \left(\begin{array}{c} \frac{1}{2}(L_x - D_x)u\left(h_x - u + \frac{1}{3}u\right) + L_x \frac{1}{2}(h-u)^2 \\[2mm] +\Phi_{0x}'h\left((L_x - D_x)\left(h_x - \frac{1}{2}u - h_{cx}'\right) + D_x\left(h_x - u - h_{cx}'\right)\right) \\[2mm] +\Phi_{0x}h\left((L_x - D_x)\left(h - h_{cx} + \frac{1}{2}u - h_x\right) + D_x\left(h - h_{cx} + u - h_x\right)\right) \end{array} \right) \\[12mm] + \dfrac{2\delta}{\frac{L_x - D_x}{2}} \left(\begin{array}{c} \frac{1}{2}L_y u\left(h_y - u + \frac{1}{3}u\right) + L_y \frac{1}{2}(h_y - u)^2 \\[2mm] +\Phi_{0y}'hL_y\left(h_y - \frac{1}{2}u - h_{cy}'\right) + \Phi_{0y}hL_y\left(h - h_{cy} - \frac{1}{2}u - h_y\right) \end{array} \right) \end{array} \right) \quad (7.72)$$

The load-carrying capacity becomes:

$$q = \frac{24 f_c h^2}{L_x^2} \cdot \frac{1}{\left(\frac{L_y}{L_x}\right)^2 \left(-1+\frac{D_x}{L_x}\right)\left(\frac{D_x}{L_x}+2\right)}$$

$$\left(\begin{array}{l} \frac{h_x}{h}\left(\begin{array}{l} \Phi_{0x}\left(1-\frac{D_x}{L_x}\right)+\Phi_{0x}{}'\left(-1+\frac{D_x}{L_x}\right)+\frac{\sigma_y}{f_c}\left(1-\frac{D_x}{L_x}\right) \\ +\frac{1}{2}\frac{u}{h}\left(1-\left(\frac{D_x}{L_x}\right)^2\right)+\frac{1}{2}\frac{h_x}{h}\left(\frac{D_x}{L_x}-1\right) \end{array} \right) \\ +\frac{h_y}{h}\left(\begin{array}{l} \Phi_{0y}\left(\frac{L_y}{L_x}\right)^2-\Phi_{0y}{}'\left(\frac{L_y}{L_x}\right)^2+\frac{\sigma_x}{f_c}\left(\frac{L_y}{L_x}\right)^2 \\ +\frac{1}{2}\frac{u}{h}\left(\frac{L_y}{L_x}\right)^2-\frac{1}{2}\frac{h_y}{h}\left(\frac{L_y}{L_x}\right)^2 \end{array} \right) \\ +\Phi_{0x}\left(-1+\frac{D_x}{L_x}\left(1-\frac{h_{cx}}{h}+\frac{1}{2}\frac{D_x}{L_x}\frac{u}{h}\right)+\frac{h_{cx}}{h}-\frac{1}{2}\frac{u}{h}\right) \\ +\Phi_{0x}{}'\left(\frac{1}{2}\frac{u}{h}+\frac{h_{cx}{}'}{h}-\frac{1}{2}\left(\frac{D_x}{L_x}\right)^2\frac{u}{h}-\frac{h_{cx}{}'}{h}\frac{D_x}{L_x}\right) \\ +\Phi_{0y}\left(\frac{L_y}{L_x}\right)^2\left(\frac{h_{cy}}{h}+\frac{1}{2}\frac{u}{h}-1\right)+\Phi_{0y}{}'\left(\frac{L_y}{L_x}\right)^2\left(\frac{1}{2}\frac{u}{h}+\frac{h_{cy}{}'}{h}\right) \\ +\frac{\sigma_y}{f_c}\left(-\frac{1}{2}+\frac{1}{2}\frac{D_x}{L_x}\right)-\frac{1}{2}\frac{\sigma_x}{f_c}\left(\frac{L_y}{L_x}\right)^2+\left(\frac{u}{h}\right)^2\left(-1-\frac{1}{6}\left(\frac{L_y}{L_x}\right)^2+\frac{1}{3}\left(\frac{D_x}{L_x}\right)^2-\frac{1}{6}\frac{D_x}{L_x}\right) \end{array} \right)$$

(7.73)

The minimum load-carrying capacity is found for:

$$\frac{dq}{d\frac{h_x}{h}} = 0 \Rightarrow$$

(7.74)

$$\frac{h_x}{h} = \frac{\sigma_y}{f_c}+\frac{1}{2}\frac{u}{h}\left(1+\frac{D_x}{L_x}\right)+\Phi_{0x}-\Phi_{0x}{}'$$

$$\frac{dq}{d\frac{h_y}{h}} = 0 \Rightarrow$$

(7.75)

$$\frac{h_y}{h} = \frac{\sigma_x}{f_c}+\frac{1}{2}\frac{u}{h}+\Phi_{0y}-\Phi_{0y}{}'$$

It appears that the axes of rotation correspond to the neutral axes for each slab part since the minimization leads to the same result as a projection equation. Similar calculations may be made for other positions of the axes of rotation and deflections and they all show that the axes of rotation correspond to the neutral axes.

For a given axial stress and deflection it is thus possible to determine the axes of rotation and thereby also the dissipation in the yield line (the simplified dissipation according to the K.W. Johansen's method).

The following equations are obtained from a projection equation of a deflected section of a slab, as shown in Figure 7.72.
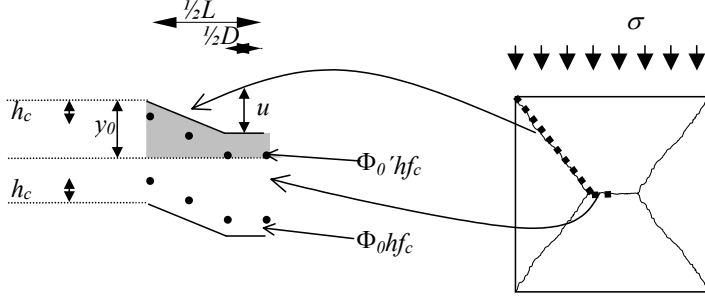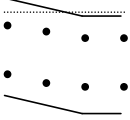

Figure 7.72. Cross-section of a deflected slab subjected to axial load.
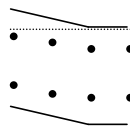
The projection equation used for the determination of the compression zone depends on both the deflection and the compression zone it self. This means that there are quite a lot of intervals to consider. They may all be seen in 11.2.An example is given below for the situation where $0<u<h_c$ & $h_c'<u+h_c'<h+h_c$ & $h-h_c<u+h-h_c<h$.

if $0<u<h_c$ & $h_c'<u+h_c'<h+h_c$ & $h-h_c<u+h-h_c<h$

and $0 \leq= y_0 < u$
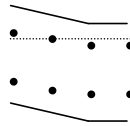
$$\frac{y_0}{h} = \frac{\sqrt{2}\sqrt{\left(1-\frac{D}{L}\right)\frac{u}{h}\left(\frac{\sigma}{f_c}+\Phi'+\Phi\right)}}{\left(1-\frac{D}{L}\right)} \quad (7.76)$$

and $u \leq y_0 < h_c$

$$\frac{y_0}{h} = \frac{1}{2}\left(2\frac{\sigma}{f_c}+2\Phi'+2\Phi+\frac{u}{h}+\frac{u}{h}\frac{D}{L}\right) \quad (7.77)$$

and $h_c \leq y_0 < u+h_c$

$$\frac{y_0}{h} = \frac{1}{2}\frac{\left(-1-\frac{D}{L}\right)\frac{u^2}{h}+-2\left(\frac{\sigma}{f_c}+\Phi'+\Phi\right)\frac{u}{h}+4\Phi'\frac{h_c}{h}\left(\frac{D}{L}-1\right)}{-2\Phi'+2\Phi'\frac{D}{L}-\frac{u}{h}} \quad (7.78)$$

and $u+h_c=y_0$

$$\left(\frac{1}{2}-\frac{1}{2}\frac{D}{L}\right)\frac{u}{h}+\Phi'-2\Phi'\frac{D}{L}-\Phi+\frac{h_c}{h}\leq\frac{\sigma}{f_c}\leq\left(\frac{1}{2}-\frac{1}{2}\frac{D}{L}\right)\frac{u}{h}-\Phi+\frac{h_c}{h}+\Phi' \qquad (7.79)$$

and $u+h_c<y_0<h-h_c$

$$\frac{y_0}{h}=\left(\frac{\sigma}{f_c}-\Phi'+\Phi+\frac{1}{2}\frac{u}{h}+\frac{1}{2}\frac{u}{h}\frac{D}{L}\right) \qquad (7.80)$$

and $h-h_c\leq y_0<h-h_c+u$

$$\frac{y_0}{h}=\frac{\frac{1}{2}\left(-1-\frac{D}{L}\right)\left(\frac{u}{h}\right)^2+\left(-\frac{\sigma}{f_c}+\Phi'-\Phi\right)\frac{u}{h}+\left(2\Phi\frac{h_c}{h}-2\Phi\right)\left(1-\frac{D}{L}\right)}{-2\Phi\left(1-\frac{D}{L}\right)-\frac{u}{h}} \qquad (7.81)$$

and $h-h_c+u\leq y_0<h$

$$\frac{y_0}{h}=\frac{\sigma}{f_c}-\Phi'-\Phi+\frac{1}{2}\frac{u}{h}\left(1+\frac{D}{L}\right) \qquad (7.82)$$

and $u+h-h_c=y_0$

$$\frac{1}{2}\left(1-\frac{D}{L}\right)\frac{u}{h}+\Phi'+\Phi+1-\frac{h_c}{h}-2\Phi\frac{D}{L}\leq\frac{\sigma}{f_c}\leq\frac{1}{2}\left(1-\frac{D}{L}\right)\frac{u}{h}+\Phi'+\Phi+1-\frac{h_c}{h} \qquad (7.83)$$

and $h<y_0\leq u+h$

$$\frac{y_0}{h}=\frac{\frac{u}{h}+1-\frac{D}{L}\pm\sqrt{-\frac{u}{h}\left(2\left(\frac{\sigma}{f_c}-1-(\Phi'+\Phi)\right)\left(1-\frac{D}{L}\right)-\frac{u}{h}\left(\frac{D}{L}\right)^2\right)}}{1-\frac{D}{L}} \qquad (7.84)$$

The dissipation is most easily calculated as the dissipation per unit rotation about the neutral axes. Using the K. W. Johansen method this may be done by taking moments about the rotation axes for each slab part.

The moments are most easily calculated as contributions from the top and bottom reinforcement and the concrete.

$$M_f=M_{f,c}+M_{f,s'}+M_{f,s} \qquad (7.85)$$

for $M_{f,c}$ we get:

if $u\leq h$

and $y_0\leq u$

$$\frac{M_{f,c}}{f_c h^2 L} = -\frac{1}{12}\left(\frac{y_0}{h}\right)^3 \frac{\left(-1+\dfrac{D}{L}\right)}{\dfrac{u}{h}} \tag{7.86}$$

and $u<y_0\leq h$

$$\frac{M_{f,c}}{f_c h^2 L} = \frac{1}{12}\left(-3\frac{u}{h}\frac{y_0}{h}+\left(\frac{u}{h}\right)^2-3\frac{u}{h}\frac{D}{L}\frac{y_0}{h}+2\left(\frac{u}{h}\right)^2\frac{D}{L}+3\left(\frac{y_0}{h}\right)^2\right) \tag{7.87}$$

and $h<y_0\leq h+u$

$$\frac{M_{f,c}}{f_c h^2 L} = \frac{1}{12}\frac{\left(\begin{array}{l}-3\left(\dfrac{u}{h}\right)^2\dfrac{y_0}{h}+\left(\dfrac{u}{h}\right)^3-3\left(\dfrac{u}{h}\right)^2\dfrac{D}{L}\dfrac{y_0}{h}+2\left(\dfrac{u}{h}\right)^3\dfrac{D}{L}+3\dfrac{u}{h}\left(\dfrac{y_0}{h}\right)^2\\[2mm]+\left(1-3\dfrac{y_0}{h}+3\left(\dfrac{y_0}{h}\right)^2-\left(\dfrac{y_0}{h}\right)^3\right)\left(1-\dfrac{D}{L}\right)\end{array}\right)}{\dfrac{u}{h}} \tag{7.88}$$

if $u>h$

and $y_0\leq h$

$$\frac{M_{f,c}}{f_c h^2 L} = -\frac{1}{12}\left(\frac{y_0}{h}\right)^3\frac{-1+\dfrac{D}{L}}{\dfrac{u}{h}} \tag{7.89}$$

and $h<y_0\leq u$

$$\frac{M_{f,c}}{f_c h^2 L} = -\frac{1}{12}\left(-1+\frac{D}{L}\right)\frac{3\left(\dfrac{y_0}{h}\right)^2-3\dfrac{y_0}{h}+1}{\dfrac{u}{h}} \tag{7.90}$$

and $u<y_0\leq h+u$

$$\frac{M_{f,c}}{f_c h^2 L} = \frac{1}{12}\frac{\left(\begin{array}{l}-3\left(\dfrac{u}{h}\right)^2\dfrac{y_0}{h}+\left(\dfrac{u}{h}\right)^3-3\left(\dfrac{u}{h}\right)^2\dfrac{D}{L}\dfrac{y_0}{h}+2\left(\dfrac{u}{h}\right)^3\dfrac{D}{L}+3\dfrac{u}{h}\left(\dfrac{y_0}{h}\right)^2\\[2mm]+\left(1-3\dfrac{y_0}{h}+3\left(\dfrac{y_0}{h}\right)^2-\left(\dfrac{y_0}{h}\right)^3\right)\left(1-\dfrac{D}{L}\right)\end{array}\right)}{\dfrac{u}{h}} \tag{7.91}$$

for $M_{f,s'}$ we get:

if $y_0\leq h_c$

$$\frac{M_{f,s'}}{f_c h^2 L} = -\frac{1}{4}\Phi'\left(-\left|2\frac{h_c}{h}+\frac{u}{h}-2\frac{y_0}{h}\right|+\left|2\frac{h_c}{h}+\frac{u}{h}-2\frac{y_0}{h}\right|\frac{D}{L}-2\frac{D}{L}\left|\frac{h_c}{h}+\frac{u}{h}-\frac{y_0}{h}\right|\right) \tag{7.92}$$

if $h_c<y_0\leq u+h_c$

$$\frac{M_{f,s'}}{f_c h^2 L} = \frac{1}{4}\Phi' \frac{\left(\left(-4\frac{y_0}{h}\frac{h_c}{h} - 2\frac{u}{h}\frac{y_0}{h} + 2\frac{h_c}{h}\frac{u}{h} + \left(\frac{u}{h}\right)^2 + 2\left(\frac{h_c}{h}\right)^2 + 2\left(\frac{y_0}{h}\right)^2\right)\left(1 - \frac{D}{L}\right) + 2\left|\frac{h_c}{h} + \frac{u}{h} - \frac{y_0}{h}\right|\frac{D}{L}\frac{u}{h}\right)}{\dfrac{u}{h}}$$

$$(7.93)$$

if $u+h_c<y_0 \leq h+u$

$$\frac{M_{f,s'}}{f_c h^2 L} = \frac{1}{4}\Phi'\left(-\left|2\frac{h_c}{h} + \frac{u}{h} - 2\frac{y_0}{h}\right| - \left|2\frac{h_c}{h} + \frac{u}{h} - 2\frac{y_0}{h}\right|\frac{D}{L} + 2\frac{D}{L}\left|\frac{h_c}{h} + \frac{u}{h} - \frac{y_0}{h}\right|\right) \qquad (7.94)$$

for $M_{f,s}$ we get:

if $y_0 \leq h-h_c$

$$\frac{M_{f,s}}{f_c h^2 L} = -\frac{1}{4}\Phi\left(-\left|2 - 2\frac{h_c}{h} + \frac{u}{h} - 2\frac{y_0}{h}\right| + \left|2 - 2\frac{h_c}{h} + \frac{u}{h} - 2\frac{y_0}{h}\right|\frac{D}{L} - 2\frac{D}{L}\left|1 - \frac{h_c}{h} + \frac{u}{h} - \frac{y_0}{h}\right|\right) \quad (7.95)$$

if $h-h_c<y_0 \leq u+h-h_c$

$$\frac{M_{f,s}}{f_c h^2 L} = -1/4\Phi\left(\frac{D}{L} - 1\right)\frac{u}{h} - 1/4\Phi\left(\left(2\frac{y_0}{h} + 2\frac{h_c}{h} - 2\right)\left(1 - \frac{D}{L}\right) - 2\left|1 - \frac{h_c}{h} + u - h - \frac{y_0}{h}\right|\frac{D}{L}\right)$$

$$-1/4\Phi\frac{\left(-2\left(\frac{y_0}{h}\right)^2 - 2\left(\frac{h_c}{h}\right)^2 + 4\frac{y_0}{h} + 4\frac{h_c}{h} - 2 - 4\frac{y_0}{h}\frac{h_c}{h}\right)\left(1 - \frac{D}{L}\right)}{\dfrac{u}{h}} \qquad (7.96)$$

if $u+h-h_c<y_0 \leq h+u$

$$\frac{M_{f,s}}{f_c h^2 L} = -\frac{1}{4}\Phi\left(-\left|2 - 2\frac{h_c}{h} + \frac{u}{h} - 2\frac{y_0}{h}\right| + \left|2 - 2\frac{h_c}{h} + \frac{u}{h} - 2\frac{y_0}{h}\right|\frac{D}{L} - 2\frac{D}{L}\left|1 - \frac{h_c}{h} + \frac{u}{h} - \frac{y_0}{h}\right|\right) \quad (7.97)$$

From the formulas above the load-carrying capacity may be found as:

Failure mode 1:

The internal work becomes:

$$W_i = 2M_{fy}\frac{\delta}{\dfrac{L_x}{2}} + 2M_{fx}\frac{\delta}{\dfrac{L_y}{2} - \dfrac{D_y}{2}} \qquad (7.98)$$

The external work becomes:

$$W_e = \delta q_1\left(\frac{1}{2}D_y L_x + \frac{1}{2}\left(L_y - D_y\right)L_x\right) + \sigma_x h 2 L_y\left(h_y - \frac{h}{2}\right)\frac{\delta}{\dfrac{1}{2}L_x} + \sigma_y h 2 L_x\left(h_x - \frac{h}{2}\right)\frac{\delta}{\dfrac{1}{2}\left(L_y - D_y\right)} \quad (7.99)$$

The work equation leads to:

$$q_{1,eq} = 12 \frac{-2M_{fx}L_x + 2\sigma_x hL_y{}^2 h_y - 2\sigma_x hL_y h_y D_y - \sigma_x h^2 L_y{}^2 + \sigma_x h^2 L_y D_y + 2\sigma_y hL_x{}^2 h_x - \sigma_y h^2 L_x{}^2 - 2M_{fy}L_y + 2M_{fy}D_y}{\left(-L_y + D_y\right)L_x{}^2\left(D_y + 2L_y\right)}$$

or

$$q_{1,eq} = 12 f_c \frac{h^2}{L_y{}^2} \frac{2\left(\dfrac{L_x}{L_y}\right)^2 \dfrac{M_{fx}}{f_c h^2 L_x} + \left(-2\dfrac{\sigma_x}{f_c}\dfrac{y_{0y}}{h} + \dfrac{\sigma_x}{f_c} + 2\dfrac{M_{fy}}{f_c h^2 L_y}\right)\left(1 - \dfrac{D_y}{L_y}\right) + \dfrac{\sigma_y}{f_c}\left(\dfrac{L_x}{L_y}\right)^2\left(1 - 2\dfrac{y_{0x}}{h}\right)}{\left(1 - \dfrac{D_y}{L_y}\right)\left(\dfrac{L_x}{L_y}\right)^2\left(\dfrac{D_y}{L_y} + 2\right)}$$

(7.100)

A similar formula is obtained for failure mode 2:

$$q_{2,eq} = 12 f_c \frac{h^2}{L_x{}^2} \frac{2\left(\dfrac{L_y}{L_x}\right)^2 \dfrac{M_{fy}}{f_c h^2 L_y} + \left(-2\dfrac{\sigma_y}{f_c}\dfrac{y_{0x}}{h} + \dfrac{\sigma_y}{f_c} + 2\dfrac{M_{fx}}{f_c h^2 L_x}\right)\left(1 - \dfrac{D_x}{L_x}\right) + \dfrac{\sigma_x}{f_c}\left(\dfrac{L_y}{L_x}\right)^2\left(1 - 2\dfrac{y_{0y}}{h}\right)}{\left(1 - \dfrac{D_x}{L_x}\right)\left(\dfrac{L_y}{L_x}\right)^2\left(\dfrac{D_x}{L_x} + 2\right)}$$

(7.101)

For a given slab having a certain deflection and failure mode (*u* and *D/L*) it is now possible to calculate the load-carrying capacity without making any numerical integrations. This leads of course to a substantial reduction of the calculations since a theoretically correct calculation involves integration over the yield line (the L_s-part).

In the following, the index $_{,eq}$ indicates that the axes of the rotation are found from equilibrium of a slab part as described above. The index $_{,up}$ indicates that the axes of rotation is found numerically from the minimum of upper bound solutions.

In order to find the minimum load-carrying capacity for a given deflection the most optimal failure mode has to be found.

In Figure 7.73 to Figure 7.75 and Figure 7.76 to Figure 7.78 the results of calculations for a square slab with axial force in two direction are shown for σ/f_c=0.1 and σ/f_c=0.4 respectively. In these plots both the results of the simplified way of calculating the load-carrying capacity (index eq) and the results of the numerical calculations (index up) are shown. Index 1 and 2 refers to the yield line pattern.

In Figure 7.75 the contributions from reinforcement (index s) and concrete (index c) to the work are plotted and thereby showing the difference between the two calculation methods.
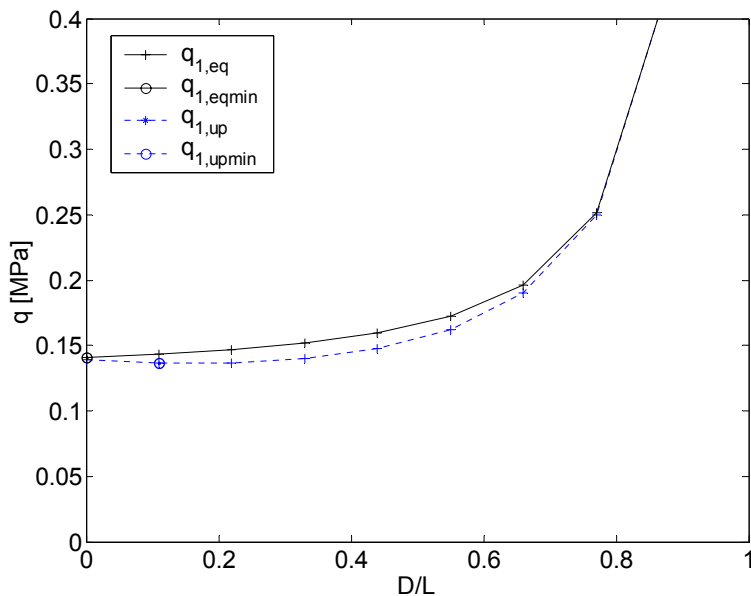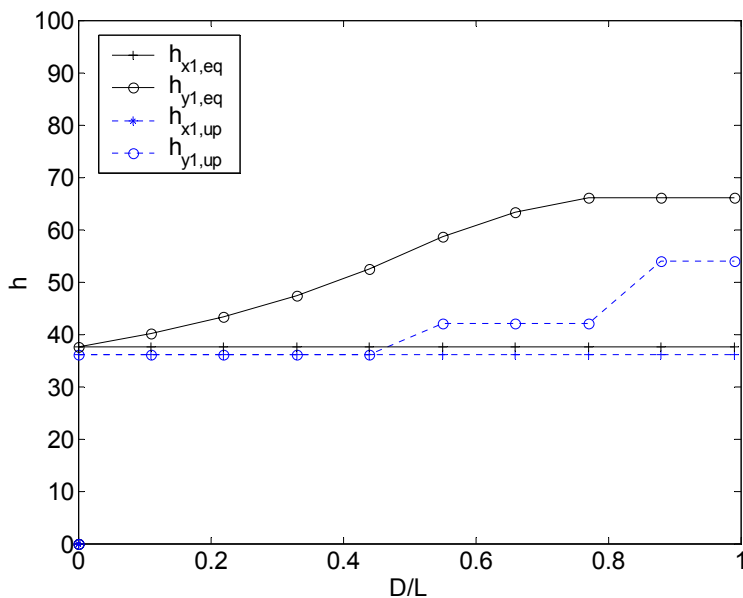
Figure 7.73.Results of calculations by equations (7.76) to (7.101) (solid) and numerical calculations (dashed) on a slab with $L_x=L_y=2000mm$, $\Phi_{0x}=\Phi_{0x}{}'=\Phi_{0y}=\Phi_{0y}{}'=0.1$, $h_c/h=0.1$, $h=60mm$, $fc=50MPa$, $u/h=1$ and $\sigma_x/f_c=\sigma_y/f_c=0.1$.

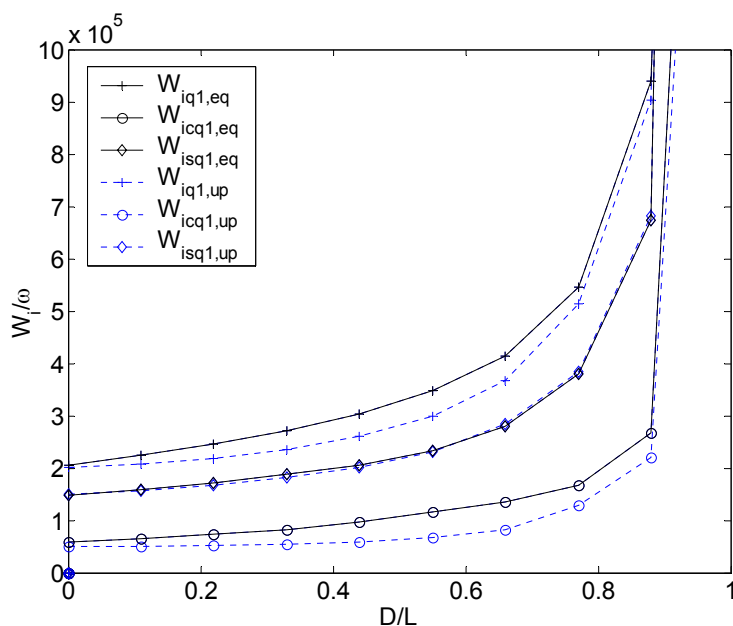*Figure 7.74.Results of calculations by equations (7.76) to (7.101) (solid) and numerical calculations (dashed) on a slab with $L_x=L_y=2000mm$, $\Phi_{0x}=\Phi_{0x}{}'=\Phi_{0y}=\Phi_{0y}{}'=0.1$, $h_c/h=0.1$, $h=60mm$, $fc=50MPa$, $u/h=1$ and $\sigma_x/f_c=\sigma_y/f_c=0.1$.*

Figure 7.75.Results of calculations by equations (7.76) to (7.101) (solid) and numerical calculations (dashed) on a slab with $L_x=L_y= 2000mm, \Phi_{0x}=\Phi_{0x}'=\Phi_{0y}=\Phi_{0y}'=0.1, h_c/h=0.1, h=60mm, fc=50MPa, u/h=1$ and $\sigma_x/f_c=\sigma_y/f_c=0.1$.
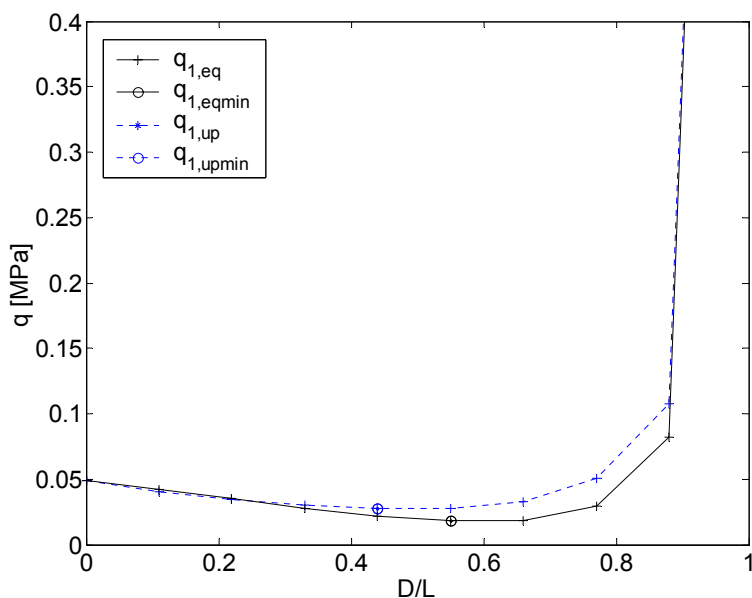

Figure 7.76.Results of calculations by equations (7.76) to (7.101) (solid) and numerical calculations (dashed) on a slab with $L_x=L_y= 2000mm, \Phi_{0x}=\Phi_{0x}'=\Phi_{0y}=\Phi_{0y}'=0.1, h_c/h=0.1, h=60mm, fc=50MPa, u/h=1$ and $\sigma_x/f_c=\sigma_y/f_c=0.4$.

Figure 7.77.Results of calculations by equations (7.76) to (7.101) (solid) and numerical calculations (dashed) on a slab with $L_x=L_y=2000mm, \Phi_{0x}=\Phi_{0x}{}'=\Phi_{0y}=\Phi_{0y}{}'=0.1, h_c/h=0.1, h=60mm, fc=50MPa, u/h=1$ and $\sigma_x/f_c=\sigma_y/f_c=0.4.$
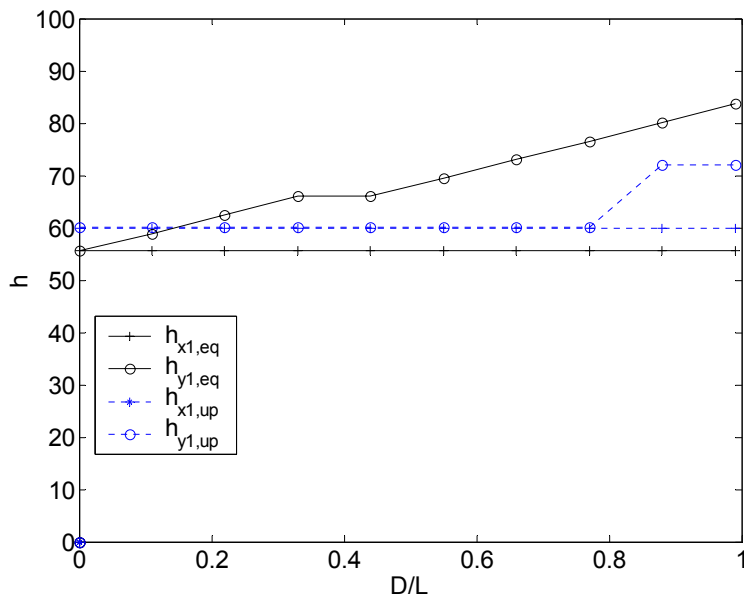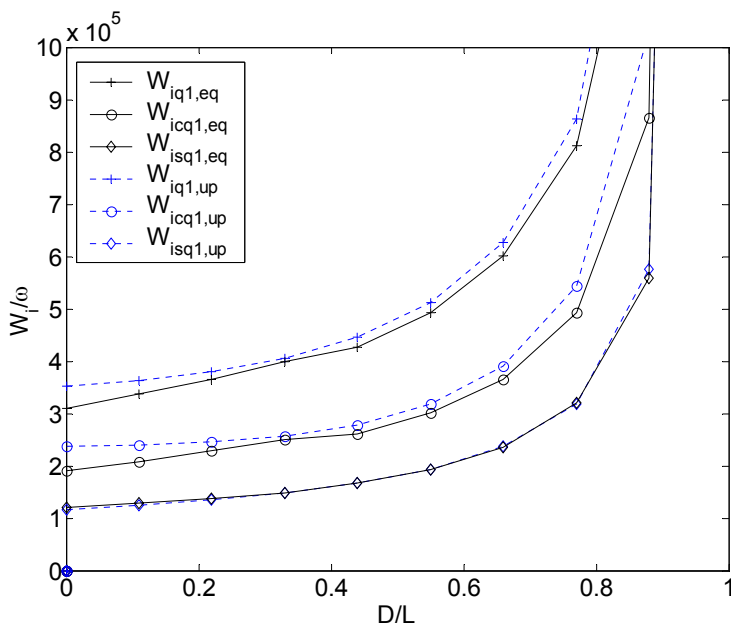

Figure 7.78.Results of calculations by equations (7.76) to (7.101) (solid) and numerical calculations (dashed) on a slab with $L_x=L_y=2000mm, \Phi_{0x}=\Phi_{0x}{}'=\Phi_{0y}=\Phi_{0y}{}'=0.1, h_c/h=0.1, h=60mm, fc=50MPa, u/h=1$ and $\sigma_x/f_c=\sigma_y/f_c=0.4.$

In the case σ/f_c=0.1 it is seen that the agreement is very good for both the load-carrying capacity and the internal work per unit deflection increase even though the position of the axes of rotation is not quite the same. Part of the error is of course due to the limited accuracy of the numerical calculations. Despite this it is seen that the position of the axes of rotation has the right performance but not entirely the correct value. The same conclusions may be made when the axial force is increased to σ/f_c=0.4.

As described previously it may be proven that equalizing the axes of rotation with the neutral axes leads to the minimum load-carrying capacity if the concrete contribution to the dissipation is calculated in the simplified way. It may be seen in these plots that it is not quite the same if the correct dissipation formulas are used but the results are close enough to furnish the correct load-carrying capacity.

It is previously shown that the simplified way of calculating the concrete contribution to the dissipation is less accurate for small values of the angle v and for large differences between the positions of the two axes of rotation. A difference in the axial force in the two directions leads to a difference in the position of the axes of rotation. Therefore, it is expected that the agreement is less good if the slab is only subjected to axial force in one direction. Results of calculations for such a case may be seen in Figure 7.79 to Figure 7.80.

It appears that the agreement is good. It is also seen that the simplified calculations lead to both over- and underestimations for different values of D/L in failure mode 2. However, it is also seen that the minimum load-carrying capacity is almost the same. It is therefore believed that the simplified method is sufficiently accurate for practical purposes.
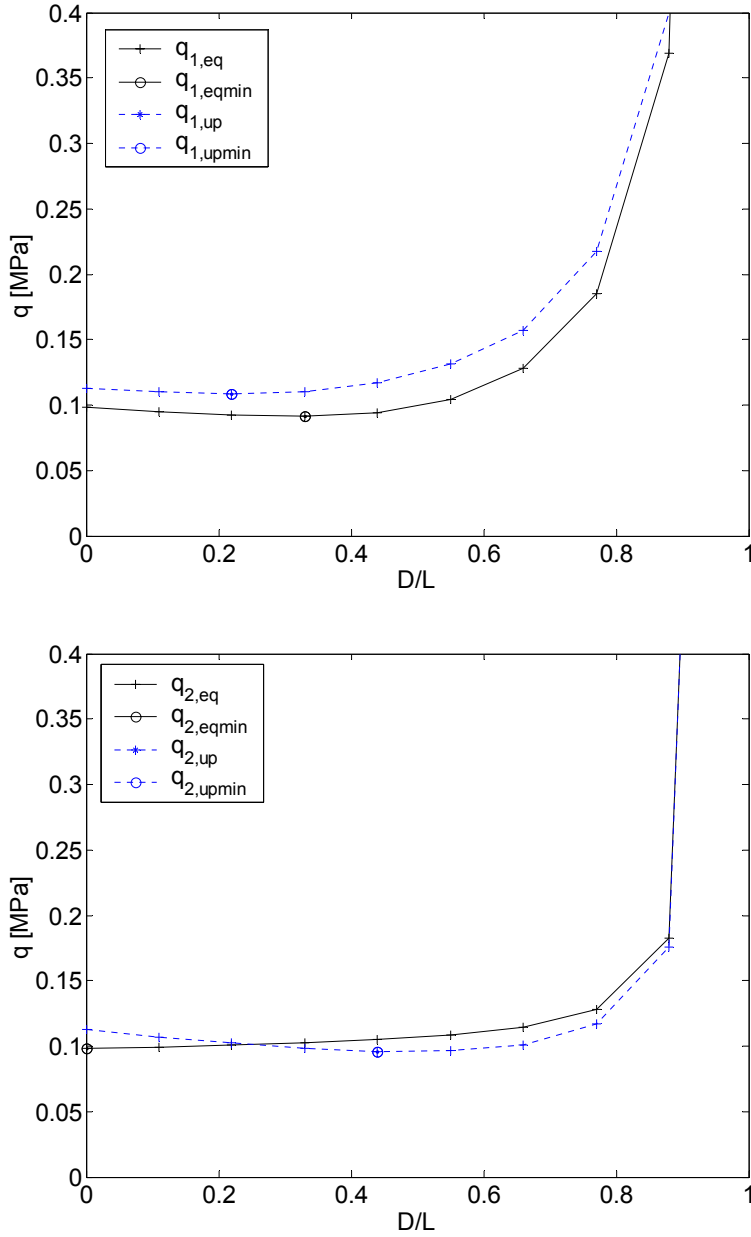
Figure 7.79.Results of calculations by equations (7.76) to (7.101) (solid) and numerical calculations (dashed) on a slab with $L_x=L_y= 2000mm, \Phi_{0x}=\Phi_{0x}{'}=\Phi_{0y}=\Phi_{0y}{'}=0.01, h_c/h=0.1,\ h=60mm, fc=50MPa, u/h=1$ and $\sigma_x/f_c=0.4,\ \sigma_y/f_c=0.$

Figure 7.80. Results of calculations by equations (7.76) to (7.101) (solid) and numerical calculations (dashed) on a slab with $L_x=L_y= 2000mm$, $\Phi_{0x}=\Phi_{0x}{}'=\Phi_{0y}=\Phi_{0y}{}'=0.01$, $h_c/h=0.1$, $h=60mm$, $fc=50MPa$, $u/h=1$ and $\sigma_x/f_c=0.4$, $\sigma_y/f_c=0$.
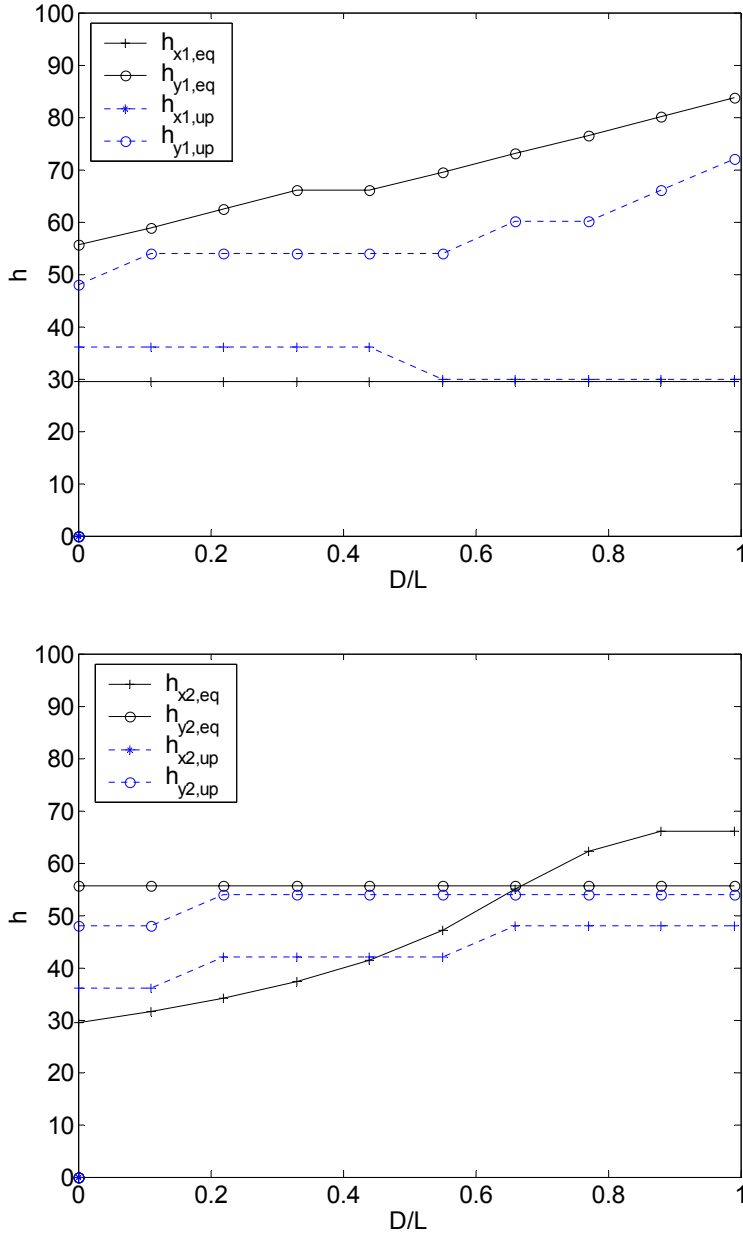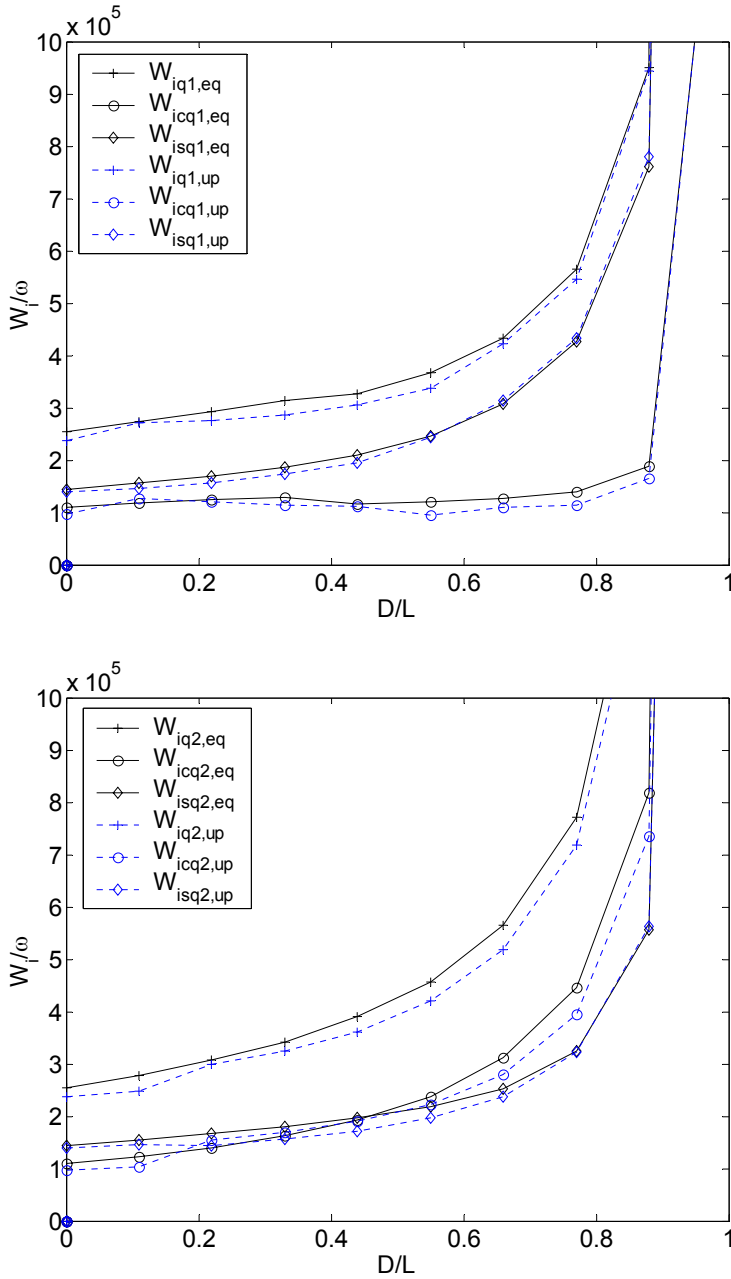
Figure 7.81 Results of calculations by equations (7.76) to (7.101) (solid) and numerical calculations (dashed) on a slab with $L_x=L_y= 2000mm, \Phi_{0x}=\Phi_{0x}{}'=\Phi_{0y}=\Phi_{0y}{}'=0.01, h_c/h=0.1, h=60mm, fc=50MPa, u/h=1$ and $\sigma_x/f_c=0.4, \sigma_y/f_c=0$

7.6 Interaction curves

It is obvious that the load-carrying capacity must be determined as the minimum for all values of *D/L*. How the load-carrying capacity should be determined in relation to the deflection is a question somewhat more difficult to answer.

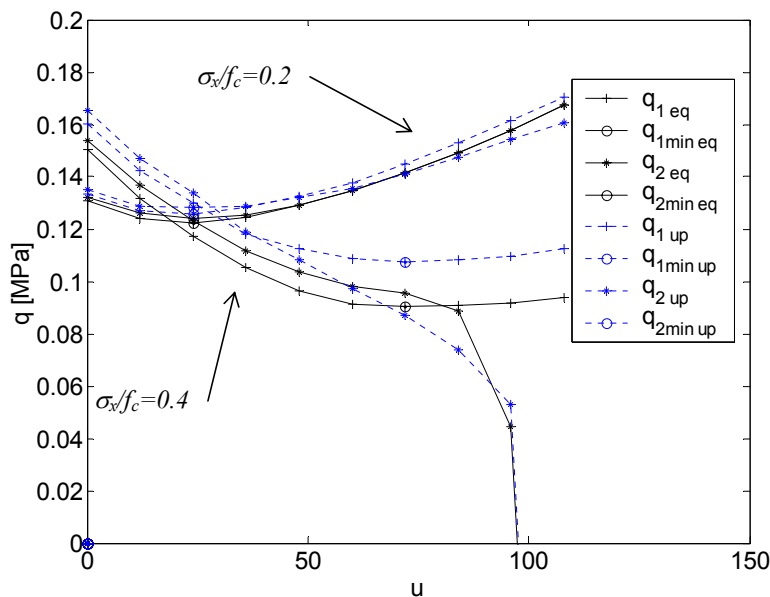In Figure 7.82 the results of calculations of the load-carrying capacity as a function of the deflection are shown.

Figure 7.82 Results of calculations by equations (8.2) to (7.101) (solid) and numerical calculations (dashed) on a slab with $L_x=L_y= 2000mm, \Phi_{0x}=\Phi_{0x}{'}=\Phi_{0y}=\Phi_{0y}{'}=0.01, h_c/h=0.1, h=60mm, fc=50MPa$ and $\sigma_x/f_c=0.4$ or 0.2, $\sigma_y/f_c=0$

For low axial force it is seen that the load-carrying capacity has a minimum with respect to the deflection. For higher axial force the load-carrying capacity decreases as the deflection increases. Assuming that the slab is perfectly rigid plastic it is obvious that the load-carrying capacity is the maximum of the load carrying capacities found for different deflections. Nevertheless, taking into consideration the actual behaviour of a concrete slab it is equally obvious that the plastic behaviour does not give the correct picture for a non-deflected slab. A more thorough investigation would take into account the actual behaviour of the concrete to determine the deflection at failure but such calculations would be cumbersome.

Instead the minimum value with respect to the deflection may be used. This is of course conservative.

Using the minimum value with respect to both *D/L* and the deflection, it is possible to calculate an interaction curve giving the load-carrying capacity for combinations of axial load and lateral load. Results from calculations with both methods are plotted in Figure 7.85 and Figure 7.88. Figure 7.85 shows results for a slab with axial force in one direction and Figure 7.88 shows results for a slab with axial force in two directions. In both cases the deflection is determined in the one corresponding to the minimum of the load-carrying capacity. It should be noted that the results are obtained through numerical calculations and that the maximum deflection is set at 110mm.
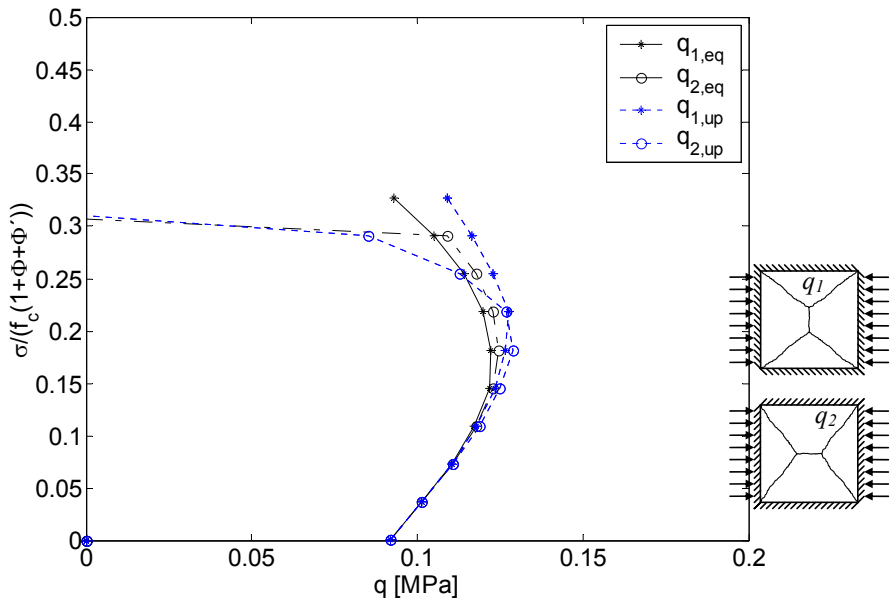

Figure 7.83 Results of calculations by equations (8.2) to (7.101) (solid) and numerical calculations (dashed) on a slab with $L_x=L_y= 2000mm, \Phi_{0x}=\Phi_{0x}{'}=\Phi_{0y}=\Phi_{0y}{'}=0.1, h_c/h=0.1, h=60mm, fc=50MPa, \sigma_y/f_c=0$.

Figure 7.84 Results of calculations by equations (8.2) to (7.101) (solid) and numerical calculations (dashed) on a slab with $L_x=L_y= 2000mm, \Phi_{0x}=\Phi_{0x}'=\Phi_{0y}=\Phi_{0y}'=0.1, h_c/h=0.1, h=60mm, fc=50MPa, \sigma_y/f_c=0$.
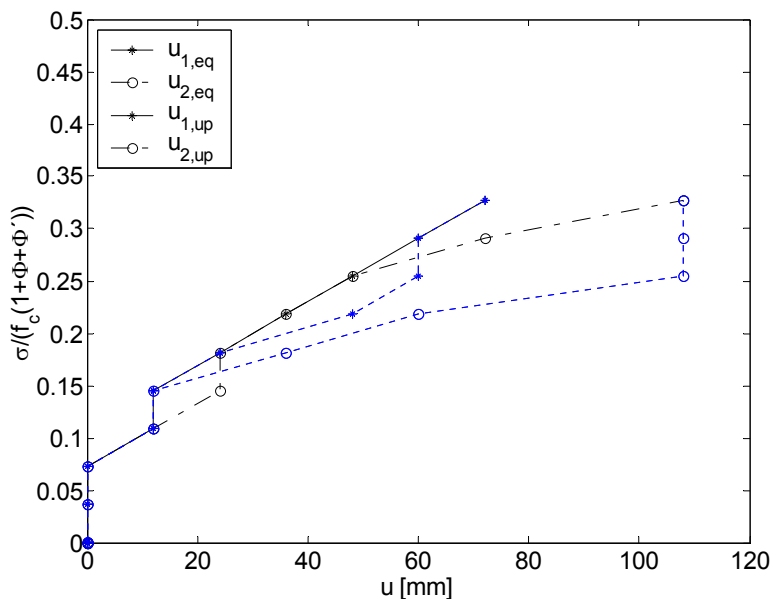

Figure 7.85. Results of calculations by equations (8.2) to (7.101) (solid) and numerical calculations (dashed) on a slab with $L_x=L_y= 2000mm, \Phi_{0x}=\Phi_{0x}'=\Phi_{0y}=\Phi_{0y}'=0.1, h_c/h=0.1, h=60mm, fc=50MPa, \sigma_y/f_c=0$.

Figure 7.86Results of calculations by equations (8.2) to (7.101) (solid) and numerical calculations (dashed) on a slab with $L_x=L_y=$ 2000mm, $\Phi_{0x}=\Phi_{0x}{}'=\Phi_{0y}=\Phi_{0y}{}'=0.1, h_c/h=0.1$, h=60mm, fc=50MPa, $\sigma_y=\sigma_x$
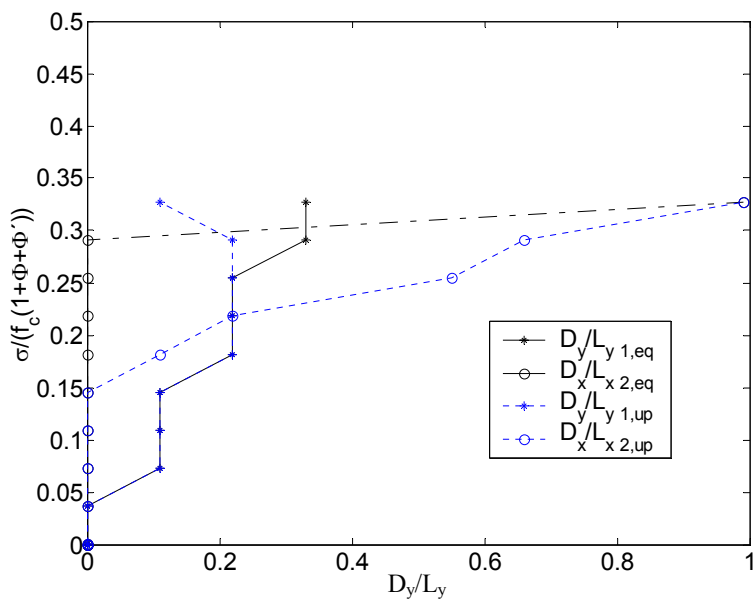

Figure 7.87Results of calculations by equations (8.2) to (7.101) (solid) and numerical calculations (dashed) on a slab with $L_x=L_y=$ 2000mm, $\Phi_{0x}=\Phi_{0x}{}'=\Phi_{0y}=\Phi_{0y}{}'=0.1, h_c/h=0.1$, h=60mm, fc=50MPa, $\sigma_y=\sigma_x$.
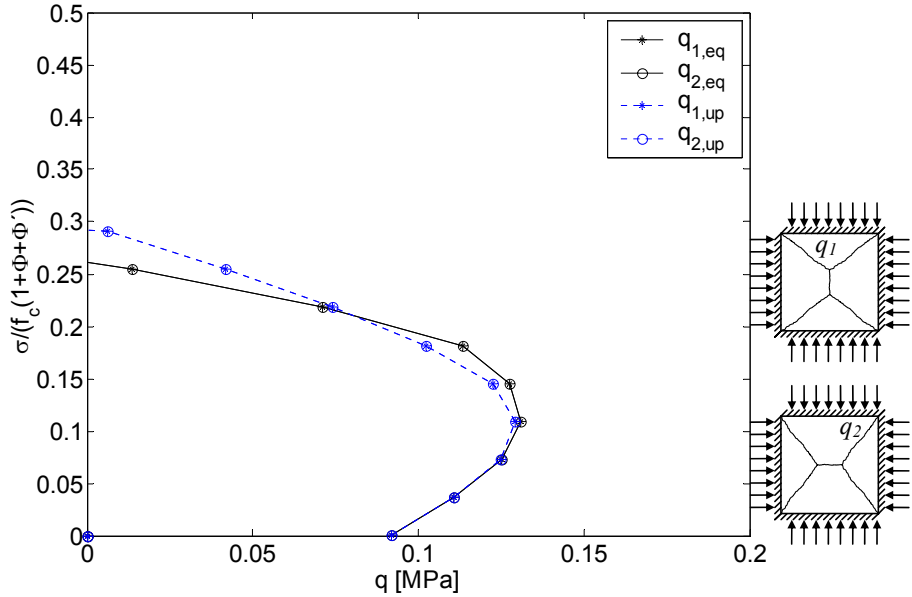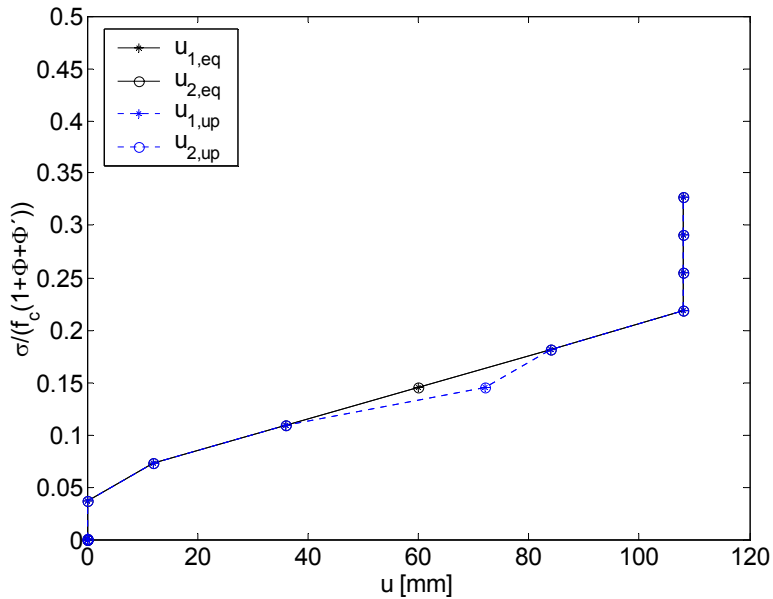
Figure 7.88. Results of calculations by equations (8.2) to (7.101) (solid) and numerical calculations (dashed) on a slab with $L_x=L_y= 2000mm, \Phi_{0x}=\Phi_{0x}{}'=\Phi_{0y}=\Phi_{0y}{}'=0.1, h_c/h=0.1, h=60mm, fc=50MPa, \sigma_y=\sigma_x$.

These figures (Figure 7.83 to Figure 7.88) confirm that using the neutral axes as the axes of rotation and combining this assumption with the simplified way of calculating the dissipation lead to a load-carrying capacity close to the theoretically correct one. This goes for slabs subjected to axial force in both one and two directions. It is also seen that the failure form (*D/L*) and the deflection at failure is not found to be the same in the two methods. Nevertheless, the most important issue here is the load-carrying capacity and it is seen that this is quite accurate.

For rectangular slabs with a L_x/L_y ratio different from one, the simplified calculation method is not as good as for the square slabs. Examples of this may be seen in Figure 7.89 to Figure 7.95
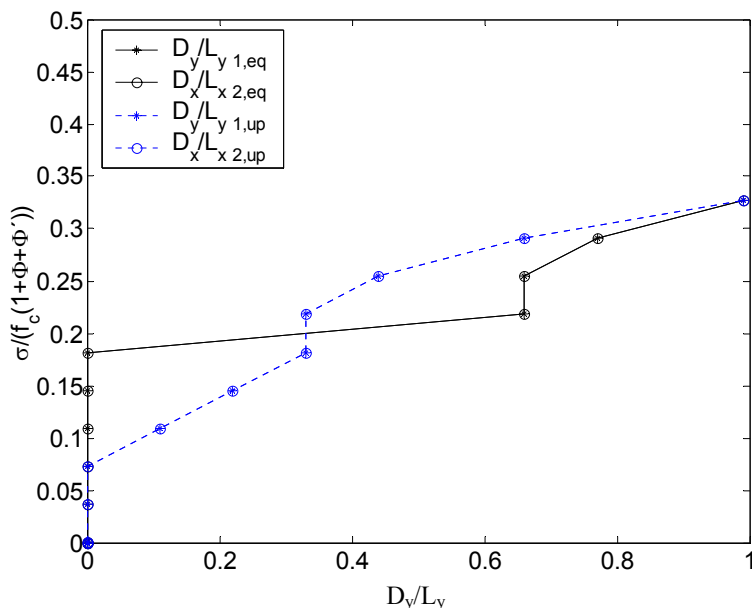
Figure 7.89. Results of calculations by equations (8.2) to (7.101) (solid) and numerical calculations (dashed) on a slab with $L_x=2000mm$, $L_y=1000mm$, $\Phi_{0x}=\Phi_{0x}{}'=\Phi_{0y}=\Phi_{0y}{}'=0.1$, $h_c/h=0.1$, $h=60mm$, $fc=50MPa$, $\sigma_y=\sigma_x$.

Figure 7.90 Results of calculations by equations (8.2) to (7.101) (solid) and numerical calculations (dashed) on a slab with $L_x=2000mm$, $L_y=1000mm$, $\Phi_{0x}=\Phi_{0x}{}'=\Phi_{0y}=\Phi_{0y}{}'=0.1$, $h_c/h=0.1$, $h=60mm$, $fc=50MPa$, $\sigma_y=\sigma_x$.

Figure 7.91 Results of calculations by equations (8.2) to (7.101) (solid) and numerical calculations (dashed) on a slab with $L_x=2000mm$, $L_y=1000mm$, $\Phi_{0x}=\Phi_{0x}{'}=\Phi_{0y}=\Phi_{0y}{'}=0.1$, $h_c/h=0.1$, $h=60mm$, $fc=50MPa$, $\sigma_y=\sigma_x$.
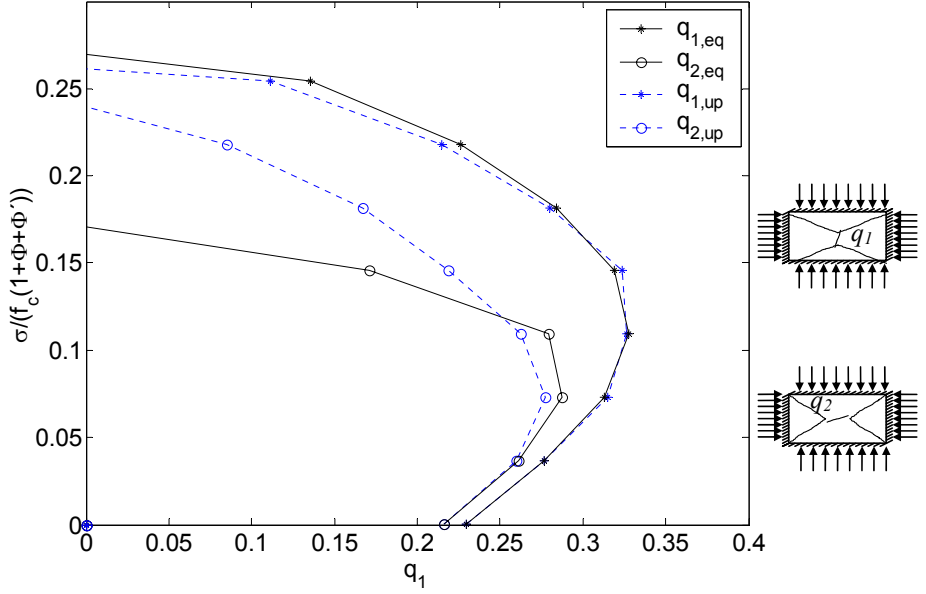

Figure 7.92 Results of calculations by equations (8.2) to (7.101) (solid) and numerical calculations (dashed) on a slab with $L_x=2000mm$, $L_y=1000mm$, $\Phi_{0x}=\Phi_{0x}{'}=\Phi_{0y}=\Phi_{0y}{'}=0.1$, $h_c/h=0.1$, $h=60mm$, $fc=50MPa$, $\sigma_y=0$.
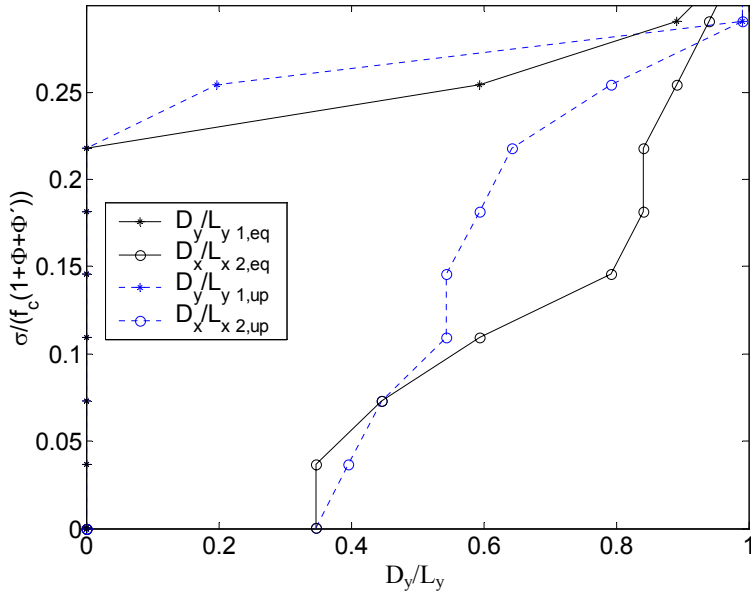
Figure 7.93 Results of calculations by equations (8.2) to (7.101) (solid) and numerical calculations (dashed) on a slab with L_x=2000mm, L_y=1000mm, Φ_{0x}=Φ_{0x}´=Φ_{0y}=Φ_{0y}´=0.1,h_c/h=0.1, h=60mm, fc=50MPa, σ_y=0.

Figure 7.94 Results of calculations by equations (8.2) to (7.101) (solid) and numerical calculations (dashed) on a slab with L_x=2000mm, L_y=1000mm, Φ_{0x}=Φ_{0x}´=Φ_{0y}=Φ_{0y}´=0.1,h_c/h=0.1, h=60mm, fc=50MPa, σ_y=0.
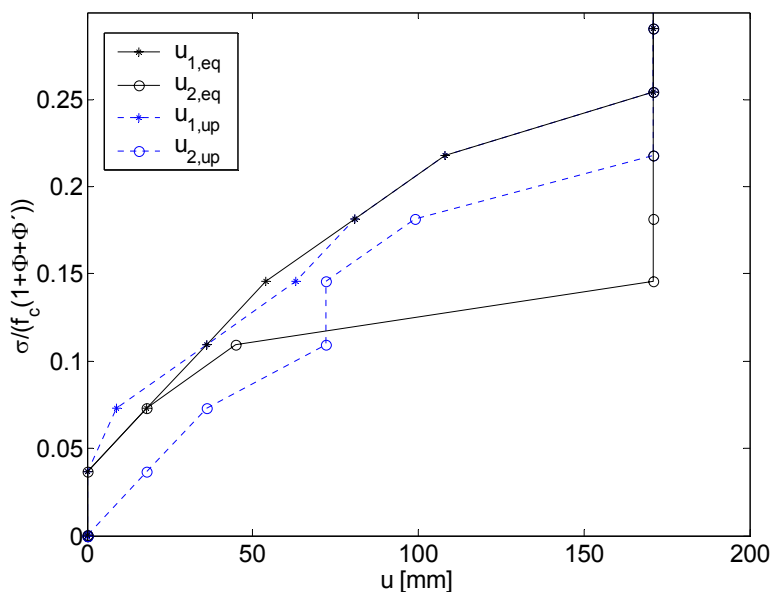
Figure 7.95. Results of calculations by equations (8.2) to (7.101) (solid) and numerical calculations (dashed) on a slab with $L_x=2000mm$, $L_y=1000mm$, $\Phi_{0x}=\Phi_{0x}{'}=\Phi_{0y}=\Phi_{0y}{'}=0.1$, $h_c/h=0.1$, $h=60mm$, $fc=50MPa$, $\sigma_x=0$.

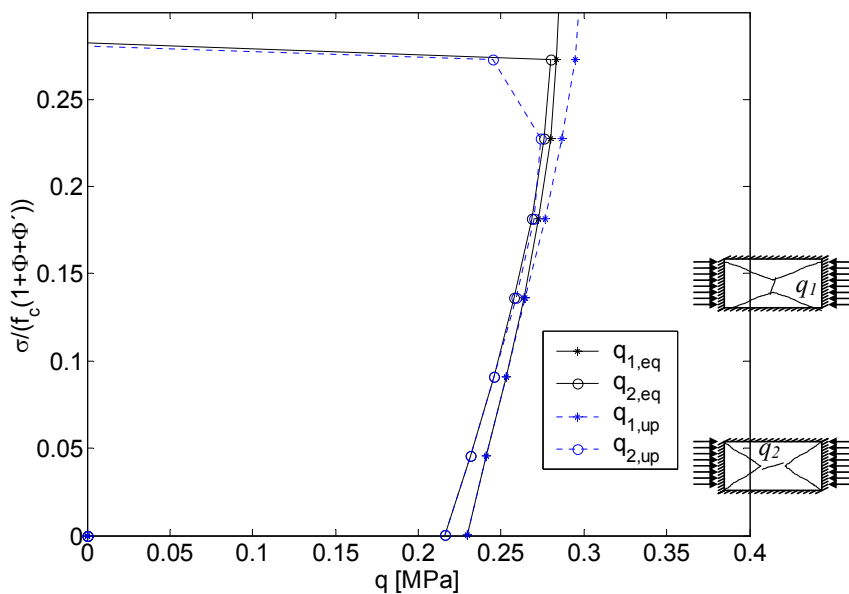*Figure 7.96 Results of calculations by equations (8.2) to (7.101) (solid) and numerical calculations (dashed) on a slab with $L_x=2000mm$, $L_y=1000mm$, $\Phi_{0x}=\Phi_{0x}{'}=\Phi_{0y}=\Phi_{0y}{'}=0.1$, $h_c/h=0.1$, $h=60mm$, $fc=50MPa$, $\sigma_x=0$.*
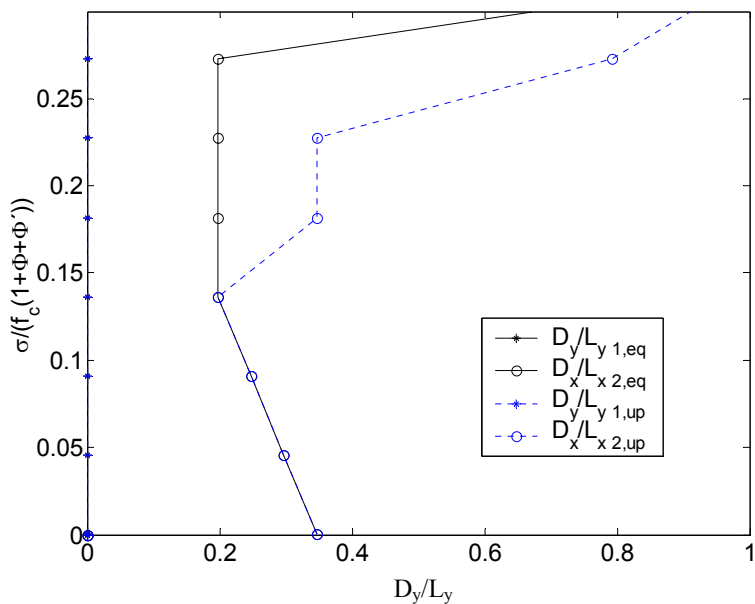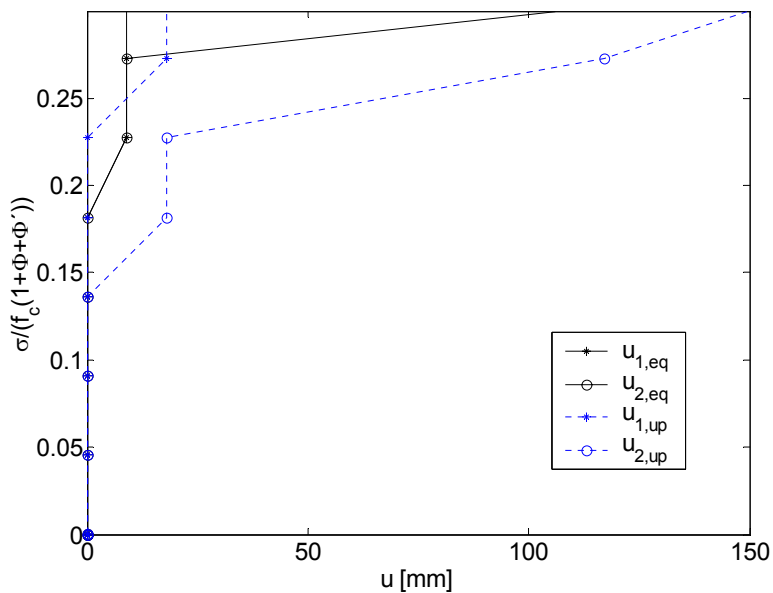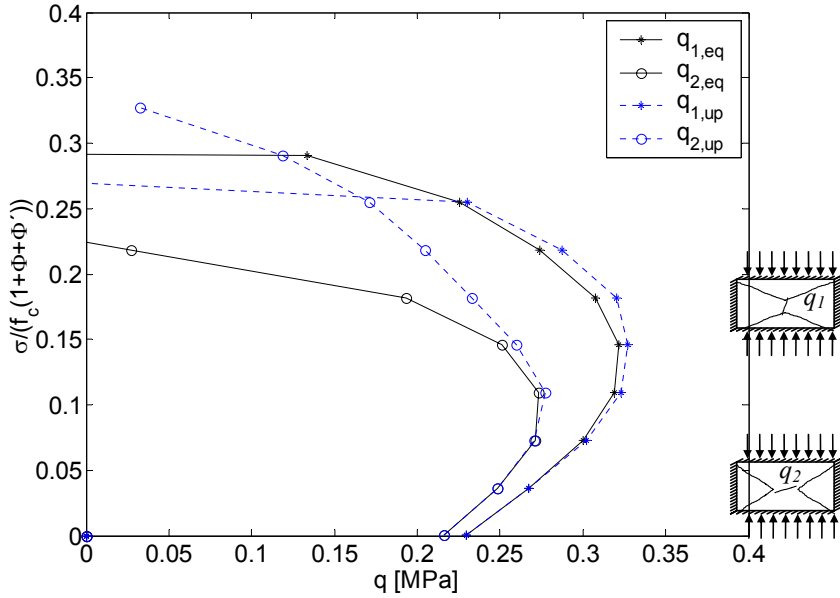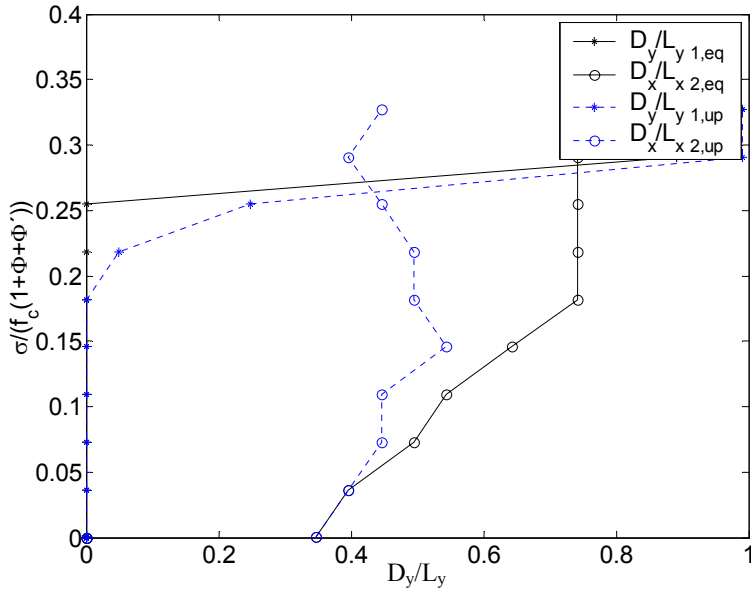
Figure 7.97 Results of calculations by equations (8.2) to (7.101) (solid) and numerical calculations (dashed) on a slab with $L_x=2000mm$, $L_y=1000mm$, $\Phi_{0x}=\Phi_{0x}{}'=\Phi_{0y}=\Phi_{0y}{}'=0.1$, $h_c/h=0.1$, $h=60mm$, $fc=50MPa$, $\sigma_x=0$.

It may be seen that the simplified calculations underestimate the load-carrying capacity somewhat for rectangular slabs with axial force in both directions and also for rectangular slabs with axial force perpendicular to the longer side. Nevertheless, it is believed that the simplified calculation method is still useful due to the simplicity of the calculations.

From the interaction curves it appears that the curve at a certain level of axial force almost makes a cut off. At this point the deflection actually goes towards infinity. In these figures the deflection is limited to 170mm in order to keep the number of calculations at a reasonable level. This axial force corresponds to stability failure. The slab may carry the load in a non-deflected state but a small deflection would lead to collapse of the slab.

In an actual slab the level of stability found in this way is of course not quite correct since the slab may be far from a plastic state close to the non-deflected state and only gets closer to plastic states as the deflection increases. Therefore, a cut off level as the one seen in the interaction diagram Figure 7.92 may not be expected to be verified by experiments.

8   Theory compared with tests

Only a few experimental investigations have been made on simply supported slabs subjected to both lateral and transverse loads. A. O. Aghayere and J. G. MacGregor (see [4]) made a test series, but because of the variation of many parameters (reinforcement ratio, concrete strength etc.) these tests are not very useful for the verification of the theory. Instead some of the tests made by L. Z. Hansen and T. Gudmand-Høyer (see[6]) are used.

The main data are given in Table 8.1 and Table 8.2.

No	f_c	E_c	f_Y	e	h	Layer	A_{sx}	h_{cx}	ρ_{0x}	l_x	h_{cv}	A_{sv}	ρ_{0v}	l_v
	[MPa]	[MPa]	[MPa]	[mm]	[mm]		[mm²/m]	[mm]	[ ]	[mm]	[mm]	[mm²/m]	[ ]	[mm]
3	60,4	18081	593	0	61,66	1	523,6	35	0,008	2000	25	523,6	0,0085	2000
4	59,5	17425	593	0	62,03	1	523,6	35	0,008	2000	25	523,6	0,0084	2000
5	58,8	17662	593	0	61,63	1	523,6	35	0,008	2000	25	523,6	0,0085	2000
6	64,6	18688	593	0	61,37	1	523,6	35	0,009	2000	25	523,6	0,0085	2000
7	64,0	18466	593	0	61,26	1	523,6	35	0,009	2000	25	523,6	0,0085	2000
8	61,4	17718	593	0	60,99	1	523,6	35	0,009	2000	25	523,6	0,0086	2000
9	66,7	18744	593	0	61,56	1	523,6	35	0,009	2000	25	523,6	0,0085	2000
16	66,7	19394	593	0	61,48	1	523,6	35	0,009	2000	25	523,6	0,0085	2000

Table 8.1. The data of the reinforced slabs.

No	q	N_x	u	Notes
	[kN/m²]	[kN/m]	[mm]	
3	74,5	0,0	78	Material failure
4	21,5	1084,1	29	Rig failure
5	33,2	462,9	53	Stability failure
6	25,1	653,3	46	Stability failure
7	41,5	436,0	61	Stability failure
8	16,7	800,0	42	Stability failure
9	8,5	1103,4	17	Material failure
16	25,1	1030,1	37	Material failure

Table 8.2. The results of the tests.

The following calculation are made for a slab with f_c=60MPa, f_y=593MPa, h=60mm, h_{cm}/h=0.5, L_x=L_y=2000mm, Φ'_x=Φ'_y=$0.0085f_y/f_c$, Φ_x=Φ_y=0 if nothing else is mentioned.

If the conservative simplified method proposed in the previous chapter is used to calculate the load-carrying capacity for the slabs tested the results in Figure 8.1 to Figure 8.3 are obtained.

Figure 8.1 Results of calculations for a slab with $f_c=60MPa$, $f_y=593MPa$, $h=60mm$, $h_{cm}/h=0.5$, $L_x=L_y=2000mm$, $\Phi'_x=\Phi'_y=0.0085f_y/f_c$, $\Phi_x=\Phi_y=0$ and $v=1$.

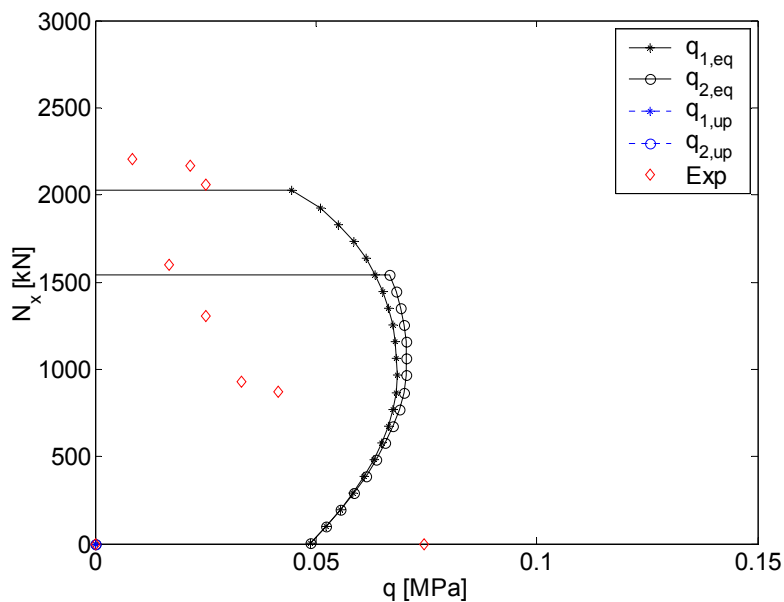*Figure 8.2 Results of calculations for a slab with $f_c=60MPa$, $f_y=593MPa$, $h=60mm$, $h_{cm}/h=0.5$, $L_x=L_y=2000mm$, $\Phi'_x=\Phi'_y=0.0085f_y/f_c$, $\Phi_x=\Phi_y=0$ and $v=1$.*

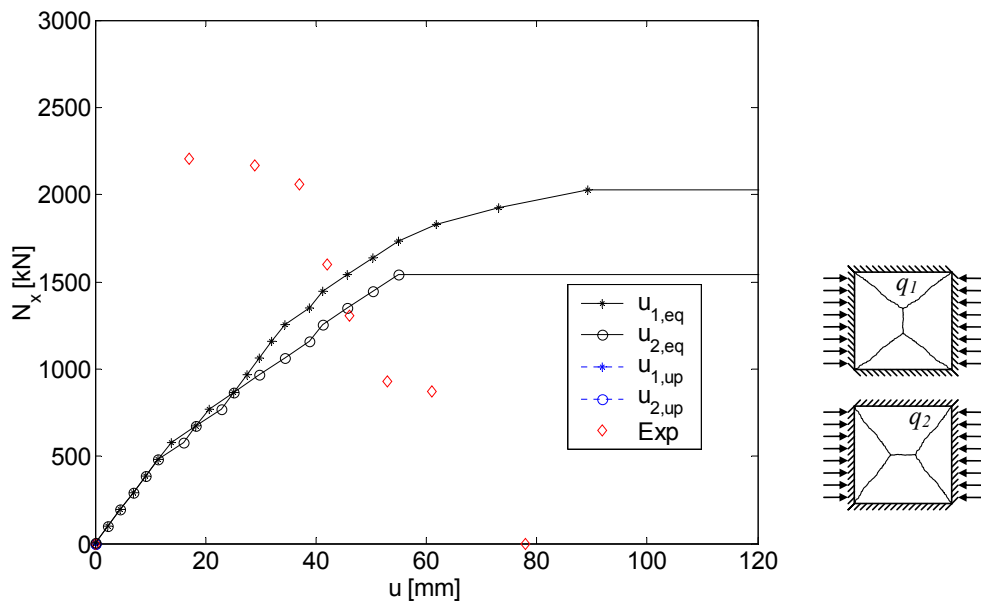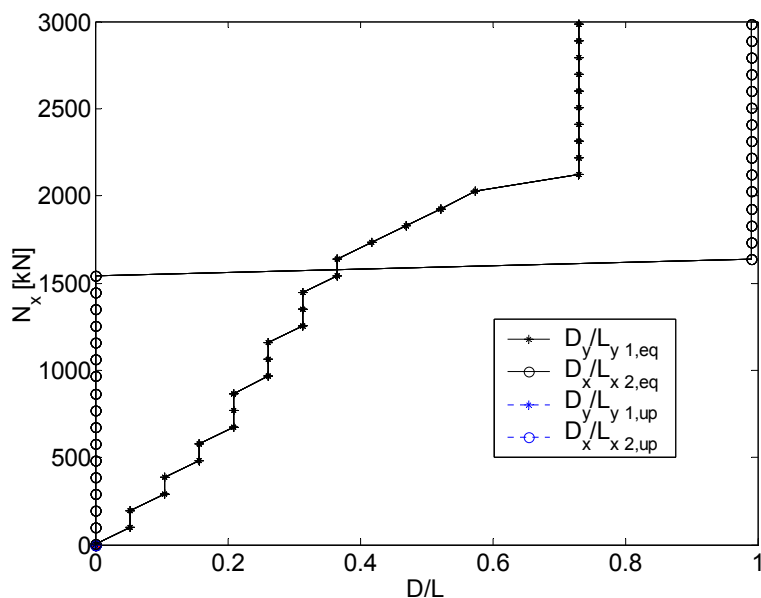*Figure 8.3 Results of calculations for a slab with f_c=60MPa, f_y=593MPa, h=60mm, h_{cm}/h=0.5, L_x=L_y=2000mm, Φ'_x=Φ'_y=0.0085f_y/f_c, Φ_x=Φ_y=0 and ν=1.*

It is obvious that the theoretical load-carrying capacity is much too high. This is of course expected since it is known that the concrete does not behave entirely according to plastic theory so an effectiveness factor should therefore be introduced.

Besides from the load-carrying capacity being much too high, also the deflection is wrong. Not only is it wrong when it comes to the numerical value but also when it comes to the relation between axial force and deflection. The experiments shows that the deflection decreases as the axial force increases and the conservative method of calculation shows the opposite relation. This tendency is also expected to a certain extent. For instance it is obvious that for no axial force the conservative method of calculation corresponds to zero deflection whereas in the tests the slabs of course will have some deflection.

In order to determine the effectiveness factor, interaction curves are found using the measured deflection (an approximate line close to the measured points). In Figure 8.4 and Figure 8.5 the results are shown for both ν=1 and ν=0.45 (f_c is set to 0.45•60MPa)

Figure 8.4. Effectivenessfactor $v=0.45$ or $v=1$. Results of calculations for a slab with $f_c=60MPa$, $f_y=593MPa$, $h=60mm$, $h_{cm}/h=0.5$, $L_x=L_y=2000mm$, $\Phi'_x=\Phi'_y=0.0085f_y/f_c$, $\Phi_x=\Phi_y=0$.

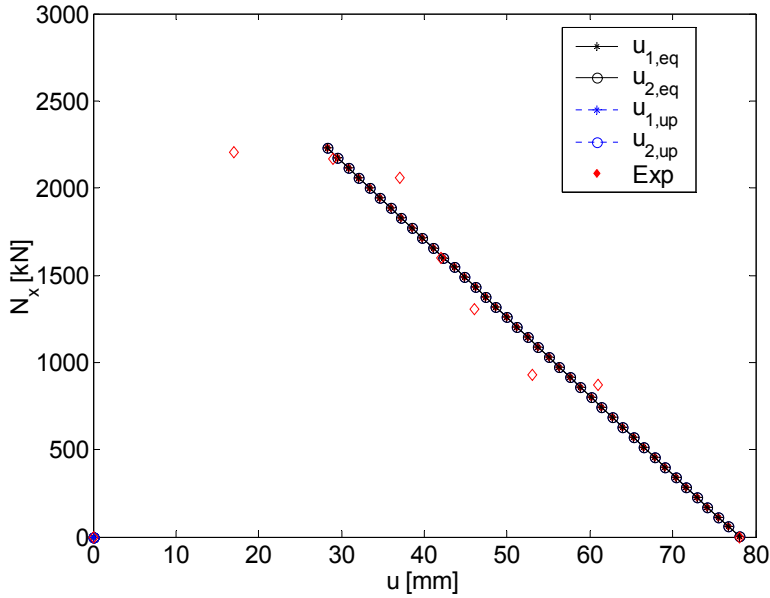*Figure 8.5 Results of calculations for a slab with $f_c=60MPa$, $f_y=593MPa$, $h=60mm$, $h_{cm}/h=0.5$, $L_x=L_y=2000mm$, $\Phi'_x=\Phi'_y=0.0085f_y/f_c$, $\Phi_x=\Phi_y=0$.*

It is seen that if v is set to 0.45 the calculations are in good agreement with the experiments.

This effectiveness factor is quite small compared to the effectiveness factors normally used in calculations of moment capacities (approx. 0.85). In evaluation of such an effectiveness factor one should keep in mind that the strains in the yield lines may be far from the yield strains. Assuming that the yield strain for concrete is 3.5 ‰ and that the yield strain is 1,465‰ for the reinforcement the deflection at the midpoint would approximately be

$$u_m = \frac{1}{10} \frac{2+1.465}{30 \cdot 1000} 2000^2 = 66mm \tag{8.1}$$

if the stresses in the mid section should be close to the yield stresses. Keeping in mind that a deflection of 66mm only leads to yielding in the top of the compression zone in the midpoint and not in the remaining parts of the yield line, it may seem reasonable that the effectiveness factor of the magnitude found above has to be used.

If ν is set to 0.45 and the conservative simplified method is used to calculate the load-carrying capacity, Figure 8.6 and Figure 8.7 are obtained.
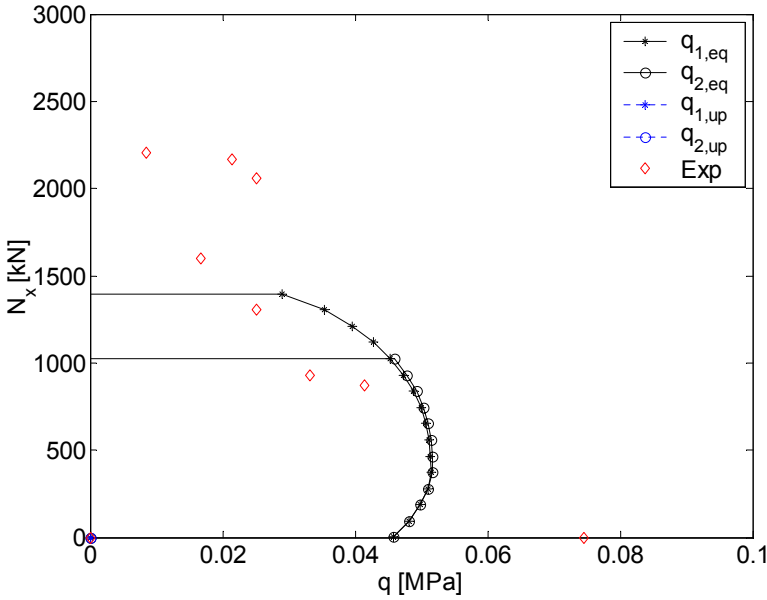

Figure 8.6. Results of calculations for a slab with f_c=60MPa, f_y=593MPa, h=60mm, h_{cm}/h=0.5, L_x=L_y=2000mm, Φ'_x=Φ'_y=0.0085f_y/f_c, Φ_x=Φ_y=0 and ν=0.45.

Figure 8.7. Results of calculations for a slab with f_c=60MPa, f_y=593MPa, h=60mm, h_{cm}/h=0.5, L_x=L_y=2000mm, Φ'_x=Φ'_y=0.0085f_y/f_c, Φ_x=Φ_y=0 and v=0.45.

It is seen that this approximation does not lead to useful results since the deviation from the tests is very large.

Another approach could be to use the deflection corresponding to yielding in mid-section (in this case 66mm) for all axial forces. A similar approach is used in calculations of reinforced concrete columns and one might suspect that it might give useful results for slabs as well. Results using this approximation may be seen in Figure 8.8 and Figure 8.9.

It appears that the results are closer to the values from tests. Nevertheless, these results only represent one slab type and further investigations and tests have to be made in order to verify the approach.

Figure 8.8. Results of calculations for a slab with f_c=60MPa, f_y=593MPa, h=60mm, h_{cm}/h=0.5, L_x=L_y=2000mm, Φ'_x=Φ'_y=0.0085f_y/f_c, Φ_x=Φ_y=0 and v=0.45.

Figure 8.9. Results of calculations for a slab with f_c=60MPa, f_y=593MPa, h=60mm, h_{cm}/h=0.5, L_x=L_y=2000mm, Φ'_x=Φ'_y=0.0085f_y/f_c, Φ_x=Φ_y=0 and v=0.45.

These comparisons with test results show that the theory developed may be used if the deflection at failure is known and a proper effectiveness factor is introduced.

If the deflection at failure is unknown the conservative simplified method may be used but it will lead to a large underestimation for low axial forces.

Using a deflection corresponding to the yield strain in concrete and reinforcement in the mid section for all levels of axial force seems to lead to reasonable agreement with tests.

From a critical point of view it may be said that this way of calculating the load-carrying capacity does not lead to any simple and useful calculation since the deflection has to be known from either experiments or from calculations that involve a much more detailed description of the behaviour of concrete.

9 Conclusion

In this paper it is shown that calculations of the load-carrying capacity of rectangular slabs using the K.W. Johansen method agree with a calculation based on the correct dissipation formulas that is sufficiently correct for practical purposes.

Furthermore, it is shown that for a deflected rectangular slab with axial force the load-carrying capacity may be calculated in the same way if the axes of rotation correspond to the neutral axes of the slab parts.

Only rectangular slabs have been treated here but the agreement between the concrete contribution to the dissipation calculated according to the K.W. Johansen method and according to the correct dissipation formulas for a Coulomb material has been investigated in general. It is shown that if the corner angle w is larger than $1/2\pi$ the Johansen simplification underestimates the dissipation and if w is less than $1/2\pi$ the simplification overestimates the dissipation.

Only tests with seven rectangular slabs with axial force in one direction have been used for verification of the theory and the conclusions are therefore not general. Furthermore, it should be noted that due to the small number of tests no great effort has been made in order to determine the effectiveness factor ν.

However, it has been shown that if a proper effectiveness factor is used, the calculations seem to be in good agreement under the condition that the deflection at failure is known.

A conservative approach using the minimum load-carrying capacity for all deflections leads to a large underestimation in some cases and thus can only be recommended as a rough estimate.

If the deflection corresponding to yield strains of the concrete and the reinforcement is used for all levels of axial force, predictions of the load-carrying capacity seem to be reasonable.

10 Literature

The list is ordered by year.

[1]   JOHANSEN, K.W., Brudlinieteorier (Yield line theories), *Copenhagen, Gjellerup, 1943.*

[2]   CALLADINE, C.R., Simple Ideas in the Large-Deflection Plastic Theory of Plates and Slabs, Engineering Plasticity, HEYMAN J. and LECKIE, F. A. eds. , *pp. 93-127, Cambridge, Cambridge University Press, 1968*

[3]   NIELSEN, M. P. and RATHKJEN, A.: Mekanik 5.1. Del 2 Skiver og plader, *Danmarks Ingeniørakadami, Bygningsafdelingen, Aalborg, Den Private Ingeniørfond, 1981.*

[4]   AGHAYERE, A. O. and MACGREGOR, J. G., Test of reinforced Concrete Plates under Combined In-Plane and Transverse Loads, *ACI Structural Journal, V. 87, No. 6, pp. 615-622, 1990*

[5]   NIELSEN, M. P.: Limit Analysis and Concrete Plasticity, *Second Edition, CRC Press, 199*8

[6]   HANSEN, L. Z., GUDMAND-HØYER, T.: Instability of Concrete Slabs, *Department of Structural Engeneering and Materials, R-042, ISSN 1601-2917, ISBN 87-7877-101-3, Technical University of Denmark, 2001*

11 Appendix

11.1.1 Results of calculations for different slabs

11.1.1.1 Square slab without axial force

Figure 11.1. Load-carrying capacity q_1 for a square slab with L=2000mm, $\Phi_0=\Phi_0'=0.1$, $h_c/h= h_c'/h=0.1$, $f_c=30MPa$ (solid) and load-carrying capacity according to (7.39) (dashed) at the left hand side and position of the axes of rotation at the right hand side.

Figure 11.2. Load-carrying capacity q_1 for a square slab with L=2000mm, $\Phi_0=\Phi_0'=0.05$, $h_c/h= h_c'/h=0.2$, $f_c=30MPa$ (solid) and load-carrying capacity according to (7.39) (dashed) at the left hand side and position of the axes of rotation at the right hand side.
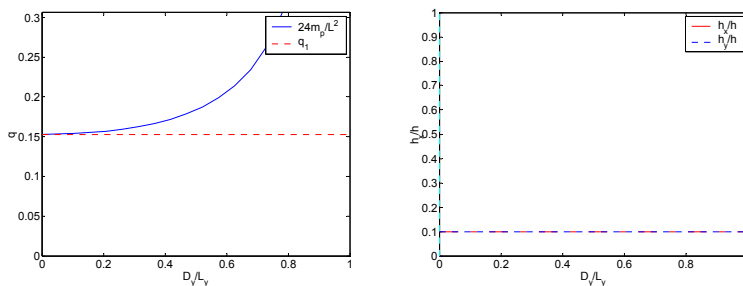
Figure 11.3. Load-carrying capacity q_1 for a square slab with L=2000mm, $\Phi_0=\Phi_0{}'=0.1$, $h_c/h= h_c{}'/h=0.2$, $f_c=30MPa$ (solid) and load-carrying capacity according to (7.39) (dashed) at the left hand side and position of the axes of rotation at the right hand side.
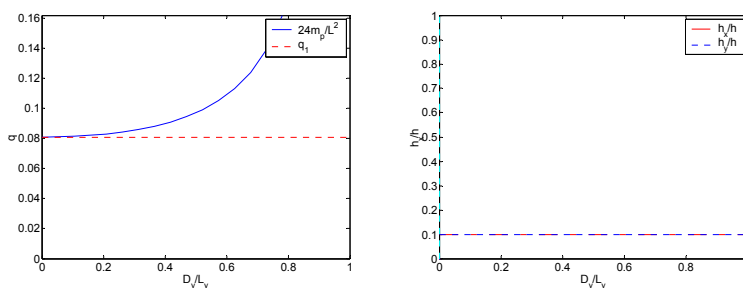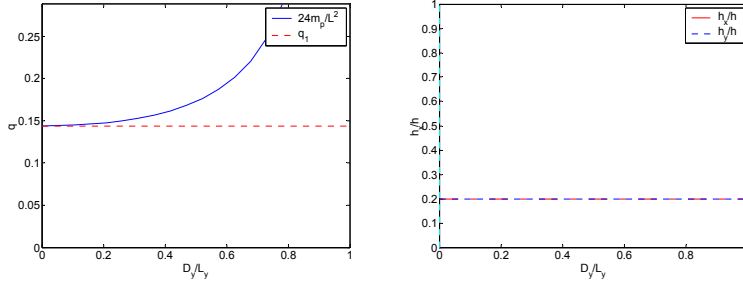
11.1.1.2 Rectangular slab without axial force

Figure 11.4. Load-carrying capacity q_1 for a rectangular slab $L_x=2000mm$, $L_y=16000mm$, $\Phi_{0x}=\Phi_{0x}{}'=\Phi_{0y}=\Phi_{0y}{}'=0.1$, $h_{cx}/h= h_{cx}{}'/h= h_{cy}/h= h_{cy}{}'/h=0.1$, $f_c=30MPa$ (solid) and load-carrying capacity according to (7.48) or (7.50) at the left hand side and position of the axes of rotation at the right hand side.

Figure 11.5. Load-carrying capacity q_1 for a rectangular slab $L_x=2000mm$, $L_y=16000mm$, $\Phi_{0x}=\Phi_{0x}{}'=\Phi_{0y}=\Phi_{0y}{}'=0.05$, $h_{cx}/h= h_{cx}{}'/h= h_{cy}/h= h_{cy}{}'/h=0.2$, $f_c=30MPa$ (solid) and load-carrying capacity according to (7.48) or (7.50) at the left hand side and position of the axes of rotation at the right hand side.

Figure 11.6. Load-carrying capacity q_1 for a rectangular slab $L_x=2000mm$, $L_y=16000mm$, $\Phi_{0x}=\Phi_{0x}{}'=0.1$, $\Phi_{0y}=\Phi_{0y}{}'=0.05$, $h_{cx}/h=h_{cx}{}'/h=h_{cy}/h=h_{cy}{}'/h=0.2$, $f_c=30MPa$ (solid) and load-carrying capacity according to (7.48) or (7.50) at the left hand side and position of the axes of rotation at the right hand side.

Figure 11.7. Load-carrying capacity q_1 for a rectangular slab $L_x=2000mm$, $L_y=4800mm$, $\Phi_{0x}=\Phi_{0x}{}'=0.7$, $\Phi_{0y}=\Phi_{0y}{}'=0.1$, $h_{cx}/h=h_{cx}{}'/h=h_{cy}/h=h_{cy}{}'/h=0.1$, $f_c=30MPa$ (solid) and load-carrying capacity according to (7.48) or (7.50) at the left hand side and position of the axes of rotation at the right hand side.

Figure 11.8. Load-carrying capacity q_1 for a rectangular slab $L_x=2000mm$, $L_y=4800mm$, $\Phi_{0x}=\Phi_{0x}{}'=0.3$, $\Phi_{0y}=\Phi_{0y}{}'=0.05$, $h_{cx}/h=h_{cx}{}'/h=h_{cy}/h=h_{cy}{}'/h=0.1$, $f_c=30MPa$ (solid) and load-carrying capacity according to (7.48) or (7.50) at the left hand side and position of the axes of rotation at the right hand side.

11.1.1.3 Rectangular slab with axial force

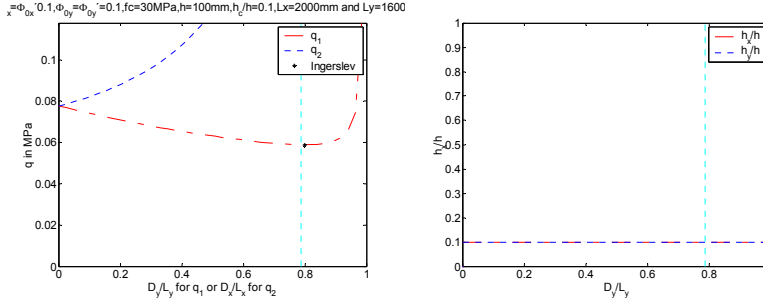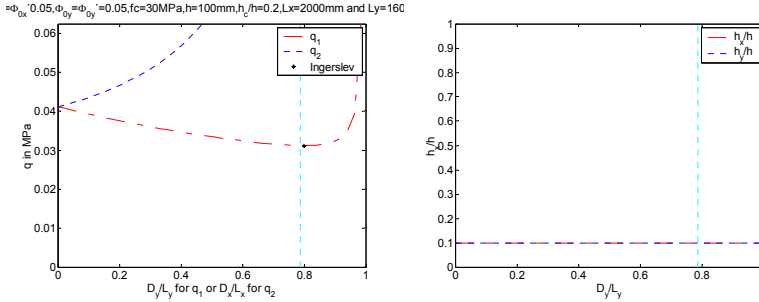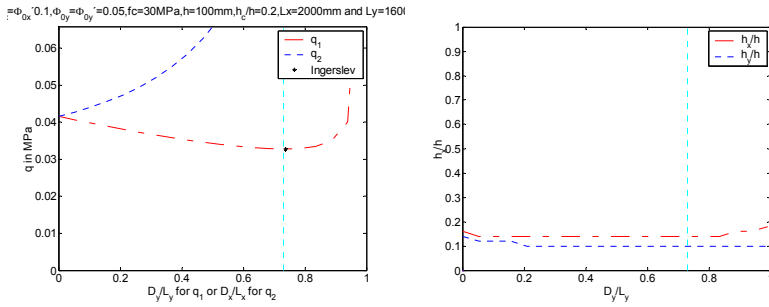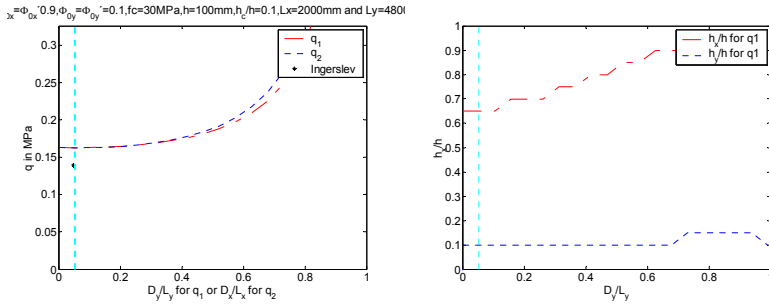*Figure 11.9. Load-carrying capacity (top left hand side), difference between the calculation methods (top right hand side), length of the part of the yield line parallel to the axes of rotation (middle left hand side), position of the axes of rotation for failure mode 1(middle left hand side) and position of the axes of rotation for failure mode 2(bottom) for a rectangular slab $L_x=2000mm$, $L_y=2000mm$, $\Phi_{0x}=\Phi_{0x}{}'=0.1$, $\Phi_{0y}=\Phi_{0y}{}'=0.1$, $h_{cx}/h= h_{cx}{}'/h= h_{cy}/h= h_{cy}{}'/h=0.1$, $f_c=30MPa$, increasing σ_x and $\sigma_y=0$.*

Figure 11.10. Load-carrying capacity (top left hand side), difference between the calculation methods (top right hand side), length of the part of the yield line parallel to the axes of rotation (middle left hand side), position of the axes of rotation for failure mode 1(middle left hand side) and position of the axes of rotation for failure mode 2(bottom) for a rectangular slab $L_x=2000mm$, $L_y=16000mm$, $\Phi_{0x}=\Phi_{0x}{}'=0.1$, $\Phi_{0y}=\Phi_{0y}{}'=0.1$, $h_{cx}/h= h_{cx}{}'/h= h_{cy}/h= h_{cy}{}'/h=0.1$, $f_c=30MPa$, increasing σ_x and $\sigma_y=0$.

11.2 Calculations of the compression depth

if $0<u<h_c$ & $h_c{}'<u+ h_c{}'<h+ h_c$ & $h-h_c<u+h-h_c<h$

and $0\leq y_0<u$

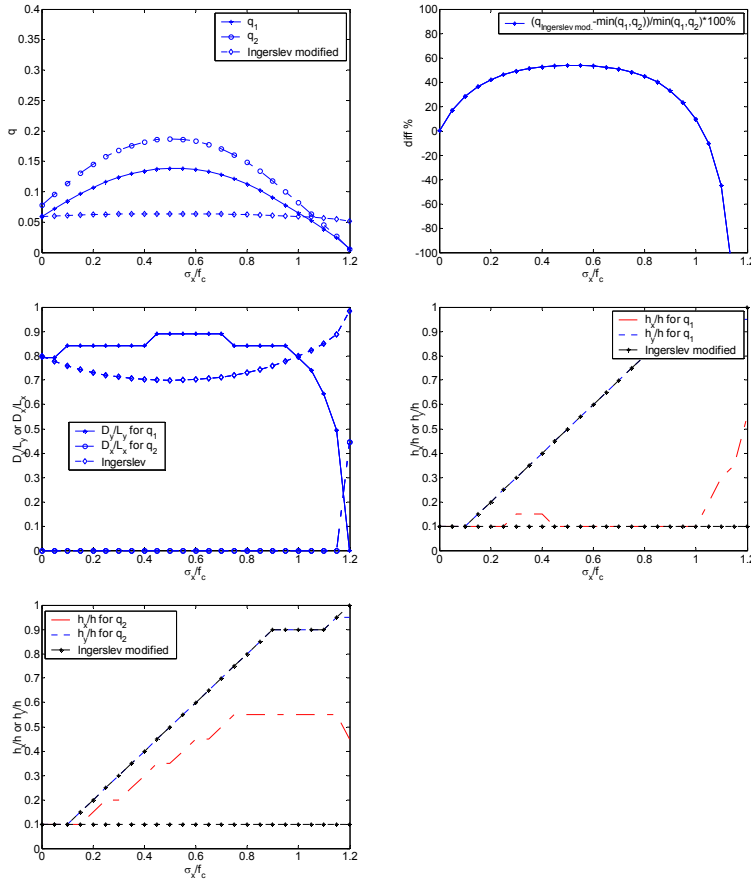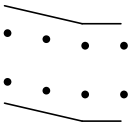$$\frac{y_0}{h} = \frac{\sqrt{2}\sqrt{\left(1-\frac{D}{L}\right)\frac{u}{h}\left(\frac{\sigma}{f_c}+\Phi'+\Phi\right)}}{\left(1-\frac{D}{L}\right)} \qquad (8.2)$$

and u≤y₀<h_c

$$\frac{y_0}{h} = \frac{1}{2}\left(2\frac{\sigma}{f_c}+2\Phi'+2\Phi+\frac{u}{h}+\frac{u}{h}\frac{D}{L}\right) \qquad (8.3)$$

and h_c≤y₀<u+h_c

$$\frac{y_0}{h} = \frac{1}{2}\frac{\left(-1-\frac{D}{L}\right)\frac{u^2}{h}+-2\left(\frac{\sigma}{f_c}+\Phi'+\Phi\right)\frac{u}{h}+4\Phi'\frac{h_c}{h}\left(\frac{D}{L}-1\right)}{-2\Phi'+2\Phi'\frac{D}{L}-\frac{u}{h}} \qquad (8.4)$$

and u+h_c=y₀

$$\left(\frac{1}{2}-\frac{1}{2}\frac{D}{L}\right)\frac{u}{h}+\Phi'-2\Phi'\frac{D}{L}-\Phi+\frac{h_c}{h} \le \frac{\sigma}{f_c} \le \left(\frac{1}{2}-\frac{1}{2}\frac{D}{L}\right)\frac{u}{h}-\Phi+\frac{h_c}{h}+\Phi' \qquad (8.5)$$

and u+h_c<y₀<h-h_c

$$\frac{y_0}{h} = \left(\frac{\sigma}{f_c}-\Phi'+\Phi+\frac{1}{2}\frac{u}{h}+\frac{1}{2}\frac{u}{h}\frac{D}{L}\right) \qquad (8.6)$$

and h-h_c≤y₀<h-h_c+u

$$\frac{y_0}{h} = \frac{\frac{1}{2}\left(-1-\frac{D}{L}\right)\left(\frac{u}{h}\right)^2+\left(-\frac{\sigma}{f_c}+\Phi'-\Phi\right)\frac{u}{h}+\left(2\Phi\frac{h_c}{h}-2\Phi\right)\left(1-\frac{D}{L}\right)}{-2\Phi\left(1-\frac{D}{L}\right)-\frac{u}{h}} \qquad (8.7)$$

and h-hc+u≤y₀<h

$$\frac{y_0}{h} = \frac{\sigma}{f_c}-\Phi'-\Phi+\frac{1}{2}\frac{u}{h}\left(1+\frac{D}{L}\right) \qquad (8.8)$$

and u+h-h_c=y₀

$$\frac{1}{2}\left(1-\frac{D}{L}\right)\frac{u}{h}+\Phi'+\Phi+1-\frac{h_c}{h}-2\Phi\frac{D}{L} \le \frac{\sigma}{f_c} \le \frac{1}{2}\left(1-\frac{D}{L}\right)\frac{u}{h}+\Phi'+\Phi+1-\frac{h_c}{h} \qquad (8.9)$$

and h<y₀≤u+h

$$\frac{y_0}{h} = \frac{\frac{u}{h} + 1 - \frac{D}{L} \pm \sqrt{-\frac{u}{h}\left(2\left(\frac{\sigma}{f_c} - 1 - (\Phi' + \Phi)\right)\left(1 - \frac{D}{L}\right) - \frac{u}{h}\left(\frac{D}{L}\right)^2\right)}}{1 - \frac{D}{L}} \qquad (8.10)$$

if $h_c' < u < h-h_c$ & $h_c' < u + h_c' < h + h_c$ & $h < u+h-h_c$

and $0 \leq y_0 < h_c$

$$\frac{y_0}{h} = \frac{\sqrt{2\left(1 - \frac{D}{L}\right)\frac{u}{h}\left(\frac{\sigma}{f_c} + \Phi' + \Phi\right)}}{1 - \frac{D}{L}} \qquad (8.11)$$

and $h_c \leq y_0 < u$

$$\frac{y_0}{h} = \frac{\left(1 - \frac{D}{L}\right)2\Phi' + \sqrt{2\left(1 - \frac{D}{L}\right)\left(\left(2\Phi'^2 + 2\Phi'\frac{h_c}{h}\right)\left(1 - \frac{D}{L}\right) + \left(\Phi + \Phi' + \frac{\sigma}{f_c}\right)\frac{u}{h}\right)}}{1 - \frac{D}{L}} \qquad (8.12)$$

and $u \leq y_0 < u+h_c$

$$\frac{y_0}{h} = \frac{\frac{1}{2}\left(-1 - \frac{D}{L}\right)\left(\frac{u}{h}\right)^2 - \left(\frac{\sigma}{f_c} + \Phi' + \Phi\right)\frac{u}{h} - 2\Phi'\frac{h_c}{h}\left(1 - \frac{D}{L}\right)}{-2\Phi'\left(1 - \frac{D}{L}\right) - \frac{u}{h}} \qquad (8.13)$$

and $u+h_c = y_0$

$$\frac{1}{2}\left(1 - \frac{D}{L}\right)\frac{u}{h} - 2\frac{D}{L}\Phi' - \Phi + \frac{h_c}{h} + \Phi' \leq \frac{\sigma}{f_c} \leq \frac{1}{2}\left(1 - \frac{D}{L}\right)\frac{u}{h} - \Phi + \frac{h_c}{h} + \Phi' \qquad (8.14)$$

and $u+h_c < y_0 < h-h_c$

$$\frac{y_0}{h} = \frac{\sigma}{f_c} - \Phi' + \Phi + \frac{1}{2}\frac{u}{h}\left(1 + \frac{D}{L}\right) \qquad (8.15)$$
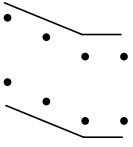
and $h-h_c \leq y_0 < h$

$$\frac{y_0}{h} = \frac{\frac{1}{2}\left(-1 - \frac{D}{L}\right)\left(\frac{u}{h}\right)^2 + \left(-\frac{\sigma}{f_c} + \Phi' - \Phi\right)\frac{u}{h} + \left(2\Phi\frac{h_c}{h} - 2\Phi\right)\left(1 - \frac{D}{L}\right)}{-2\Phi\left(1 - \frac{D}{L}\right) - \frac{u}{h}} \qquad (8.16)$$

and $h \leq y_0 < u+h-h_c$

$$\frac{y_0}{h} = \frac{\frac{u}{h}(-1-2\Phi)\left(1-\frac{D}{L}\right) \pm \sqrt{\begin{array}{c}\left(1-\frac{D}{L}\right)\left(\Phi+\Phi'-\frac{\sigma}{f_c}+1\right)2\frac{u}{h}+\left(4\Phi\frac{h_c}{h}+4\Phi^2\right)\left(1+\left(\frac{D}{L}\right)^2\right)\\ -8\Phi^2\frac{D}{L}-8\Phi\frac{D}{L}\frac{h_c}{h}+\left(\frac{u}{h}\right)^2\left(\frac{D}{L}\right)^2\end{array}}}{1-\frac{D}{L}} \quad (8.17)$$
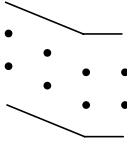
and $u+h-h_c=y_0$

$$1-\frac{D}{L}\frac{h_c}{h}+\Phi'+\Phi-2\Phi\frac{D}{L}+\frac{-\frac{1}{2}\left(\frac{h_c}{h}\right)^2\left(1-\frac{D}{L}\right)}{\frac{u}{h}} \leq \frac{\sigma}{f_c} \leq 1-\frac{D}{L}\frac{h_c}{h}+\Phi'+\Phi+\frac{-\frac{1}{2}\left(\frac{h_c}{h}\right)^2\left(1-\frac{D}{L}\right)}{\frac{u}{h}} \quad (8.18)$$

and $u+h-h_c<y_0\leq u+h$

$$\frac{y_0}{h} = \frac{\frac{u}{h}+1-\frac{D}{L} \pm \sqrt{\frac{u}{h}\left(2\left(1-\frac{D}{L}\right)\left(1-\frac{\sigma}{f_c}+\Phi'+\Phi\right)-\frac{u}{h}\left(\frac{D}{L}\right)^2\right)}}{1-\frac{D}{L}} \quad (8.19)$$

if $h_c'<u<h-h_c$ & $h-h_c<u+h_c'<h$ & $h<u+h-h_c$

and $0\leq y_0<h_c$

$$\frac{y_0}{h} = \frac{\pm\sqrt{2\left(1-\frac{D}{L}\right)\frac{u}{h}\left(\frac{\sigma}{f_c}+\Phi'+\Phi\right)}}{1-\frac{D}{L}} \quad (8.20)$$

and $h_c\leq y_0<u$

$$\frac{y_0}{h} = \frac{2\Phi'\left(1-\frac{D}{L}\right)+\sqrt{2\left(1-\frac{D}{L}\right)\left(\frac{\sigma}{f_c}\frac{u}{h}+\left(2\Phi'^2+2\Phi'\frac{h_c}{h}\right)\left(1-\frac{D}{L}\right)+(\Phi'+\Phi)\frac{u}{h}\right)}}{-1+\frac{D}{L}} \quad (8.21)$$

and $u\leq y_0<h-h_c$

$$\frac{y_0}{h} = \frac{\frac{1}{2}\left(1+\frac{D}{L}\right)\left(\frac{u}{h}\right)^2+\left(\frac{\sigma}{f_c}+\Phi'+\Phi\right)\frac{u}{h}+2\Phi'\frac{h_c}{h}\left(1-\frac{D}{L}\right)}{2\Phi\left(1-\frac{D}{L}\right)+\frac{u}{h}} \quad (8.22)$$

and $u+h_c=y_0$

$$\frac{1}{2}\left(1-\frac{D}{L}\right)\frac{u}{h}-2(\Phi+\Phi')\frac{D}{L}+\Phi'+\Phi+\frac{h_c}{h}+\frac{4\Phi\frac{h_c}{h}-2\Phi-4\Phi\frac{D}{L}\frac{h_c}{h}+2\Phi\frac{D}{L}}{\frac{u}{h}}$$

$$\leq\frac{\sigma}{f_c}\leq \tag{8.23}$$

$$\frac{1}{2}\left(1-\frac{D}{L}\right)\frac{u}{h}-2\Phi\frac{D}{L}+\Phi'+\Phi+\frac{h_c}{h}+\frac{4\Phi\frac{h_c}{h}-2\Phi-4\Phi\frac{D}{L}\frac{h_c}{h}+2\Phi\frac{D}{L}}{\frac{u}{h}}$$

and $h-h_c<y_0<u+h_c$

$$\frac{y_0}{h}=\frac{\frac{1}{2}\left(1+\frac{D}{L}\right)\left(\frac{u}{h}\right)^2+\left(\frac{\sigma}{f_c}+\Phi'+\Phi\right)\frac{u}{h}+2\left(-\Phi\frac{h_c}{h}+\Phi+\Phi'\frac{h_c}{h}\right)\left(1-\frac{D}{L}\right)}{2(\Phi+\Phi')\left(1-\frac{D}{L}\right)+\frac{u}{h}} \tag{8.24}$$

and $u+h_c\leq y_0<h$

$$y01=\frac{\frac{1}{2}\left(1+\frac{D}{L}\right)\left(\frac{u}{h}\right)^2+\left(\frac{\sigma}{f_c}-\Phi'+\Phi\right)\frac{u}{h}+\left(2\Phi-2\Phi\frac{h_c}{h}\right)\left(1-\frac{D}{L}\right)}{2\Phi\left(1-\frac{D}{L}\right)+\frac{u}{h}} \tag{8.25}$$

and $h\leq y_0<u+h-h_c$

$$\frac{y_0}{h}=\frac{2\Phi\left(1-\frac{D}{L}\right)+\frac{u}{h}+1-\frac{D}{L}\pm\sqrt{\begin{array}{c}\left(2\frac{u}{h}+2\Phi\frac{u}{h}-2\frac{\sigma}{f_c}\frac{u}{h}+2\Phi'\frac{u}{h}\right)\left(1-\frac{D}{L}\right)+\left(4\Phi\frac{h_c}{h}+4\Phi^2\right)\left(1+\left(\frac{D}{L}\right)^2\right)\\-8\Phi^2\frac{D}{L}+\left(\frac{u}{h}\right)^2\left(\frac{D}{L}\right)^2-8\Phi\frac{D}{L}\frac{h_c}{h}\end{array}}}{1-\frac{D}{L}}$$

$$\tag{8.26}$$

and $u+h-h_c=y_0$

$$1-\frac{D}{L}\frac{h_c}{h}+\Phi'+\Phi-2\Phi\frac{D}{L}-\frac{\frac{1}{2}\left(\frac{h_c}{h}\right)^2\left(1-\frac{D}{L}\right)}{\frac{u}{h}}\leq\frac{\sigma}{f_c}\leq1-\frac{D}{L}\frac{h_c}{h}+\Phi'+\Phi-\frac{\frac{1}{2}\left(\frac{h_c}{h}\right)^2\left(1-\frac{D}{L}\right)}{\frac{u}{h}} \tag{8.27}$$

and $u+h-h_c<y_0\leq u+h$

$$\frac{y_0}{h}=\frac{\frac{u}{h}+1-\frac{D}{L}\pm\sqrt{\frac{u}{h}\left(2\left(1-\frac{\sigma}{f_c}+\Phi'+\Phi\right)\left(1-\frac{D}{L}\right)+\frac{u}{h}\left(\frac{D}{L}\right)^2\right)}}{1-\frac{D}{L}} \tag{8.28}$$

if $h-h_c<u<h$ & $h<u+h_c'$ & $h<u+h-h_c$

and $0\leq y_0<h_c$

$$\frac{y_0}{h} = \frac{\sqrt{2\left(1-\dfrac{D}{L}\right)\dfrac{u}{h}\left(\dfrac{\sigma}{f_c}+\Phi'+\Phi\right)}}{1-\dfrac{D}{L}} \qquad (8.29)$$

and $h_c\leq y_0<h-h_c$

$$\frac{y_0}{h} = \pm\frac{-2\Phi'\left(1-\dfrac{D}{L}\right)+\sqrt{2\left(1-\dfrac{D}{L}\right)\left(\dfrac{u}{h}\left(\dfrac{\sigma}{f_c}+\Phi+\Phi'\right)+\left(2\Phi'^2+2\Phi'\dfrac{h_c}{h}\right)\left(1-\dfrac{D}{L}\right)\right)}}{1-\dfrac{D}{L}} \qquad (8.30)$$

and $h-h_c\leq y_0<u$

$$\frac{y_0}{h}=\frac{2\left(\Phi'+\Phi\right)\left(1-\dfrac{D}{L}\right)\pm\sqrt{2\left(1-\dfrac{D}{L}\right)\left(\begin{array}{l}2\left(\Phi'^2+\Phi^2+\Phi+2\Phi'\Phi-\Phi\dfrac{h_c}{h}+\Phi'\dfrac{h_c}{h}\right)\left(1-\dfrac{D}{L}\right)\\+\left(\Phi+\Phi'+\dfrac{\sigma}{f_c}\right)\dfrac{u}{h}\end{array}\right)}}{1-\dfrac{D}{L}} \qquad (8.31)$$

and $u+h_c=y_0$

$$1-\frac{D}{L}+\frac{D}{L}\frac{h_c}{h}+\left(\Phi+\Phi'\right)\left(1-2\frac{D}{L}\right)+\frac{\left(1-\dfrac{D}{L}\right)\left(-2\Phi-\dfrac{1}{2}+\dfrac{h_c}{h}+4\Phi\dfrac{h_c}{h}-\dfrac{1}{2}\left(\dfrac{h_c}{h}\right)^2\right)}{\dfrac{u}{h}}$$

$$\leq\frac{\sigma}{f_c}\leq \qquad (8.32)$$

$$1-\frac{D}{L}+\frac{D}{L}\frac{h_c}{h}+\Phi\left(1-2\frac{D}{L}\right)+\Phi'+\frac{\left(1-\dfrac{D}{L}\right)\left(-2\Phi-\dfrac{1}{2}+\dfrac{h_c}{h}+4\Phi\dfrac{h_c}{h}-\dfrac{1}{2}\left(\dfrac{h_c}{h}\right)^2\right)}{\dfrac{u}{h}}$$

and $u<y_0<h$

$$\frac{y_0}{h}=\frac{\dfrac{1}{2}\left(1+\dfrac{D}{L}\right)\left(\dfrac{u}{h}\right)^2+\left(\dfrac{\sigma}{f_c}+\Phi'+\Phi\right)\dfrac{u}{h}+2\left(\Phi+\Phi'\dfrac{h_c}{h}-\Phi\dfrac{h_c}{h}\right)\left(1-\dfrac{D}{L}\right)}{2\left(\Phi+\Phi'\right)\left(1-\dfrac{D}{L}\right)+\dfrac{u}{h}} \qquad (8.33)$$

and $h \leq y_0 < u+h_c$

$$\frac{y_0}{h} = \frac{\left(1+\frac{D}{L}\right)(-2\Phi - 2\Phi' - 1) - \frac{u}{h} + \sqrt{\begin{aligned} &\left(1-\frac{D}{L}\right)\left(+2\frac{u}{h}+2\Phi\frac{u}{h}\right) \\ &+\left(1+\left(\frac{D}{L}\right)^2\right)\left(4\Phi'^2+4\Phi^2+4\Phi\frac{h_c}{h}-4\Phi'\frac{h_c}{h}+8\Phi'\Phi+4\Phi'\right) \\ &+\left(+2\frac{D}{L}\frac{u}{h}-2\frac{u}{h}\right)\left(\frac{\sigma}{f_c}-\Phi'\right) \\ &+8\frac{D}{L}\left(-\Phi^2-\Phi'^2-\Phi\frac{h_c}{h}+\Phi'\frac{h_c}{h}-\Phi'\right) \\ &-16\Phi'\Phi\frac{D}{L}+\left(\frac{u}{h}\right)^2\left(\frac{D}{L}\right)^2 \end{aligned}}}{-1+\frac{D}{L}} \quad (8.34)$$

and $u+h_c \leq y_0 < u+h-h_c$

$$\frac{y_0}{h} = \frac{2\Phi\frac{D}{L}-\frac{u}{h}-2\Phi-1+\frac{D}{L} + \sqrt{\begin{aligned} &2\frac{u}{h}\left(\left(\Phi'+1+\Phi-\frac{\sigma}{f_c}\right)\left(1-\frac{D}{L}\right)\right)+4\Phi\left(\left(1+\left(\frac{D}{L}\right)^2\right)\left(\frac{h_c}{h}+\Phi\right)-2\frac{D}{L}\frac{h_c}{h}\right) \\ &-8\Phi^2\frac{D}{L}+\left(\frac{u}{h}\right)^2\left(\frac{D}{L}\right)^2 \end{aligned}}}{-1+\frac{D}{L}} \quad (8.35)$$

and $u+h-h_c = y_0$

$$1-\frac{h_c}{h}\frac{D}{L}+\Phi'+\Phi-2\Phi\frac{D}{L}-\frac{\frac{1}{2}\left(\frac{h_c}{h}\right)^2\left(1-\frac{D}{L}\right)}{\frac{u}{h}} \leq 1-\frac{h_c}{h}\frac{D}{L}+\Phi'+\Phi-\frac{\frac{1}{2}\left(\frac{h_c}{h}\right)^2\left(1-\frac{D}{L}\right)}{\frac{u}{h}} \quad (8.36)$$

and $u+h-h_c < y_0 \leq u+h$

$$\frac{y_0}{h} = \frac{-\frac{u}{h}-1+\frac{D}{L}+\sqrt{\frac{u}{h}\left(2\left(1-\frac{D}{L}\right)\left(1-\frac{\sigma}{f_c}+\Phi'+\Phi\right)+\frac{u}{h}\left(\frac{D}{L}\right)^2\right)}}{-1+\frac{D}{L}} \quad (8.37)$$

if $h < u$ & $h < u+h_c'$ & $h < u+h-h_c$

and $0 \leq y_0 < h_c$

- 109 -

$$\frac{y_0}{h} = \frac{\sqrt{2\left(1-2\frac{D}{L}\right)\frac{u}{h}\left(\Phi'+\Phi+\frac{\sigma}{f_c}\right)}}{1-\frac{D}{L}} \qquad (8.38)$$

and $h_c \leq y_0 < h-h_c$

$$\frac{y_0}{h} = \frac{-2\left(1-\frac{D}{L}\right) \pm \sqrt{2\left(1-\frac{D}{L}\right)\left(\left(\frac{\sigma}{f_c}+\Phi'+\Phi\right)\frac{u}{h}+\left(2\Phi'^2+2\Phi'\frac{h_c}{h}\right)\left(1-\frac{D}{L}\right)\right)}}{1-\frac{D}{L}} \qquad (8.39)$$

and $h-h_c \leq y_0 < h$

$$\frac{y_0}{h} = \frac{2(-\Phi'-\Phi)\left(1-\frac{D}{L}\right) \pm \sqrt{2\left(1-\frac{D}{L}\right)\left(2\left(1-\frac{D}{L}\right)\left(+\Phi'\frac{h_c}{h}-\Phi\frac{h_c}{h}+2\Phi'\Phi-\Phi'^2+\Phi+\Phi^2\right)+\left(+\Phi+\frac{\sigma}{f_c}+\Phi'\right)\frac{u}{h}\right)}}{1-\frac{D}{L}}$$
$$(8.40)$$

and $u+h_c=y_0$

$$1-\frac{D}{L}+\frac{D}{L}\frac{h_c}{h}-2\Phi\frac{D}{L}-2\frac{D}{L}\Phi'+\Phi+\Phi'+\frac{\left(\frac{h_c}{h}-\frac{1}{2}-\frac{1}{2}\left(\frac{h_c}{h}\right)^2+4\Phi\frac{h_c}{h}-2\Phi\right)\left(1-\frac{D}{L}\right)}{\frac{u}{h}}$$

$$\leq \frac{\sigma}{f_c} \leq \qquad (8.41)$$

$$1-\frac{D}{L}+\frac{D}{L}\frac{h_c}{h}-2\Phi\frac{D}{L}+\Phi+\Phi'+\frac{\left(\frac{h_c}{h}-\frac{1}{2}-\frac{1}{2}\left(\frac{h_c}{h}\right)^2+4\Phi\frac{h_c}{h}-2\Phi\right)\left(1-\frac{D}{L}\right)}{\frac{u}{h}}$$

and $h<y_0<u$

$$\frac{y_0}{h} = \frac{\left(\frac{\sigma}{f_c}+\Phi'+\Phi\right)\frac{u}{h}+\left(\frac{1}{2}+2\Phi-2\Phi\frac{h_c}{h}+2\Phi'\frac{h_c}{h}\right)\left(1-\frac{D}{L}\right)}{\left(1-\frac{D}{L}\right)(2\Phi'+2\Phi+1)} \qquad (8.42)$$

and $u \leq y_0 < u+h_c$

$$\frac{y_0}{h} = \frac{-\dfrac{u}{h}+\dfrac{D}{L}-2\Phi'+2\Phi'\dfrac{D}{L}-2\Phi-1+2\Phi\dfrac{D}{L}\pm\sqrt{\begin{array}{l}2\dfrac{D}{L}\dfrac{\sigma}{f_c}\dfrac{u}{h}-2\dfrac{\sigma}{f_c}\dfrac{u}{h}-2\dfrac{u}{h}\Phi\dfrac{D}{L}-8\Phi'\dfrac{D}{L}\\[2mm] +2\Phi\dfrac{u}{h}+4\Phi\dfrac{h_c}{h}-4\Phi'\dfrac{h_c}{h}+2\Phi'\dfrac{u}{h}+4\Phi'+2\dfrac{u}{h}\\[2mm] +8\Phi'\dfrac{D}{L}\dfrac{h_c}{h}-8\Phi\dfrac{D}{L}\dfrac{h_c}{h}+4\Phi\left(\dfrac{D}{L}\right)^2\dfrac{h_c}{h}\\[2mm] -4\Phi'\left(\dfrac{D}{L}\right)^2\dfrac{h_c}{h}+8\Phi'\left(\dfrac{D}{L}\right)^2\Phi-2\dfrac{D}{L}\Phi'\dfrac{u}{h}\\[2mm] -2\dfrac{u}{h}\dfrac{D}{L}+\left(\dfrac{u}{h}\right)^2\left(\dfrac{D}{L}\right)^2+8\Phi'\Phi+4\Phi'\left(\dfrac{D}{L}\right)^2-8\Phi^2\dfrac{D}{L}\\[2mm] +4\Phi^2+4\Phi^2\left(\dfrac{D}{L}\right)^2+4\Phi'^2-8\Phi'^2\dfrac{D}{L}+4\Phi'^2\left(\dfrac{D}{L}\right)^2\\[2mm] -16\Phi'\Phi\dfrac{D}{L}\end{array}}}{-1+\dfrac{D}{L}}$$

(8.43)

and $u+h_c \leq y_0 < u+h-h_c$

$$\frac{y_0}{h} = \frac{1-\dfrac{D}{L}+2\Phi-2\Phi\dfrac{D}{L}+\dfrac{u}{h}\pm\sqrt{\begin{array}{l}2\dfrac{u}{h}-2\dfrac{u}{h}\dfrac{D}{L}\Phi'+2\Phi'\dfrac{u}{h}+2\Phi\dfrac{u}{h}\\[2mm] +2\dfrac{u}{h}\dfrac{D}{L}\dfrac{\sigma}{f_c}-2\dfrac{\sigma}{f_c}\dfrac{u}{h}-2\dfrac{u}{h}\dfrac{D}{L}\Phi-2\dfrac{D}{L}\dfrac{u}{h}\\[2mm] +\left(\dfrac{u}{h}\right)^2\left(\dfrac{D}{L}\right)^2-8\Phi\dfrac{D}{L}\dfrac{h_c}{h}+4\Phi\dfrac{h_c}{h}+4\Phi\left(\dfrac{D}{L}\right)^2\dfrac{h_c}{h}\\[2mm] +4\Phi^2-8\Phi^2\dfrac{D}{L}+4\Phi^2\left(\dfrac{D}{L}\right)^2\end{array}}}{1-\dfrac{D}{L}}$$

(8.44)

and $u+h-h_c=y_0$

$$1-\frac{D}{L}\frac{h_c}{h}+\Phi'+\Phi-2\Phi\frac{D}{L}+\frac{-\dfrac{1}{2}\left(\dfrac{h_c}{h}\right)^2\left(1-\dfrac{D}{L}\right)}{\dfrac{u}{h}}$$

$$\leq \frac{\sigma}{f_c} \leq$$

(8.45)

$$1-\frac{D}{L}\frac{h_c}{h}+\Phi'+\Phi+\frac{-\dfrac{1}{2}\left(\dfrac{h_c}{h}\right)^2\left(1-\dfrac{D}{L}\right)}{\dfrac{u}{h}}$$

and u+h-h_c<y_0≤u+h

$$\frac{y_0}{h} = \frac{\dfrac{u}{h}+1-\dfrac{D}{L} \pm \sqrt{\dfrac{u}{h}\left(2\left(1-\dfrac{D}{L}\right)\left(1-\dfrac{\sigma}{f_c}+\Phi'+\Phi\right)+\dfrac{u}{h}\left(\dfrac{D}{L}\right)^2\right)}}{1-\dfrac{D}{L}}$$

(8.46)

DTU